AD-A066 388 NAVAL POSTGRADUATE SCHOOL MONTEREY CALIF F/G 20/1
COMPARISON OF THEORETICAL AND EXPERIMENTAL SOUND RADIATION PATT--ETC(U)
DEC 78 T O KIYAR

UNCLASSIFIED NL

1 OF 2
ADA
066388

NAVAL POSTGRADUATE SCHOOL

Monterey, California

THESIS

COMPARISON OF THEORETICAL AND EXPERIMENTAL SOUND RADIATION PATTERNS FROM A WATER LOADED FLEXURAL DISK TRANSDUCER

by

Tekin O. Kiyar

December 1978

Thesis Advisor: O.B. Wilson, Jr.

Approved for public release; distribution unlimited.

UNCLASSIFIED

SECURITY CLASSIFICATION OF THIS PAGE (When Data Entered)

REPORT DOCUMENTATION PAGE		READ INSTRUCTIONS BEFORE COMPLETING FORM
1. REPORT NUMBER	2. GOVT ACCESSION NO.	3. RECIPIENT'S CATALOG NUMBER (9)
4. TITLE (and Subtitle) (6) Comparison of Theoretical and Experimental Sound Radiation Patterns from a Water Loaded Flexural Disk Transducer.		5. TYPE OF REPORT & PERIOD COVERED Master's Thesis December 1978
		6. PERFORMING ORG. REPORT NUMBER
7. AUTHOR(s) (10) Tekin O. Kiyar		8. CONTRACT OR GRANT NUMBER(s)
9. PERFORMING ORGANIZATION NAME AND ADDRESS Naval Postgraduate School Monterey, California 93940		10. PROGRAM ELEMENT, PROJECT, TASK AREA & WORK UNIT NUMBERS
11. CONTROLLING OFFICE NAME AND ADDRESS Naval Postgraduate School Monterey, California 93940		12. REPORT DATE (11) December 1978
		13. NUMBER OF PAGES 109
14. MONITORING AGENCY NAME & ADDRESS (if different from Controlling Office) Naval Postgraduate School Monterey, California 93940 (12) 110p.		15. SECURITY CLASS. (of this report) Unclassified
		15a. DECLASSIFICATION/DOWNGRADING SCHEDULE

16. DISTRIBUTION STATEMENT (of this Report)

Approved for public release; distribution unlimited.

17. DISTRIBUTION STATEMENT (of the abstract entered in Block 20, if different from Report)

Approved for public release; distribution unlimited.

18. SUPPLEMENTARY NOTES

19. KEY WORDS (Continue on reverse side if necessary and identify by block number)

20. ABSTRACT (Continue on reverse side if necessary and identify by block number)

Measurements of the sound radiation patterns in water from the flexural vibrations of a clamped-edge steel disk have been made and are compared with the results of theoretical calculations made by Alper and Magrab (Journal of Acoustical Society of America, Vol. 48, Number 3, pp. 681-691, 1970) for the two lowest order circularly symmetric modes of disk vibration. → next page

DD FORM 1473, 1 JAN 73 EDITION OF 1 NOV 65 IS OBSOLETE

S/N 0102-014-6601 |

UNCLASSIFIED

SECURITY CLASSIFICATION OF THIS PAGE (When Data Entered)

251450 1

LB

Although some differences were expected and were found due to the experimental condition which only approximated the assumptions made in the theory, it was found that the major features of the measured patterns agreed reasonably well with the theoretical patterns.

The results have applicability to the design of sound source which could be used in underwater tracking of vehicles on a test range.

ACCESSION for		
NTIS	White Section	☑
DDC	Buff Section	☐
UNANNOUNCED		☐
JUSTIFICATION		
BY		
DISTRIBUTION/AVAILABILITY CODES		
Dist.	AVAIL. and/or SPECIAL	
A		

Approved for public release; distribution unlimited.

Comparison of Theoretical and Experimental Sound Radiation Patterns from a Water Loaded Flexural Disk Transducer

by

Tekin O. Kiyar
Lieutenant, Turkish Navy
B.S.E.E., Naval Postgraduate School, 1978

Submitted in partial fulfillment of the
requirements for the degree of

MASTER OF SCIENCE IN ENGINEERING ACOUSTICS

from the

NAVAL POSTGRADUATE SCHOOL
December 1978

Author: Tekin Kiyar

Approved by: O.B. Wilson, Jr.
Thesis Advisor

William B. Zeleny
Second Reader

Chairman, Department of Physics and Chemistry

William M. Tolles
Dean of Science and Engineering

ABSTRACT

Measurements of the sound radiation patterns in water from the flexural vibrations of a clamped-edge steel disk have been made and are compared with the results of theoretical calculations made by Alper and Magrab (Journal of Acoustical Society of America, Vol. 48, Number 3, pp. 681-691, 1970) for the two lowest order circularly symmetric modes of disk vibration.

Although some differences were expected and were found due to the experimental condition which only approximated the assumptions made in the theory, it was found that the major features of the measured patterns agreed reasonably well with the theoretical pattern.

The results have applicability to the design of sound source which could be used in underwater tracking of vehicles on a test range.

TABLE OF CONTENTS

LIST OF FIGURES

LIST OF SYMBOLS

a	Plate radius
C_0	Sound velocity of fluid
C_s	Shear wave velocity in the plate $[G/\rho]^{1/2}$
d_q^{mn}	Coefficients in the spheroidal wave functions expansions
e_{mj}	See Eq. (46)
$\vec{e}_\eta$	Unit Vector Normal to surface of constant η
$\vec{e}_\xi$	Unit Vector Normal to surface of constant ξ
$\vec{e}_\theta$	Unit Vector Normal to surface of constant θ
$\hat{f}$	Force per unit area (space dependent only)
G	Shear Modulus of the plate
h	Plate thickness
i	$(-1)^{1/2}$
k	Wave number in acoustic medium
k_T^2	Empirical Shear Coefficient for plate
p	Acoustic Pressure
ρ_0	Density of Fluid Medium
ρ	Density of Plate Material per unit volume
ν	Poisson's ratio
ϕ	Velocity Potential
$\hat{q}$	External Load on the Plate (space dependent only)
η, ξ, θ	Dimensionless oblate spheroidal coordinates
γ	$h/[a\sqrt{12}]$
J_m, I_m	Bessel functions of first and second kind of order m

κ	$(1-\nu)/2$
$R_{mn}^{j}(-i\Omega, i\xi)$	Radial Function for oblate spheroidal coordinate (j = 1,2,3,4.)
$S(-i\Omega, \eta)$	Angular Function for oblate spheriodal coordinates
$\delta(x)$	Delta Function
A_{mn}, D_{mn}	Coefficients
$\hat{w}$	Dimensionless Transverse Displacement
u	$\frac{r}{a}$
$\psi_u(u,\theta)$	Rotation angle of normal to plate surface in u direction
$\psi_\theta(u,\theta)$	Rotation angle of normal to plate surface in θ direction
ω	Angular Frequency
τ	ωt
Ω	ka; frequency parameter
Ω_{mj}	In Vacuo Eigenvalues for clamped circular plate
$\vec{V}$	Velocity Vector
V_η	Velocity Normal to surface of constant η

ACKNOWLEDGEMENTS

I would like to express my appreciation to Dr. S. Alper for making available his doctoral thesis and computer programs. Also I want to thank Mr. Robert Moeller of the Physics and Chemistry Department Shop for his construction of the mechanical apparatus and LT N. Bradshaw, USN, and the Navy Fleet Numerical Weather Central for her assistance and the computer time and the Naval Undersea Warfare Engineering Station, Keyport, Washington, for their support.

I would like to thank Professor O. B. Wilson for his guidance, counsel, patience and motivation for the preparation of this thesis.

I am especially grateful and would like to thank and to express my sincere appreciation to the Turkish Navy and to my Country for providing this opportunity.

I. INTRODUCTION

A high frequency broad-band transducer which has a broad radiation pattern in a half-space is required for acoustic tracking of underwater vehicles in situations where the vehicle carries the sound source and the receivers are fixed. [1] The underwater ranges at the Naval Undersea Warfare Engineering Station (NUWES), Keyport, Washington, are of this type. During tests of production torpedoes and new torpedo designs, the torpedo is tracked in three dimensions as it moves through the water.

The tracking is accomplished using an array of hydrophones mounted on the bottom of the acoustic range which receives acoustic pulses radiated periodically from a projector mounted on each vehicle on the range. Currently, an acoustic projector mounted flush with the bottom of the torpedo sends out a 75kHz coded pulse that is picked up by the hydrophones. A shore-based computer receives the information from the range hydrophones and computes the location and speed of the torpedo during the run.

For the NUWES Keyport ranges, the signal to noise ratio requirements and the expected maximum transmission loss between source and the receivers places a minimum requirement on source level which is quite high. In addition, the pitch and roll motions of the torpedo and the effect of surface reflection of the sound has led to a specification of a broad beam

width. Specifically, current requirements are for a uniform source level within a conical volume about 150° wide centered on the vertical axis of the transducer.

The projectors are required to operate acoustically unloaded (in air) 95 percent of the time, since the unit is turned on before launch and continues running after recovery. Another requirement placed on the projector to be used in higher speed vehicles is that the radiating surface be flush with the body of the vehicle.

These various requirements place extreme demands on the physical properties of materials used in the transducer and create difficult problems of building a transducer which also has reasonable life expectancy and reasonable cost.

Another approach to this problem is the use of a flexural wave transducer as a broad-beam, broad-band-width source which would be readily adaptable to flush-mounting, a necessary requirement for high speed torpedoes. The possibility of using the torpedo hull itself as the radiating surface is especially attractive for the low drag, laminar flow shapes expected to become used in the future. Present designs use a transducer which is inserted into a recess in the hull. Although this is relatively smooth, it is not adequately smooth for ultra-low drag laminar flow.

Some early work in this area was done by Barlow at NUWES (private communication). The first previous work at the Naval Postgraduate School on this subject was done by LT Sevdik [1]. His calculations were based on classical plate theory as described in Morse and Ingard [2] and Malechi [3], which does

not take into account of effects of transverse shear and rotatory inertia. Among the results of Sevdik's work was the noting of damping of the plate natural frequencies by fluid loading and of inconsistencies in the change of flexural wave phase speed with frequency for transducers of differing thickness.

Mindlin [4] includes these effects in a three-dimensional plate theory and shows that classical plate theory begins to differ markedly from three-dimensional theory at frequencies above that at which the flexural wavelength is about ten times the plate thickness. His theory gives flexural-wave speed values for a given ratio of plate thickness to flexural wave length which are lower than those from classical plate theory.

Feit [5] considers the case of an infinite plate excited by a simple harmonic point source and which is fluid loaded on one side. He discusses the significant changes in the theoretical radiation patterns that result at frequencies above and below the critical frequency, that frequency at which the flexural wave speed in the plate equals the speed of sound in the fluid. His work is based on the Mindlin-Timoshenko plate theory.

An experimental investigation was conducted of the effects of fluid loading on axially symmetric flexural waves in a circular aluminum plate 25 in. in diameter and 5/16 in. thick by LT Jarvis [7] in 1977. Jarvis' results are in good agreement with the Mindlin-Timoshenko plate theory for the speed of the flexural wave as a function of frequency. Jarvis' results clearly show a change in the radiation resistance as

frequency increases, as evidenced by the increased damping of the plate natural frequencies with increasing frequency. At frequencies below the critical frequency, the fluid adds inertia which causes a lower flexural wave speed. Above the critical frequency, the wave speed increasesabruptly to about the value for the unloaded plate, indicating that the radiation reactance (inertial) becomes very much smaller above the critical frequency.

Until the work of Alper and Magrab [6], a "closed form" solution of the coupled vibration of a finite circular plate clamped in an infinite, rigid baffle had not been obtained for either classical plate theory or the Mindlin-Timeshenko plate theory.

The first treatment of this problem was given by Lord Rayleigh [8] Mindlin [10] andDeresciewicz [9] have shown that the normal modes and natural frequencies of a plate of finite thickness are different and more numerous in a given frequency band that are given by classical plate theory.

Reisman and Greene [11] have studied the "in vacuo" response of clamped circular plates to suddenly applied loads using the Mindlin-Timoshenko plate theory. They found that except for the first three or four natural frequencies of very thin plates (diameter to thickness ratio 40 or more) there was no similarity between the natural frequency spectra of the Mindlin-Timoshenko theory and classical theory. The difference in transient responses were also significant.

In the Alper-Magrab paper the acoustic pressure distribution is obtained in a half space bounded by an infinite rigid

baffle containing a clamped circular plate which is driven from the "in vacuo" side by a simple harmonic force having an arbitrary spatial distribution. A closed form solution is obtained which is valid for both the near and far fields. The analysis uses oblate spheroidal coordinates to obtain the solution of the wave equation in the fluid. These coordinates are chosen because a bounding surface of one of the coordinates is represented entirely by the circular plate, and a bounding surface of another coordinate is represented entirely by the infinite baffle with a circular opening the same size as the plate diameter. The third coordinate is identical to one of the polar coordinates, the coordinates in which the plate motion is obtained. As a result, the otherwise fairly complicated coupled problem is reduced to two simpler boundary value problems which can be solved separately and the solutions coupled by the continuity condition at their common boundary. The resulting solution for the acoustic field is given by an expansion in spheroidal wave functions. Pressure at any point in the field can be evaluated by inserting the value of the wave functions at the point.

This is in contrast to previous known attempts to solve this problem, all of which have resulted in the need to perform difficult double (surface) integrations numerically with each integration valid for only one point in the field. Furthermore, all known previous work has been restricted to the classical plate theory.

In the following pages, a brief review is presented of Alper's theoretical work as reported in his doctoral thesis [16]

and from the point of view of using the results as a design tool for a transducer.

As part of the present thesis, experimental work was conducted as a test of the Alper-Magrab theory, using measurements of the radiated beam pattern from a transducer. These results are presented and compared with Alper's calculation.

Finally, a modification of the Alper-Magrab computer program is included as an appendix in a form suitable for running on the Navy Fleet Numerical Weather Facility Computer (CDC-6500-"HAL").

II. THEORETICAL CONSIDERATIONS

A. APPROACH

An outline of the approach to the problem [16] of calculating the sound field from the flexual vibration in a clamped edge plate is:

(1) The wave equation governing the motion in the acoustic fluid is transformed into oblate spheroidal coordinates.

(2) Using the Mindlin-Timoshenko plate theory, the eigen frequencies and eigen functions of the plate are determined for a clamped circular plate using polar cylindrical coordinates.

(3) The solution to the forced vibration problem is expressed as the collection of all possible combinations of the plate eigenfunctions and is introduced into the appropriate nonhomogeneous differential equation governing the plate motion which contains a term representing the surface force acting on the plate [the surface force is the sum of the applied force and the fluid pressure (in terms of velocity potential expressed by the means of spheroidal wave functions)]. The resulting equations are then reduced to algebraic equations in the two sets of arbitrary coefficients (plate motion and fluid motion) by using the orthogonality property of the "in vacuo" eigenfunctions of the plate.

(4) Because the velocities of the plate and of the fluid must equal each other at the interface of the plate on fluid, the appropriate derivatives of the plate displacement and fluid

velocity potential are equated. Orthogonality of the spheroidal wave functions then yields another set of algebraic equations.

(5) Combining (3) and (4) and solving the result gives equations which express the pressure at every point in terms of spheroidal wave functions, thus leading to a knowledge of pressure at the point of interest at a given frequency.

B. SOLUTION

The following steps are from the work of Alper [16]. As seen in Figure 1 a circular plate is clamped in an infinite rigid baffle, represented by the x, y plane. The upper part is filled with fluid and there is vacuum in the lower part. A spatially arbitrary, harmonic, transverse force is applied to the "in-vacuo" side of the plate. The objective is to calculate the far field pressure in the acoustic fluid produced by the forced motion of the plate. The equation of motion in the fluid is

$$a^2 \nabla^2 = \Omega^2 \frac{\partial^2 \phi}{\partial \tau^2} \tag{1}$$

where

$\Omega =$ ka, frequency parameter

$\tau = \omega t$, dimensionless time.

$\phi =$ dimensionless velocity potential

$$p = \Omega^2 \frac{\partial \phi}{\partial \tau} \qquad \text{dimensionless pressure} \tag{2}$$

$$V = -a \nabla \phi \qquad \text{dimensionless velocity} \tag{3}$$

We will look for harmonic solutions of the form

$$\phi = \hat{\phi} e^{i\tau} \tag{4}$$

where

$\hat{\phi}$ = magnitude of velocity potential and is a function of space coordinates only.

Hence, putting Eq. (4) into Eq. (2) gives

$$p = i\Omega^2 \hat{\phi} e^{i\tau} = \hat{p} e^{i\tau} \qquad (5)$$

Again, $\hat{p} = i\Omega^2 \hat{\phi}$ is a function of space coordinates only.

Also, putting Eq. (4) into Eq. (1) gives

$$a^2\nabla^2(\hat{\phi} e^{i\tau}) - \Omega^2(i^2 \hat{\phi} e^{i\tau}) = 0$$

$$(a^2\nabla^2 + \Omega^2)\hat{\phi} = 0 \qquad (6)$$

Eq. (6) is the dimensionless Helmholtz equation. Its solutions must satisfy the boundary conditions in the fluid. Except for the conditions at the plate, these are:

(a) The fluid velocity normal to the rigid baffle must be zero.

(b) Only outgoing waves are accepted.

Oblate spheroidal coordinates, which are shown in Figure 2 [Van Buren, King, Baier, and Hanish, Ref. 17], are the most suitable for these boundary conditions.

When the confocal ellipses and hyperbolas having an inter-focal distance of plate diameter 2a are rotated about the minor axis (z axis), flattened ellipsoids and hyperboloids of one sheet are obtained. Under the transformation to dimensionless coordinates η and ξ.

$$x = a\,[(1-\eta^2)(\xi^2+1)]^{1/2} \quad \cos\theta$$
$$y = a\,[(1-\eta^2)(\xi^2+1)]^{1/2} \quad \sin\theta \qquad (7)$$
$$z = a\,[\eta\xi].$$

The ξ= constant surface is an ellipsoid of revolution. The cross section perpendicular to the x or y axis is an ellipse,

while that perpendicular to the z axis is a circle. In the xy plane the eccentricity of the ellipse is $\frac{1}{\xi}$ and the semimajor axis is ξ. Hence the bigger ξ is, the larger the ellipse, and the more nearly circular it becomes. The surface $\xi = 0$ is a circular disk of radius a in the xy plane. The surface $\xi = \infty$ is a sphere of radius ∞. The η = constant surface is a hyperboloid of revolution of one sheet with anasymptotic cone whose generating line passes through the origin and is inclined at the angle $\eta = \cos \nu_0$ to the z axis. The cross section perpendicular to the z axis is an ellipse, sections perpendicular to the x or y axis are hyperbolas. The surface $\eta = 0$ is the xy plane except for the circular disk $\xi = 0$. The surface $|\eta| = 1$ is the z axis. The intersection of η and ξ constant surfaces is a circle. The angle θ, measured from the x axis towards the y axis determines a point on this circle.

Domains are:

$$0 \leq \eta \leq 1 \quad , -\infty < \xi < \infty \quad , 0 \leq \theta \leq 2\pi$$

Eq. (23) becomes, in oblate spheroidal coordinates,

$$\left[\frac{\partial}{\partial \eta}(1-\eta^2)\frac{\partial}{\partial \eta} + \frac{\partial}{\partial \xi}(\xi^2+1)\frac{\partial}{\partial \xi} + \frac{\xi^2+\eta^2}{(\xi^2+1)(\eta^2+1)}\frac{\partial^2}{\partial \theta^2} + \Omega^2(\xi^2+\eta^2)\right]\hat{\phi} = 0 \tag{8}$$

The general solution of this by separation of variables gives

$$\hat{\phi}_{mn} = S_{mn}(-i\Omega,\eta)\, R_{mn}(-i\Omega, i\xi)\, \Theta_m(\theta) \tag{9}$$

where $\Theta_m(\theta) = \begin{Bmatrix} \cos m\theta \\ \sin m\theta \end{Bmatrix}$ and

$S_{mn}(-i\Omega, \eta)$ and $R_{mn}(-i\Omega, i\xi)$ represent angular and radial functions respectively. Putting the general solution Eq. (9) into the Helmholtz equation Eq. (8) leads to two ordinary differential equations.

$$\frac{d}{d\eta}\left[(1-\eta^2)\frac{d}{d\eta} S_{mn}(-i\Omega,\eta)\right] + \left[\lambda_{mn} + \Omega^2\eta^2 - \frac{m^2}{1-\eta^2}\right] S_{mn}(-i\Omega,\eta) = 0 \qquad (10)$$

$$\frac{d}{d\xi}\left[(\xi^2+1)\frac{d R_{mn}(-i\Omega,i\xi)}{d\xi}\right] - \left[\lambda_{mn} + \Omega^2\xi^2 - \frac{m^2}{\xi^2+1}\right] R_{mn}(-i\Omega,i\xi) = 0 \qquad (11)$$

where λ_{mn} is the separation constant and $m = 0,1,2,3\ldots\ldots$.

After mathematical calculations

$$\hat{\phi}_{mn} = A_{mn} S^{(1)}_{mn}(-i\Omega,\eta) R^{(4)}_{mn}(-i\Omega,i\xi)\, \Theta_m(\theta) \qquad (12)$$

(n-m) are even values

where A_{mn} = constant,

$$S_{mn}^{(1)}(-i\Omega, \eta) = \sum_{q=0}^{\infty} d_q^{mn}(-i\Omega)\, P^m_{m+q}(\eta)$$

is the oblate angular function of the first kind, and

$P^m_{m+q}(\eta)$

is the associated Legendre function of order m and degree (m+q).

From [ref. 16, pp. 17-23].

$$R^{(4)}_{mn}(-i\Omega, i\xi) = R^{(1)}_{mn}(-i\Omega, i\xi) - i\, R^{(2)}_{mn}(-i\Omega, i\xi).$$

In the development of Eq. (12) some of the possible solutions are rejected. The coefficient of the second independent solution of Eq (4), which is $S^{(2)}_{mn}(-i\Omega, \eta)$, is chosen to be zero, because at $\eta = 1$ this function goes infinity. The coefficient of the other independent solution combination of Eq. (11), which is $R^{(3)}_{mn}(-i\Omega, i\xi)$, is also chosen to be zero, because only outgoing waves are considered. $R^{(1)}_{mn}$ & $R^{(2)}_{mn}(-i\Omega, i\xi)$ can be calculated in power expansion given by Flammer [ref. 18]. Also by expanding Eq. (3) in oblate spheroidal coordinates yields

$$\vec{V} = \left[\vec{e}_\eta \sqrt{\frac{1-\eta^2}{\eta^2+\xi^2}} \frac{\partial \phi}{\partial \eta} + \vec{e}_\xi \sqrt{\frac{\xi^2+1}{\eta^2+\xi^2}} \frac{\partial \phi}{\partial \xi} + \vec{e}_\theta \frac{1}{\sqrt{(1-\eta^2)(\xi^2+1)}} \frac{\partial \phi}{\partial \theta} \right] \tag{13}$$

where $\vec{e}_\eta$, $\vec{e}_\xi$ and $\vec{e}_\theta$ are the unit vectors normal to the η, ξ and θ surfaces, respectively. The velocity component normal to the η surface is

$$V_\eta = -\sqrt{\frac{1-\eta^2}{\eta^2+\xi^2}} \frac{\partial \phi}{\partial \eta} \tag{14}$$

The baffle plane corresponds to $\eta = 0$. The rigid baffle condition requires that

$$V_\eta \Big|_{\eta=0} = 0 = \frac{\partial \phi}{\partial \eta} \Big|_{\eta=0} \tag{15}$$

Using Eq. (12) for Eq. (15) yields

$$\frac{d S^{(1)}_{mn}(-i\Omega, \eta)}{d\eta} \Big|_{\eta=0} = 0 \tag{16}$$

After using the power expansion for $S_{mn}^{(1)}(-i\Omega,\eta)$, odd values of (n-m) simply could not satisfy Eq. (16). Therefore odd values of (n-m) are rejected and hence it is found that Eq. (12) exists only for even values of (n-m).

Summation of all acceptable solutions yields

$$\hat{\phi} = \sum_{m=0}^{\infty} \sum_{n=m,m+2,m+4}^{\infty} A_{mn} S_{mn}^{(1)}(-i\Omega,\eta) R_{mn}^{(4)}(-i\Omega,i\xi)\,\Theta_m(\theta). \tag{17}$$

In the case of axisymmetric motion, m = 0 and then the far field solution becomes

$$\hat{\phi}_{of} = \frac{ie^{-i\Omega\xi}}{\Omega\xi} \sum_{n=0,2,4}^{\infty} (-1)^{n/2} A_{on} S_{on}^{(1)}(-i\Omega,\eta) \tag{18}$$

C. MINDLIN-TIMOSHENKO PLATE ANALYSIS [REFS 6 and 16]:

The dimensionless equations of motion in polar coordinates for simple harmonic excitation are:

$$K\left[\left(\nabla_{u,\theta}^2 \hat{\psi}_u - \frac{2}{u^2}\frac{\partial\hat{\psi}_\theta}{\partial\theta} - \frac{\hat{\psi}_u}{u^2}\right) + \frac{\partial\Phi}{\partial u} - \frac{k_T^2}{\gamma^2}\left(\hat{\psi}_u + \frac{\partial\hat{w}}{\partial u}\right) + \frac{c_o^2}{c_s^2}\Omega^2\hat{\psi}_u\right] = 0 \tag{19a}$$

$$K\left[\left(\nabla_{u,\theta}^2 + \frac{2}{u^2}\frac{\partial\hat{\psi}_u}{\partial\theta} - \frac{\hat{\psi}_\theta}{u^2}\right) + \frac{1}{u}\frac{\partial\Phi}{\partial\theta} - \frac{k_T^2}{\gamma^2}\left(\hat{\psi}_\theta + \frac{1}{u}\frac{\partial\hat{w}}{\partial\theta}\right) + \frac{c_o^2}{c_s^2}\Omega^2\hat{\psi}_\theta\right] = 0 \tag{19b}$$

$$\nabla^2_{u,\theta}\hat{w} + \Phi + \left[\frac{c_o}{c_s}\frac{\Omega}{k_T}\right]^2 \hat{w} = \frac{a}{h}\left[-\hat{q}(u,\theta) + \hat{p}_a(u,\theta)\right]\frac{1}{k_T^2 G}$$

(19c)

and $$\Phi = \frac{\partial\hat{\psi}_u}{\partial u} + \frac{\hat{\psi}_u}{u} + \left(\frac{1}{u}\right)\frac{\partial\hat{\psi}_\theta}{\partial\theta}$$

where $\Omega^2 = k^2a^2$

$\hat{w}(u,\theta)$ = dimensionless transverse displacement

$K = \dfrac{1-\nu}{2}$

$\nabla^2_{u,\theta} = \dfrac{\partial^2}{\partial u^2} + \dfrac{\partial}{u\,\partial u} + \dfrac{\partial^2}{u^2\partial\theta^2}$

$\gamma = h/a\sqrt{12}$

k_T^2 = empirical shear coefficient for plate.

$\hat{\psi}_u(u,\theta)$ and $\hat{\psi}_\theta(u,\theta)$ are the angles of rotation of the normal to the plate's middle surface a result of bending in the u and θ direction respectively.

$u = \dfrac{r}{a}$

$\hat{q}(u,\theta)$ = spatially distributed harmonic external load

$\hat{p}_a(u,\theta)$ = reaction of the fluid pressure to $\hat{q}(u,\theta)$

$\hat{\psi}_u = \hat{\psi}_r$

For $\hat{q} = 0$ (free vibration) solutions to Eq. (19) are

$$\hat{\psi}_u = (\sigma_1 - 1)\frac{\partial\hat{w}_1}{\partial u} + (\sigma_2 - 1)\frac{\partial\hat{w}_2}{\partial u} + \frac{1}{u}\frac{\partial\hat{H}}{\partial\theta}$$

$$\hat{\psi}_\theta = (\sigma_1 - 1)\frac{1}{u}\frac{\partial \hat{w}_1}{\partial \theta} + (\sigma_2 - 1)\frac{1}{u}\frac{\partial \hat{w}_2}{\partial \theta} - \frac{\partial \hat{H}}{\partial \theta} \qquad (20)$$

$$\hat{w} = \hat{w}_1 + \hat{w}_2 \; ,$$

If $\hat{w}_1$, $\hat{w}_2$ and $\hat{H}$ satisfy

$$(\nabla^2_{u,\theta} + \alpha_1^2)\,\hat{w} = 0$$

$$(\nabla^2_{u,\theta} + \alpha_2^2)\,\hat{w} = 0$$

$$(\nabla^2_{u,\theta} + \alpha_3^2)\,\hat{H} = 0 \qquad (21)$$

where

$$(\alpha_1^2, \alpha_2^2) = \left(\frac{c_o}{c_s}\right)^2 \frac{\Omega^2}{2}\left\{\left(\frac{1}{k_T^2} + K\right) \pm \sqrt{\left(\frac{1}{k_T^2} - K\right) + \frac{4K}{\left(\gamma \frac{c_o}{c_s}\Omega\right)^2}}\right.$$

$$(\sigma_1, \sigma_2) = \frac{(\alpha_2^2, \alpha_1^2)}{\alpha_3^2 K} \qquad (21a)$$

$$\alpha_3^2 = \left(\frac{c_o}{c_s}\right)^2 \Omega^2 - \frac{k_T^2}{\gamma^2}$$

Solutions to Eq. (21) under the condition that they will be finite at u = 0 are:

$$\left.\begin{aligned}
\hat{w}_1 &= \sum_{m=0}^{\infty} B_{1m} J_m(\alpha_1 u)\,\Theta_m \\
\hat{w}_2 &= \sum_{m=0}^{\infty} B_{2m} J_m(\alpha_2 u)\,\Theta_m \\
\hat{H} &= \sum_{m=0}^{\infty} B_{3m} J_m(\alpha_3 u)\,\Theta'_m
\end{aligned}\right\} \quad \Omega^2 > \frac{k_T^2}{\gamma^2 \frac{c_o^2}{c_s^2}} \qquad (22)$$

and

$$\left.\begin{aligned}
\hat{w}_1 &= \sum_{m=0}^{\infty} B_{1m} J_m(\alpha_1 u)\,\Theta_m \\
\hat{w}_2 &= \sum_{m=0}^{\infty} B_{2m} I_m(|\alpha_2| u)\,\Theta_m \\
\hat{H} &= \sum_{m=0}^{\infty} B_{3m} I_m(|\alpha_3| u)\,\Theta_m
\end{aligned}\right\} \quad \Omega^2 < \frac{k_T^2}{\gamma^2 \frac{c_o^2}{c_s^2}} \qquad (23)$$

Since $J_m(ix) = i^m I_m(x)$ only Eq. (22) can be used without losing generality.

Boundary conditions for a clamped plate are

$$\hat{w}(1,\theta) = 0$$
$$\hat{\psi}_u(1,\theta) = 0$$
$$\hat{\psi}_\theta(1,\theta) = 0 \qquad (24)$$

Combining EQ. (20) and (22) yields

$$\hat{\psi}_u(u,\theta) = \sum_{m=0}^{\infty} \left\{ (\sigma_1 - 1)\frac{dJ_m(\alpha_1 u)}{du} B_{1m} + (\sigma_2 - 1)\frac{dJ_m(\alpha_2 u)}{du} B_{2m} - \frac{m^2}{u} J_m(\alpha_3 u) B_{3m} \right\} \Theta_m(\theta)$$

$$\hat{\psi}_\theta(u,\theta) = \sum_{m=0}^{\infty} \left\{ (\sigma_1 - 1)\frac{J_m(\alpha_1 u)}{u} B_{1m} + (\sigma_2 - 1)\frac{J_m(\alpha_2 u)}{u} B_{2m} - \frac{dJ_m(\alpha_3 u)}{du} B_{3m} \right\} \Theta'_m(\theta)$$

$$\hat{w}(u,\theta) = \sum_{m=0}^{\infty} \left\{ J_m(\alpha_1 u) B_{1m} + J_m(\alpha_2 u) B_{2m} \right\} \Theta_m(\theta) \qquad (25)$$

where $\Theta'_m = \dfrac{d\Theta_m}{d\theta}$

Applying the boundary conditions, Eqs. (24) to (25) and the requirement that solutions will be non-trivial the characteristic equations are obtained

$$\left. m^2(\sigma_2 - \sigma_1) J_m(\alpha_1) J_m(\alpha_2) J_m(\alpha_3) + \left\{ J'_m(\alpha_3 u)\left[(\sigma_1 - 1) J_m(\alpha_2 u) J'_m(\alpha_1 u) - (\sigma_2 - 1) J_m(\alpha_2 u) J'_m(\alpha_1 u) \right] \right\} \right|_{u=1} = 0 \qquad (26)$$

where m = 0,1,2, ... and derivatives are w.r.t. u. The dimensionless frequencies Ω_{mj}, m = 0,1,2, ...; j = 1, 2, ..., for which Eq. (26) is satisfied are the eigenfrequencies to which there are corresponding values α_{1mj}, α_{2mj}, α_{3mj}, σ_{1mj} and σ_{2mj}. The corresponding eigenfunctions are

$$\hat{w}_{mj} = W_{mj}(u)\,\Theta_m(\theta)$$

$$= \left\{ J_m(\alpha_{1mj}) - \frac{J_m(\alpha_{1mj})}{J_m(\alpha_{2mj})} J_m(\alpha_{2mj}u) \right\} \Theta_m(\theta) \qquad \text{(a)}$$

$m = 0, 1, 2, \ldots; \; j = 1, 2, \ldots .$

$$\hat{\psi}_{u,mj} = \Psi_{u,mj}(u)\,\Theta_m(\theta)$$

$$= \left\{ (\sigma_{1mj}-1)\left[\frac{m}{u} J_m(\alpha_{1mj}u) - \alpha_{1mj} J_{m+1}(\alpha_{1mj}u)\right] - (\sigma_{2mj}-1)\frac{J_m(\alpha_{1mj})}{J_m(\alpha_{2mj})} \right.$$

$$\times \left[\frac{m}{u} J_m(\alpha_{2mj}u) - \alpha_{2mj} J_{m+1}(\alpha_{2mj}u)\right] \qquad \text{(27)}$$

$$\left. - \frac{(\sigma_{1mj}-\sigma_{2mj})(m^2/u) J_m(\alpha_{1mj}) J_m(\alpha_{3mj}u)}{m J_m(\alpha_{3mj}) - \alpha_{3mj} J_{m+1}(\alpha_{3mj})} \right\} \Theta_m(\theta) \qquad \text{(b)}$$

and $$\hat{\psi}_{\theta,mj} = \Psi(u)\,\Theta_m(\theta) = \left\{ (\sigma_{1mj}-1)\frac{J_m(\alpha_{1mj}u)}{u} - (\sigma_{2mj}-1)\frac{J_m(\alpha_{1mj})}{J_m(\alpha_{2mj})}\frac{J_m(\alpha_{2mj}u)}{u} \right.$$

$$\left. - \frac{(\sigma_{1mj}-\sigma_{2mj}) J_m(\alpha_{1mj}) \left[\frac{m}{u} J_m(\alpha_{3mj}u) - \alpha_{3mj} J_{m+1}(\alpha_{3mj})\right]}{m J_m(\alpha_{3mj}) - \alpha_{3mj} J_{m+1}(\alpha_{3mj})} \right\} \Theta'_m(\theta) \qquad \text{(c)}$$

$m = 0, 1, 2, \ldots ; \; j = 1, 2, \ldots .$

In the case of axisymmetric motion, m = 0, Eq. (26) takes the form (eliminating the derivatives)

$$\alpha_3 J_1(\alpha_3)\left[(\sigma_1-1)\alpha_1 J_0(\alpha_2) J_1(\alpha_1) - (\sigma_2-1)\alpha_2 J_0(\alpha_2)\right] = 0 \qquad \text{(28)}$$

and the eigenfunctions

$$\hat{w}_j = J_0(\alpha_{1j} u) - \frac{J_0(\alpha_{1j})}{J_0(\alpha_{2j})} J_0(\alpha_{2j} u)$$

$$\hat{\psi}_{u,j} = -(\sigma_{1j} - 1)\alpha_{1j} J_1(\alpha_{1j} u) + (\sigma_{2j} - 1)\frac{J_0(\alpha_{1j})}{J_0(\alpha_{2j})}\alpha_{2j} J_1(\alpha_{2j} u)$$

$$\hat{\psi}_{\theta,j} = 0 \tag{29}$$

because $\Theta_m'(\theta) = 0$. Thus, there is no coupling between $\hat{w}$ or $\hat{\psi}_u$ and $\hat{\psi}_\theta$ in axisymmetric motion.

There can be rotations $\hat{\psi}_\theta \neq 0$ that are axisymmetric, but they will be independent of $\hat{w}$ and $\hat{\psi}_u$.

The characteristic equation for independent axisymmetric $\hat{\psi}_\theta$ motion is obtained from Eq. (28) by setting the factor

$$\alpha_3 J_1(\alpha_3) = 0. \tag{30}$$

When the roots of Eq. (30) are inserted into α_3^2 the Ω values are obtained for axisymmetric $\hat{\psi}_\theta$ motion. The applied force is normal to the plate here and these modes are of no interest. This can be seen easily after calculating a value for $w^2 = \left\{1 + \frac{\alpha_3^2}{\pi^2 (a/h)^2}\right\}(\pi c_s/h)^2$.

For a thick steel plate, for example, $\frac{h}{a} = 0.2$, $\Omega > 37$ and for a thin plate Ω would be even greater.

Finally, Eq. (28) for this problem takes the form

$$(\sigma_1 - 1)\alpha_1 J_0(\alpha_2) J_1(\alpha_1) - (\sigma_2 - 1)\alpha_2 J_0(\alpha_1) J_1(\alpha_2) = 0 \tag{31}$$

By using Eq. (21a) the roots Ω_j of this equation can be obtained. Symmetric eigenfrequencies for $\frac{h}{a} = 0.04$ and $\frac{h}{a} = 0.2$ are given in Table I of Ref. 16.

$$\alpha^2 < 0 \quad \text{when} \quad \Omega^2 < \frac{12 k_T^2 (a/h)^2}{(c_o/c_s)^2} \tag{32}$$

Then calling

$\beta^2 = -\alpha^2$ when $\alpha_2{}^2 < 0$, the characteristic Eq. (31) for axisymmetric motion becomes

$$(\sigma_1 - 1)\alpha_1 \, I_0(\beta) \, J_1(\alpha_1) + (\sigma_2 - 1)\beta \, J_0(\alpha_1) \, I_1(\beta) = 0 \tag{33}$$

and corresponding eigenfunctions are

$$\hat{w}_j = J_0(\alpha_{1j} u) - \frac{J_0(\alpha_{1j})}{I_0(\beta_j)} I_0(\beta_j u)$$

$$\hat{\psi}_{uj} = -(\sigma_{1j} - 1)\alpha_{1j} \, J_1(\alpha_{1j} u) - (\sigma_2 - 1) \frac{J_0(\alpha_{1j})}{I_0(\beta_j)} \beta_j I_1(\beta_j u) \tag{34}$$

D. COUPLING OF ACOUSTIC FLUID AND PLATE

The following developments are also taken from Alper and Magrab [6]. On the $\xi = 0$ surface, which represents the plate, boundary conditions are: The normal fluid velocity and the acoustic pressure on the fluid are equal to the transverse plate velocity and the pressure on the boundary of the plate, respectively.

Using Eq. (30),

$$V_\xi \Big|_{\xi=0} = -\sqrt{\frac{\xi^2+1}{\eta^2+\xi^2}} \, \frac{\partial \phi}{\partial \xi}\Big|_{\xi=0} = \frac{1}{\eta} \frac{\partial \phi}{\partial \xi}\Big|_{\xi=0} \tag{35}$$

$$V_z = -\frac{1}{\eta} \frac{\partial \phi}{\partial \xi}\Big|_{\xi=0} = i \, \hat{w} \tag{36}$$

The external force (applied force per unit area plus acoustic pressure at the plate boundary of fluid) is given as

$$\hat{q}(u,\theta) = \hat{f}(u,\theta) - i \frac{\rho_0}{\rho} \frac{c_0^2}{c_s^2} \Omega^2 \hat{\phi}(\eta, 0, \theta) \tag{37}$$

Hence, if Eq. (37) is substituted into Eq. (19c), then, use of Eqs. (19) and (36) couples the motion of the plate and the acoustic fluid, so that solutions for $\hat{\phi}$ and $\hat{w}$ can be found under the specified force distribution $\hat{f}$. When $q = 0$ and $\Omega = \Omega_{mj}$, the eigenfunctions ($\hat{w}_{mj}$, $\hat{w}_{u,mj}$, $\hat{\psi}_{\theta,mj}$) satisfying combined Eq. (19) and Eq. (37) could be found.

Let the solution for the plate motion be expressed as expansions in its eigenfunctions:

$$\hat{w} = \sum_{m=0}^{\infty} \sum_{j=1}^{\infty} D_{mj} \hat{w}_{mj}$$

$$\hat{\psi}_u = \sum_{m=0}^{\infty} \sum_{j=1}^{\infty} D_{mj} \hat{\psi}_{u,mj}$$

$$\hat{\psi}_\theta = \sum_{m=0}^{\infty} \sum_{j=1}^{\infty} D_{mj} \psi_{\theta,mj} \tag{38}$$

Putting Eq. (38) into the linear and homogenous combination of Eq. (19) and (37) there is obtained:

$$\left(\frac{c_0}{c_s}\right)^2 \sum_{m=0}^{\infty} \sum_{j=1}^{\infty} D_{mj} (\Omega^2 - \Omega_{mj}^2) \hat{\psi}_{u,mj} = 0$$

$$\left(\frac{c_0}{c_s}\right)^2 \sum_{m=0}^{\infty} \sum_{j=1}^{\infty} D_{mj} (\Omega^2 - \Omega_{mj}^2) \hat{\psi}_{\theta,mj} = 0$$

$$\left(\frac{c_0}{c_s}\right)^2 \sum_{m=0}^{\infty} \sum_{j=1}^{\infty} D_{mj} (\Omega^2 - \Omega_{mj}^2) \hat{w}_{mj} = -\frac{a}{h} \hat{q} \tag{39}$$

The orthogonality condition for a clamped circular Mindlin-Timoshenko plate is defined as

$$\int_0^{2\pi} \int_0^1 \left[\gamma^2 \left\{ \hat{\psi}_{u,mj} \hat{\psi}_{u,nk} + \hat{\psi}_{\theta,mj} \hat{\psi}_{\theta,nk} \right\} + \hat{w}_{mj} \hat{w}_{nk} \right] u\,du\,d\theta$$

$$= \delta_{mn} \delta_{kj} (1 - \delta_{0m}) \pi N_{mj} \tag{40}$$

where δ_{ij} is the Kronecker delta and

$$N_{mj} = \int_0^1 \left[\gamma^2\left\{\Psi_{u,mj} + m^2\Psi_{\theta,mj}\right\} + W_{mj}^2\right] u \cdot du \qquad (41)$$

Using Eq. (27a) and performing appropriate integrations

$$N_{mj} = G_m(\alpha_{1mj}) - \frac{\delta_{mj}}{\alpha_{1mj}^2 - \alpha_{2mj}^2} H_m(\alpha_{1mj}, \alpha_{2mj}) + \delta_{2mj}^2 G_m(\alpha_{2mj})$$
$$+ \gamma^2 \Big\{ m\Big[\beta_{1mj} J_m(\alpha_{1mj}) - \beta_{2mj} J_m(\alpha_{2mj}) - \frac{\beta_{3mj}}{m} J_m(\alpha_{3mj})\Big]^2$$
$$+ \sum_{i=1}^{2} \beta_{imj}^2 \alpha_{imj}^2 G_{m+1}(\alpha_{imj}) + \beta_{3mj} G_{m+1}(\alpha_{3mj}) \alpha_{3mj}^2$$
$$- \frac{\beta_{1mj}\beta_{2mj}\alpha_{1mj}\alpha_{2mj}}{\alpha_{1mj}^2 - \alpha_{2mj}^2} H_{m+1}(\alpha_{1mj}, \alpha_{2mj}) \Big\}, \quad \text{for } \Omega^2 > \frac{k_T^2}{\left(\gamma \frac{c_o}{c_s}\right)^2}$$

$$N_{mj} = G_m(\alpha_{1mj}) - \frac{\hat{\delta}_{mj}}{\alpha_{1mj}^2 + |\alpha_{2mj}|^2} \hat{H}_m(\alpha_{1mj}, \alpha_{2mj}) + \hat{\delta}_{mj}^2 \hat{G}_m(\alpha_{2mj})$$
$$+ \gamma^2 \Big\{ m\Big[\beta_{1mj} J_m(\alpha_{1mj}) - \beta_{2mj} I_m(|\alpha_{2mj}|) - \hat{\beta}_{3mj} \frac{I_m(|\alpha_{3mj}|)}{m}\Big]^2$$
$$+ \beta_{1mj}^2 \alpha_{1mj}^2 G_{m+1}(\alpha_{1mj}) + \hat{\beta}_2^2 |\alpha_{2mj}|^2 \hat{G}_{m+1}(\alpha_{2mj}) + \frac{\beta_{3mj}}{m^2} |\alpha_{3mj}|^2 G_{m+1}(\alpha_{3mj})$$
$$+ \frac{\beta_{3mj}\hat{\beta}_{2mj}\alpha_{1mj}|\alpha_{2mj}|}{\alpha_{1mj}^2 + |\alpha_{2mj}|^2} \hat{H}_{m+1}(\alpha_{1mj}, \alpha_{2mj}) \Big\},$$

$$\text{for } \Omega^2 < \frac{k_T^2}{\left(\gamma \frac{c_o}{c_s}\right)^2}$$

in which

$$\gamma^2 = \frac{1}{2}\left(\frac{h}{a}\right)^2$$

$$\delta_{mj} = \frac{J_m(\alpha_{1mj})}{J_m(\alpha_{2mj})}$$

$$\hat{\delta}_{mj} = \frac{J_m(\alpha_{1mj})}{I_m(|\alpha_{2mj}|)}$$

$$\beta_{1mj} = (\sigma_{1mj} - 1)$$

$$\beta_{2mj} = (\sigma_{2mj} - 1)$$

$$\hat{\beta}_{2mj} = (\sigma_{2mj} - 1)\,\hat{\delta}_{mj}$$

$$\beta_{3mj} = \frac{(\sigma_{1mj} - \sigma_{2mj})\, m^2 J_m(\alpha_{1mj})}{m J_m(\alpha_{3mj}) - \alpha_{3mj} J_{m+1}(\alpha_{3mj})}$$

$$\hat{\beta}_{3mj} = \frac{(\sigma_{1mj} - \sigma_{2mj})\, m^2 J_m(\alpha_{1mj})}{m I_m(|\alpha_{3mj}|) + |\alpha_{3mj}|\, I_{m+1}(|\alpha_{3mj}|)}$$

$$G_m(x) = \left[J_m^2(x) - J_{m-1}(x)\, J_{m+1}(x)\right]\cdot\frac{1}{2}$$

$$\hat{G}_m(x) = \left[I_m^2(x) - I_{m+1}(x)\, I_{m-1}(|x|)\right]\frac{1}{2}$$

$$H_m(x_1, x_2) = \left[x_1 J_m(x_2)\, J_{m+1}(x_1) - x_2 J_m(x_1)\, J_{m+1}(x_2)\right].2$$

$$\hat{H}_m(x_1, x_2) = \left[x_1 J_m(|x_2|)\, J_{m+1}(x_1) + |x_2|\, J_m(x_1)\, I_{m+1}(|x_2|)\right].2$$

For the axisymmetric case, m = 0.

Multiplying the first of Eq. (39) by $\gamma^2 \hat{\psi}_{u,mj} u\,du\,d\theta$, the second by $\gamma^2 \psi_{\theta,mj} u\,du\,d\theta$, and the third by $\hat{w}_{mj}\, u\,du\,d\theta$, adding the three equations and integrating over $0 \leq \theta \leq 2\pi$, $0 \leq u \leq 1$ and using the orthogonality condition Eq. (40) leads to

$$\left(\frac{c_o}{c_s}\right)^2 D_{mj}(1+\delta_{om})\pi N_{mj}\left(\Omega^2-\Omega^2_{mj}\right) = -\frac{a}{h}\int_0^{2\pi}\int_0^1 \hat{q}\,\hat{w}_{mj}\, u\,du\,d\theta \qquad (42)$$

m = 0,1,2,...; j = 1,2 .

By expressing $f(u,\theta)$ in a Fourier series $\hat{f}(u,\theta) = \sum_{m=0}^{\infty} F_m(u)\,\Theta_m(\theta)$.

$$F_m(u) = \frac{1}{(1+\delta_{om})\pi}\int_0^{2\pi} \hat{f}(u,\theta)\,\Theta_m(\theta)\,d\theta \qquad (43)$$

and using Eq. (12) to express $\hat{\phi}$ there results

$$\hat{q} = \sum_{m=0}^{\infty} F_m(u)\,\Theta_m(\theta) - i\frac{\rho_o}{\rho}\left(\frac{c_o}{c_s}\Omega\right)^2 \sum_{m=0}^{\infty}\sum_{n=m,m+2,m+4}^{\infty} A_{mn} S^{(1)}_{mn}(-i\Omega,\eta)\, R^{(4)}_{mn}(-i\Omega,0)\,\Theta_m(\theta) \qquad (44)$$

Combining Eq. (42), (43) and (44) and performing integration with respect to θ yields

$$\left(\frac{c_o}{c_s}\right)^2 D_{mt} N_{mt}\left(\Omega^2-\Omega^2_{mt}\right) = -\frac{a}{h}\left[e_{mt} - i\frac{\rho_o}{\rho}\left(\frac{c_o}{c_s}\Omega\right)^2 \sum_{n=m,m+2,m+4}^{\infty} A_{mn} R^{(4)}_{mn}(-i\Omega,0)\, g_{m,nt}\right] \qquad (45)$$

m = 0,1,2,...; t = 1,2, ...

where $$g_{m,nj} = \int_0^1 W_{mj}(u)\, S_{mn}^{(1)}(-i\Omega,\eta)\, u\, du$$

and $$e_{mj} = \int_0^1 F_m(u)\, W_{mj}(u)\, u \cdot du \qquad . \qquad (46)$$

Expressions for $g_{m,nj}$ are

$$g_{m,nj} = \begin{cases} g_{mnj1} - \delta_{mj}\, g_{mnj2}\ ; \ \alpha_{2mj}^2 > 0 \\ g_{mnj1} - \hat{\delta}_{mj}\, g_{mnj2}\ ; \ \alpha_{2mj} < 0 \end{cases} \qquad (47)$$

where
$$g_{mnj\epsilon} = \frac{1}{2}\sum_{k=0}^{\infty} a_{2k}^{mn} \sum_{q=0}^{\infty} \frac{(-1)^q}{q!\,(m+q)!\,(k+m+q+1)} \left(\frac{\alpha_{\epsilon mj}}{2}\right)^{2q+m}$$

ϵ = 1,2 and

$$g_{mnj2} = \frac{1}{2}\sum_{k=0}^{\infty} a_{2k}^{mn} \sum_{q=0}^{\infty} \frac{1}{q!\,(m+q)!\,(k+m+q+1)} \left(\frac{|\alpha_{2mj}|}{2}\right)^{2q+m}$$

For the axisymmetric case m = 0.

Combining Eq. (12) and (36) and using the first of Eq. (38) for w yields

$$i\sum_{j=1}^{\infty} D_{mj} W_{mj}(u) = -\frac{1}{\eta}\sum_{n=m,m+2,m+4}^{\infty} A_{mn}\, S_{mn}^{(1)}(-i\Omega,\eta)\, \frac{dR_{mn}^{(4)}}{d\xi}(-i\Omega, i\xi)\bigg|_{\xi=0}$$

(48)

The functions $S_{mn}^{(1)}(-i\Omega,\eta)$, (n-m) even, are orthogonal on the interval $0 \leq \eta \leq 1$. The orthogonality condition is

$$\int_0^1 S_{mn}^{(1)}(-i\Omega,\eta)\, S_{mn'}^{(1)}(-i\Omega,\eta) = T_{mn}\,\delta_{nn'} \tag{49}$$

(n-m) even; m = 0,1,2, ...

where

$$T_{mn} = \int_0^1 \left[S_{mn}^{(1)}(-i\Omega,\eta)\right]^2 d\eta = \sum_{q=0,2,4}^{\infty} \frac{(q+2m)!\left[d_q^{mn}(-i\Omega)\right]^2}{(2q+2m+1)\,q!} \tag{50}$$

(n-m) even.

Multiplying Eq. (48) by $S_{mn'}^{(1)}(-i\Omega,\eta)\eta\, d\eta$, integrating over the interval $0 \leq \eta \leq 1$, solving for A_{mn} and using the definition Eq. (46) yields:

$$A_{mn} = \frac{-i}{T_{mn}\, R_{mn}^{(4)\prime}(-i\Omega,0)} \sum_{j=1}^{\infty} D_{mj}\, g_{m,nj} \tag{51}$$

m = 0,1,2, ... ; n = m, m+2, m + 4.

Putting Eq. (51) into Eq. (45)

$$\frac{\rho_0}{\rho}\left(\frac{c_0}{c_s}\Omega\right)^2 \sum_{j=1}^{\infty}\left(\sum_{\substack{n=m,\\ m+2,m+4}}^{\infty} \frac{R_{mn}^{(4)}(-i\Omega,0)}{T_{mn}\, R_{mn}^{(4)\prime}(-i\Omega,0)}\, g_{m,nj}\, g_{m,nt}\right) D_{mj} \tag{52}$$

$$-\frac{h}{a}\left(\frac{c_0}{c_s}\right)^2 N_{mt}\left(\Omega^2-\Omega_{mt}^2\right) D_{mt} = e_{mt}$$

m = 0, 1, 2, ...; t = 1, 2, ...

This represents an infinite number of sets of infinitely long linear non-homogenous equations in the coefficients D_{mj}. For each value of m, there is a set of equations, t = 1,2, ...

The infinite set of equations, yields solutions for D_{mj}; j = 1, 2, ... which, when put Eq. (38) gives the displacements of the plate and, when put into Eq. (51), gives the coefficients A_{mn}. The coefficients A_{mn} are then used to determine the m^{th} harmonic of the potential field using Eq. (12) and thereby the m^{th} harmonic of the pressure using Eq. (5).

Instead of using an infinite set of equations there is a necessity to use truncation with a resulting limitation on accuracy (N = number of terms in the truncated solutions). Alper [16] found that for the far field pressure using N = 11 for thin ($\frac{h}{a}$ = 0.04) and N= 16 for thick ($\frac{h}{a}$ = 0.2) plates gives solutions which are accurate to within 0.2 percent.

Alper calculated patterns for the first three resonant frequencies for thin ($\frac{h}{a}$ = 0.04) and thick ($\frac{h}{a}$ = 0.2) steel plates. These are presented in Figures 3 and 4. Calculated pressures in the far field on the plate axis as a function of dimensionless frequency for thin and thick plates are presented in Figures 5 and 6. Physical properties for steel plates with water as the fluid medium are: $k_T^2 = 0.86$, $\nu = 0.3$, $\frac{c_o}{c_s} = 0.42$, $\rho_o/\rho = 0.132$ and $\rho_o = 1$.

As a result it was decided that the best choice for building a transducer to meet the desired specifications would be a thick plate. A sketch illustrating the form of plate displacement for the first ($\Omega = 1.9$) and second ($\Omega = 6.9$) symmetric modes is presented in Figure 7.

The computer programs used for the theoretical calculations, which were designed for a CDC 6400 computer, were obtained from

Dr. Alper. These have been modified for the CDC 6500 and are listed in Appendix A. A shortage of time prohibited actual use of these modified programs for design work.

III. EXPERIMENTAL PROCEDURES

An experimental test of the calculations of Alper and Magrab was conducted. A small, clamped edge plate transducer was constructed with dimensions which corresponded to the published calculated results for the thick plate, as shown in Figure 8. The material used is steel. The ratio of plate thickness to radius, h/a, was chosen to be 0.2. The thickness was chosen so that the second, in-fluid resonance mode would be about 75kHz. This corresponds to a value of the parameter $\Omega = 6.9$. Exterior dimensions were determined by the positioning and mounting hole on the cylindrically-shaped torpedo extension section, which served as the acoustic baffle for the transducer. The height of the outer cylindrical section at the rear was chosen to be about 3/4 wave length in order to create a high acoustic impedance for the plate edge in the neighborhood of 75kHz.

The driver for this transducer consisted of a piezoelectric ceramic longitudinal vibrator, similar to the sketch shown in Figure 9. The ceramic, a lead-zirconate titanate type, consisted of two axially polarized circular discs with a hole in the center. Masses on the ends and a clamping screw were constructed and their dimensions were selected to make the half-wavelength (free-free) longitudinal resonance to occur near 75kHz. A silicone grease was used between joints to ensure good acoustic coupling.

In order to provide a more nearly point source of excitation, the area of contact of the driver with the plate was reduced by the use of a small nut on the clamping screw between the driver and the plate. Later, measurements were made with the full face of the vibrator clamped to the plate.

Resonance frequencies of the completed transducer assembly were determined using measurements of the electrical admittance of the piezoelectric elements. A Dranetz Impedance-Admittance meter was used for this purpose. Typical graphical results of conductance versus frequency are shown in Figures 12 through 14.

The construction of the longitudinal vibrator used in the acoustic measurements prohibited the obtaining of a satisfactory isolation of the electrodes from electrical ground of the system, needed for making electrical admittance measurements with the unit in water. Therefore, resonance frequencies were not measured in water. However, measurements were conducted of resonances of the driver with the transducer in air and in water using a different, isolated driver. This driver was a radially polarized cylinder of barium titanate, 2.54 cm long by 1.27 cm outside diameter. It was clamped to the plate using a screw and an end mass. Although the free-free half wave length resonance frequency for this element differed by several kilohertz from that of the other driver, the observed resonances of the combined systems differed only slightly. The change in resonance frequency caused by the immersion in water was within the uncertainty of frequency setting. The effects of radiation damping on the sharpness resonance was noted.

The acoustical measurements consisted of measuring the far field acoustic pressure as a function of angle. The arrangement of apparatus is shown in schematic form in Figures 10-11. A pulse method was used. Although the walls and floor of the water tanks are essentially anechoic, the reflection from the water-air surface can be significant, necessitating the use of a box-car integrator. The gate of the box-car integrator was adjusted so that only the sound wave traveling by a direct path from the source to the hydrophone was measured.

The cylindrical baffle consists of an aluminum alloy casting about 26.25 cm long and 32.4 cm outside diameter. Plastic end caps were used. The wall thickness is not uniform but is about 2.2 cm. A sketch is shown in Figure 12.

The transducer is bolted into a hole which is located as shown. Lead weights were added inside the cylinder to make the assembly negatively buoyant.

The rotation system could be arranged to measure the radiation pattern about either the longitudinal axis of the cylinder or the perpendicular axis. Measurements about both axes were made. The mechanical drive used to rotate the transducer includes a potentiometer on the gear train which produces a D.C. voltage proportional to angle of rotation. This voltage is applied to the x axis of x-y plotter. The calibrated LC-10 hydrophone used as a receiver and the transducer were separated by a distance of 1 m with the hydrophone and the center of the transducer at a depth of 1.92 . The

output of the hydrophone was amplified, rectified by the envelope detector and fed to the box-car integrator. In order to eliminate the effects of surface reflections, and minimize the effects of standing waves in the tank a pulsed signal was used. The box-car integrator, gated to the direct path pulse produces a D.C. voltage that is proportional to the average amplitude of the received pulse envelope. This D.C. voltage is fed to the logarithmic converter which generates the ordinate of the beam pattern. The attenuator is used to calibrate the y axis to provide a decibel scale. It is needed because of the nonlinearity of the envelope detector.

Each radiation pattern was calibrated by adjusting the x-y recorder and driving voltage to obtain at least half scale reading on the integrator, and then by the means of attenuator, decibel increments on the y scale were marked.

Results of radiation patterns about the perpendicular axis and the cylindrical axis are shown in Figures 20 and 21 and Figures 22 and 23, respectively. These were made with a small area of coupling between the driver and the plate. Then, with the small brass nut removed from the coupling between driver and plate the area of contact was increased to that of the disk at the end of the driver. Rotation was about the vertical axis. Results are shown in Figures 24 through 26.

The box-car integrator gate width was suitably maintained to ensure that the integration would be done at steady state region of received signal.

After some experimental work was done it was noticed that bubbles produced in the water greatly affect the results and

reduce loading effects of the fluid. Hence to prevent this effect a long brush was used for both hydrophone and transducer. Before each pattern was recorded, the source and receiver were brushed off in order that no effects due to bubbles would occur.

A second series of measurements using the composite driver with small coupling area was conducted. The objective was two-fold. The first was to identify the modes of vibration associated with the several resonance frequencies noted previously and, particularly, to determine which were the first and second modes. The second objective was to recheck the results of earlier measurements.

For the driver alone (free-free) conductance plotted as a function of frequency is shown in Fig. 13. Two resonances are noted. It seemed clear from observing the sensitivity to clamping provided by grasping it with one's fingers that the uppermost resonance involved flexural plate resonance of the lower and mass. The lower resonance appeared to be the usual free-free mode of vibration.

When this driver is mounted on the transducer, a number of resonances can be observed. A plot of driver conductance as a function of frequency is presented in Figures 14 and 15, for the transducer alone and for the case where the transducer is mounted in the cylindrical baffle.

A small capacitive displacement probe was used to measure the relative displacement amplitude at various positions on the outer face of the transducer. The probe consisted essentially of an 8 mm. diameter flat electrode which could be

positioned very close to the plate (about 0.1 mm). This electrode and the plate itself formed an electrical capacitor. The electrical circuit provided polarization potential for this capacitor and measured the amplitude of the alternating potential caused by changing capacitance when the plate vibrated. Although the probe measures the average effect of change in capacitance over a distance of 6 or 8 mm, it was sufficiently sensitive to get a reasonable estimate of the relative amplitude of plate motion as a function of distance from the center of the disk. A schematic representation of the displacement measurement apparatus is shown in Figure 16.

A plot of the relative amplitudes is presented in Figures 17 and 18 for each of the transducer resonances noted previously. The motion for the 01 and 02 modes was re-confirmed after the transducer was clamped in the cylindrical baffle.

IV. DISCUSSION OF RESULTS

A. EFFECTS OF AXIS OF ROTATION ON PATTERN

Radiation patterns were obtained for the same transducer but with different axis of rotation, one parallel to the cylinder axis and the other perpendicular to the cylinder axis. The results for two such measurements are presented in Figures 20-21 and 22-23.

It is concluded that although some differences between experimental patterns exist, these do not obscure the basic features of the radiation pattern to be used for comparison between theory and experiment. For purposes of convenience, all remaining patterns were made by rotating the baffle about its perpendicular axis.

B. EFFECTS OF VARYING AREA OF CONTACT BETWEEN DRIVER AND PLATE

Some radiation pattern measurements were made in which the size of the contact area between the longitudinal vibrates was increased from about 5 mm diameter to the diameter of the driver end mass, 17 mm. Since the diameter of the driver end mass is comparable to the dimension of the first nodal circle for the 02 mode of the plate, it should be expected that the details of the displacement of the plate at the higher frequencies would not be a good approximation to that assumed for the point drive case. The radiation patterns made at high frequencies using this larger area of coupling were very complicated and difficult to interpret and they are not included here. The pattern at

low frequencies made with the larger area of coupling were not significantly different from those using the small coupling area. These are presented in Figures 24 through 26.

C. IDENTIFICATION OF MODES OF VIBRATION OF THE PLATE

The existence of a number of resonances in the neighborhood of frequencies calculated for the 01 and 02 modes of the transducer plate appear to be due to the frequency dependent impedance of the various parts attached to the plate. The driver element is one such attachment. However, the boundary conditions at the plate edge are probably more important. The massive cylinder at the rear of the plate was intended to provide a high mechanical impedance at the plate edge to simulate the clamped edge condition. An outer flange of thickness comparable to (but larger than) that of the plate itself was needed to secure the transducer in the baffle. There were several modes of vibration which involved significant vibration of the outer flange. Some of these modes were damped where the transducer was clamped into the baffle. It is concluded that the resonances at 31 and 63.9 kHz were associated with the clamped edge plate modes having mode number 01 and 02, respectively.

D. RADIATION PATTERNS

The comparison between the radiation patterns calculated by Alper [16] and those measured in these experiments must take into account several factors which can give rise to differences.

First, the assumed clamped edge boundary condition is only approximated in the tests.

Second, the baffle used is cylindrical in shape and is therefore neither infinite nor plane, so the assumption of the theory of an infinite plane baffle is not well approximated even though the diameter of the cylinder is about 7.5 times the diameter of the plate.

Third, the fact that the baffle is not perfectly rigid permits some coupling of flexural wave energy from the plate into the baffle and the possibility of additional radiation of sound into the water from the baffle itself.

Fourth, the area of contact between the driver and the center of the plate was made as small as possible but it was not a point driving force, as assumed in the theory.

The comparison between theoretical and experimental radiation patterns should best be made by inspecting Figures 3 and 4 and 27 and 29. The theoretical patterns due to Alper (shown in Figure 19) have been redrawn in the rectangular log-linear plot format used for the experimental data.

The experimental pattern which should correspond most closely to the 01 mode is Figure 27 at a frequency of about 31 kHz.

Those which should correspond most closely to the 02 mode are shown in Figures 20-22-29 at a frequency of 63 kHz.

For the 31 kHz pattern it is seen that there are some small oscillations of about 3 dB near the center of a single major lobe. The level of this lobe at the 90° angle is down about 18 dB below the axial value. This contrasts with the theoretical 90° value of about -2 dB. The reasons for this disagreement

are not known, but it is believed that an important contributor is the finite size and curvature of the baffle.

For the 63 kHz patterns, there are some features which correspond well to the theoretical pattern. The angular position of the first minimum is at about 23 degrees, very close to the theoretical value of 22.5 degrees. The level of the measured maximum of the size lobe is about the same as that of the major lobe. The theoretical curves indicate a side lobe maximum level of -2.5 dB located at 48° and a level at 90° of -5.6 dB. The experimentally observed level at 90° is about -20 dB. Again, this lower level near 90° is believed to be due largely to the finite baffle dimension. The additional structure on the measured patterns is believed to be due to radiation of sound from the baffle.

Illustrations of the complexity of radiation patterns at other higher frequencies are shown in Figures 21-23-30. The frequencies here correspond to resonances in which there are additional displacements of the transducer parts particularly the outer flange (see Figures 16-17). Very likely the baffle itself was also excited into some flexural modes of vibration.

It is concluded that the major features of the radiation patterns measured agree with those of the Alper theory and that the differences are probably due to boundary conditions of the plate which did not meet those assumed in the theory.

E. RECOMMENDATIONS

Since the goal for this effort was to develop the Alper-Magrab theory as a design tool for the development of a flexural

disk transducer that might be suitable for use as a sound source on underwater test range tracking, the following comments and recommendations seem to be appropriate.

The adaptation of Alper's program to fit the CDC 6500 Computer, HAL, is virtually complete. Shortage of time precluded completion of this part of the work. It is recommended that the work be finished and that it be used as intended.

It appears that some sort of variation on the radiation pattern from the second radially symmetric plate mode does offer the potential for controlling the source level near the axis and yet maintain a relatively broad beam width for the secondary lobes. The patterns observed here show a deep but narrow null at about 22 degrees off the central axis. It may be possible that this null could reduced by proper distribution of excitation force on the plate. It also is possible that the effect of this narrow null on range tracking is acceptable. It is recommended that the experience of this work be employed to construct and test on the tracking range a flexural disk transducer which operates in this mode.

The smoothest radiation pattern is given by the plate operating in the first symmetric mode. The transducer used in these tests was not optimized for this mode. It is likely that a transducer designed to operate in this mode at 75 kHz would have such a small plate diameter that a problem would exist in fitting an adequate sized driver into the available space. If the program development tool becomes workable, calculations should be made to test the design at 75kHz to determine feasibility.

A much more likely application for a flexural disk source operating in the first mode appears to be at frequencies significantly lower than 75 kHz, such as are used on other test ranges.

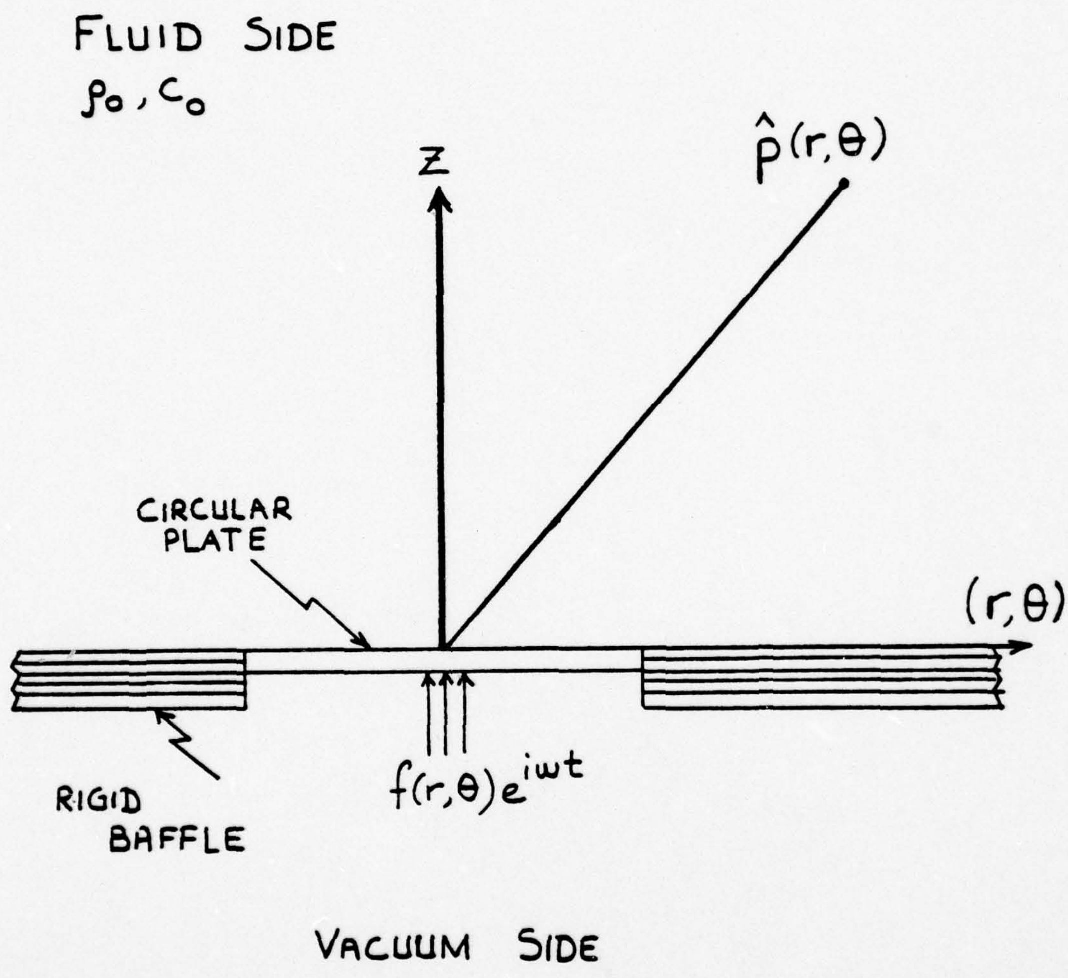

Figure 1. Geometry of Problem

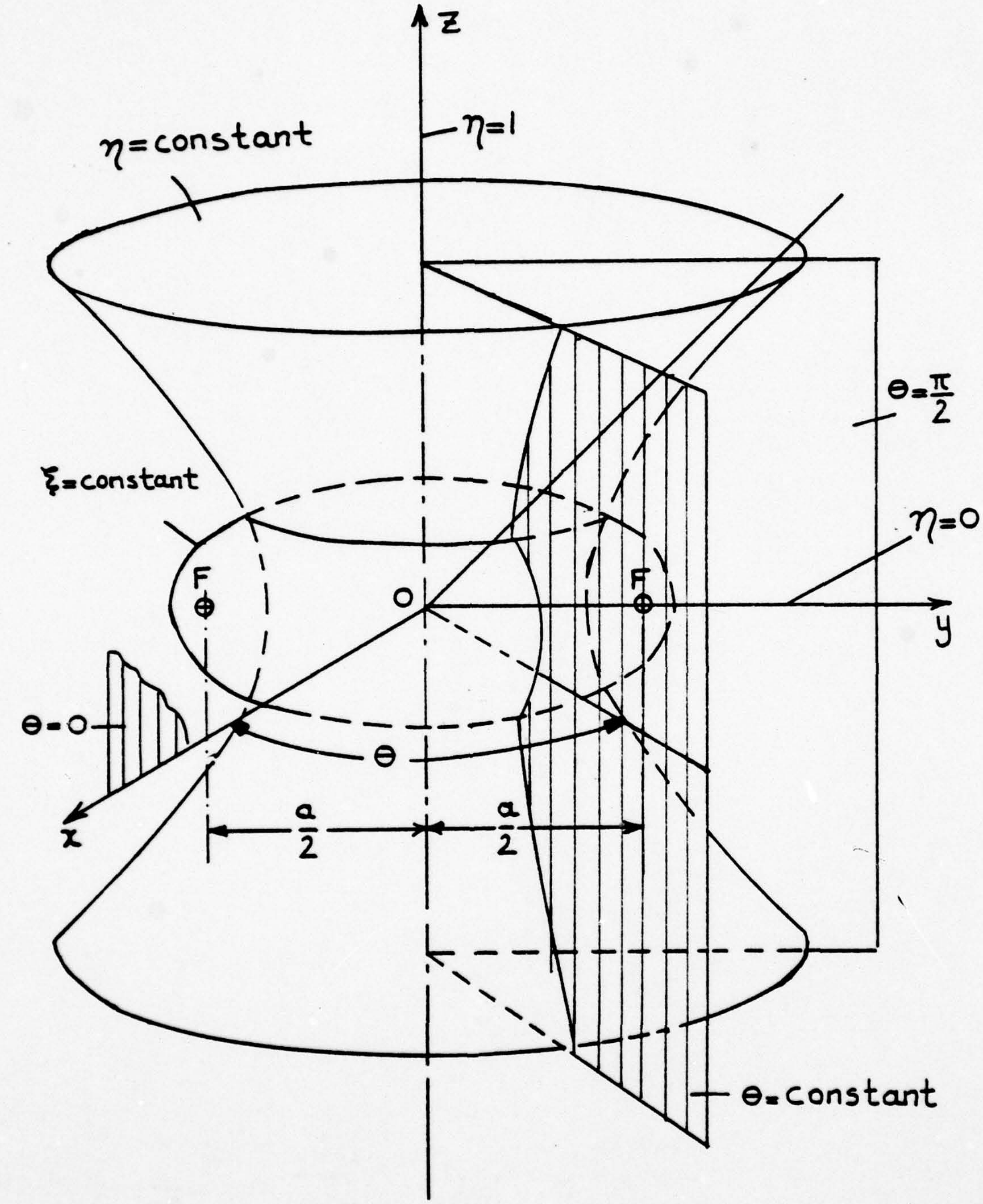

Figure 2. Oblate Spheroidal Coordinate System

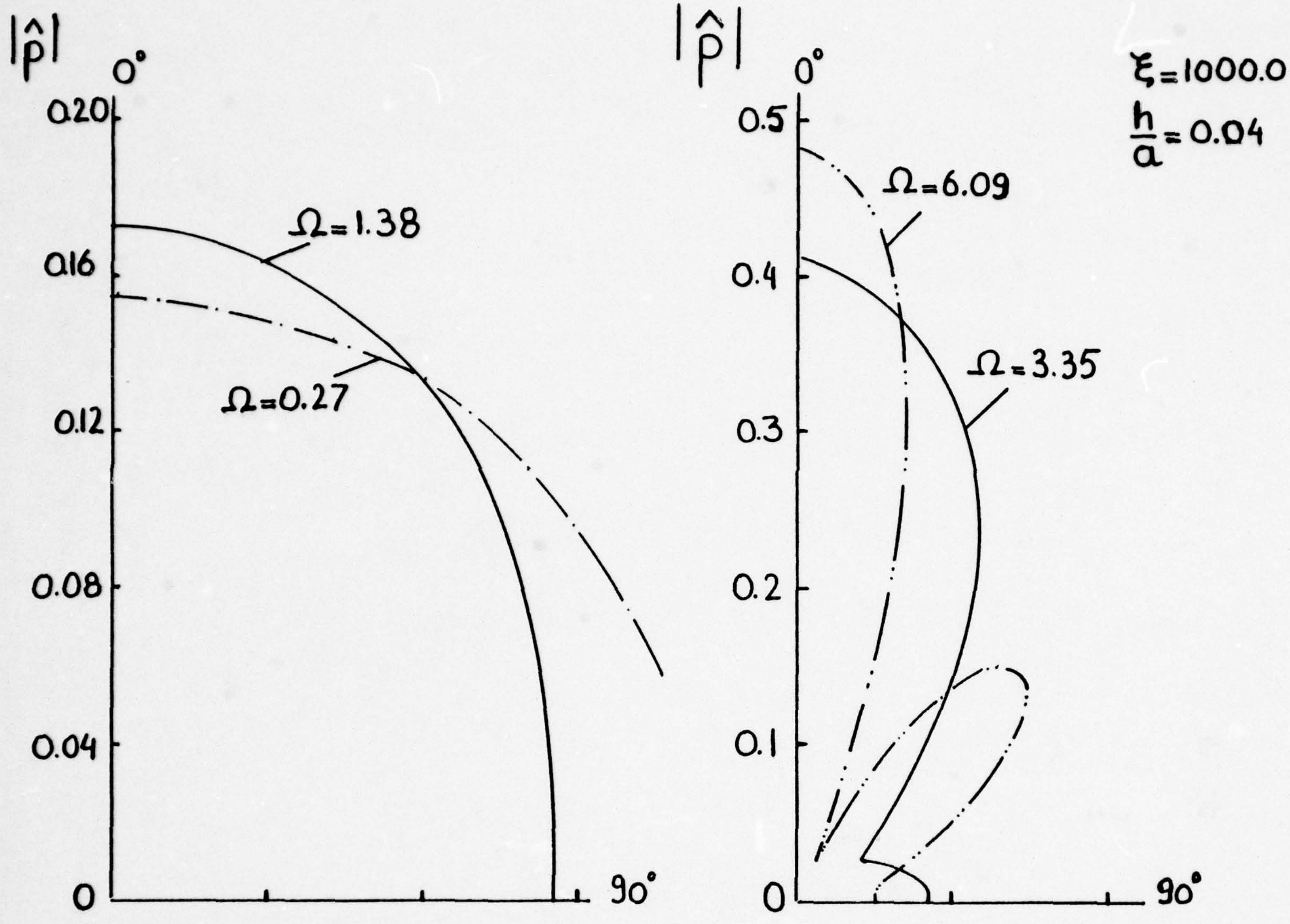

Figure 3. Far Field Beam Patterns for Thin Plate
(From Alper, Ref. 16)

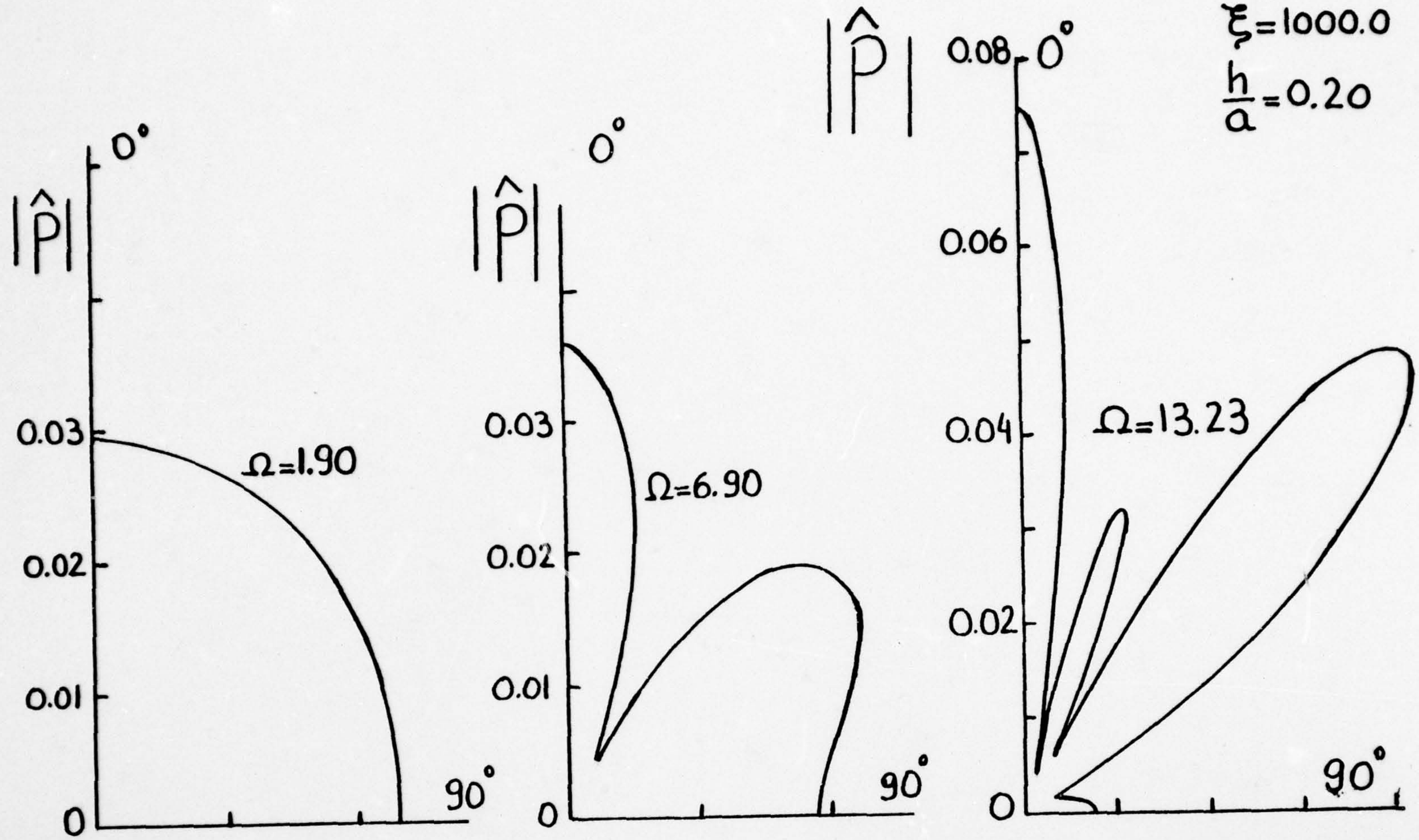

Figure 4. Far Field Beam Patterns for Thick Plate
(From Alper, Ref. 16)

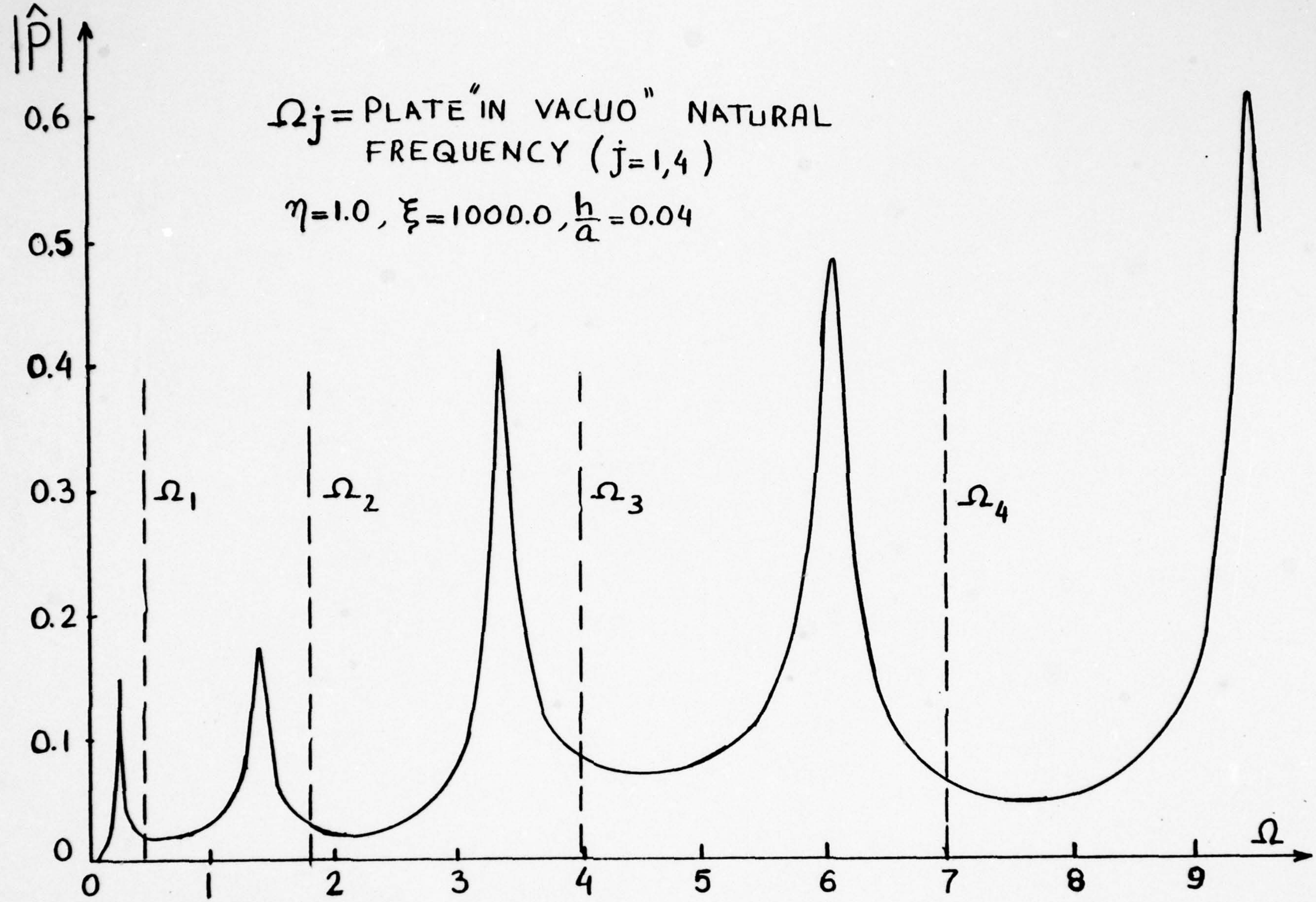

Figure 5. Pressure in Far Field on Plate Axis as a Function of Dimensionless Frequency. (From Alper, Ref. 16)

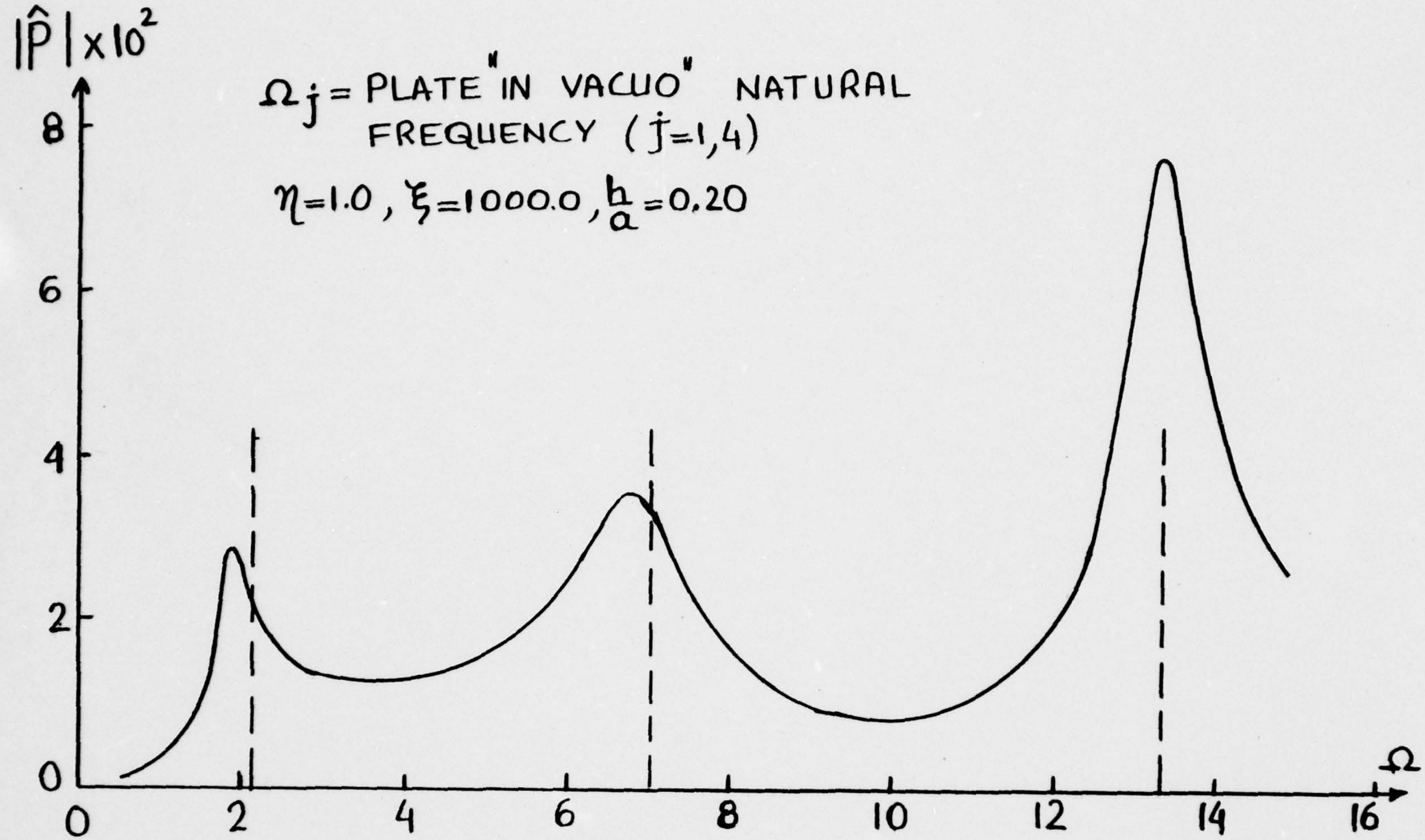

Figure 6. Pressure in Far Field on Plate Axis as a Function of Dimensionless Frequency. (From Alper, Ref. 16)

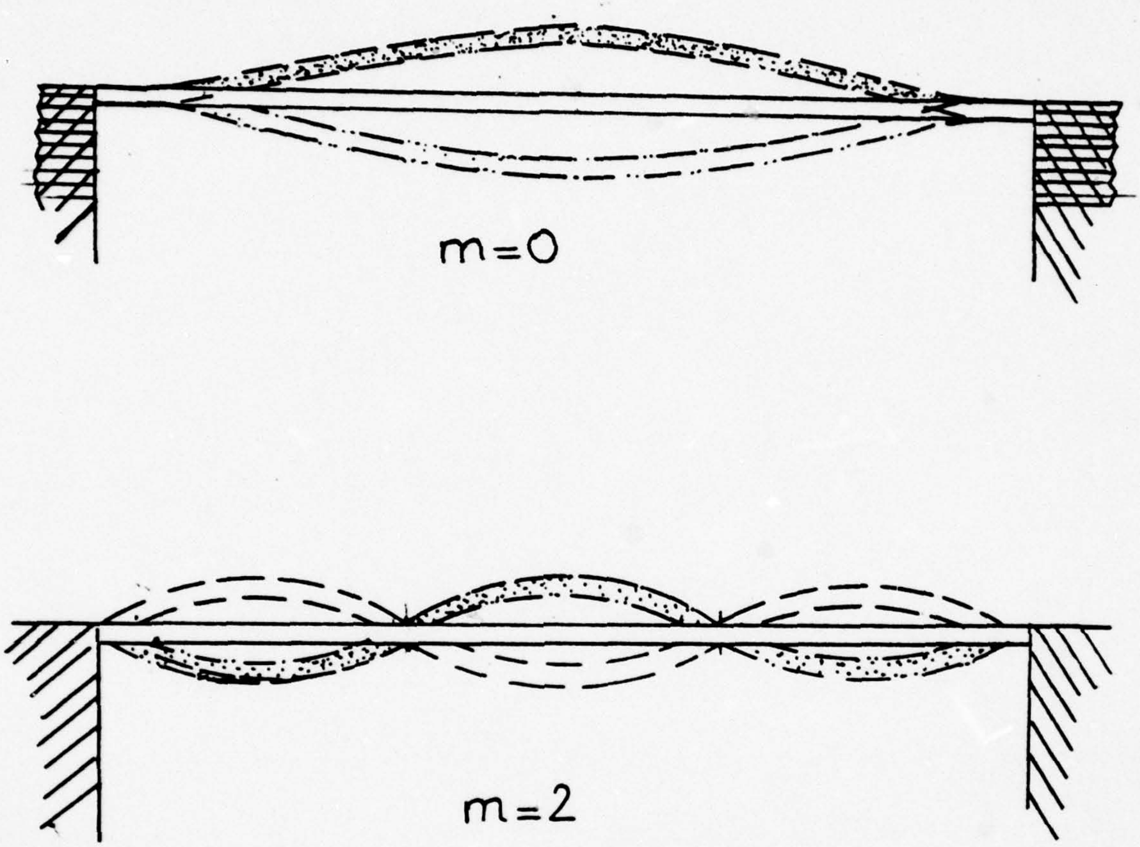

Figure 7. Form of Plate Displacement
(Schematic)

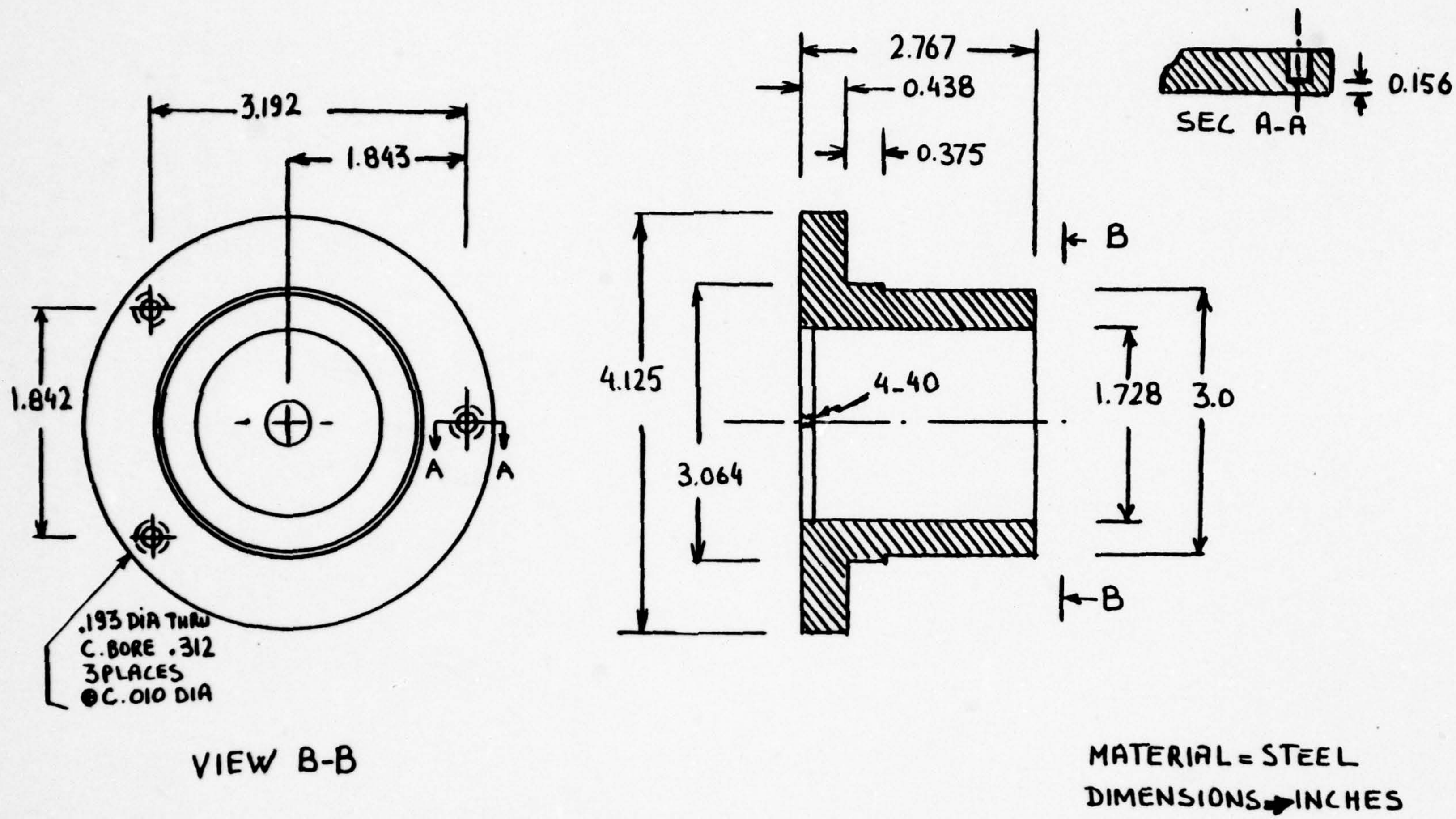

Figure 8. Transducer Dimensions

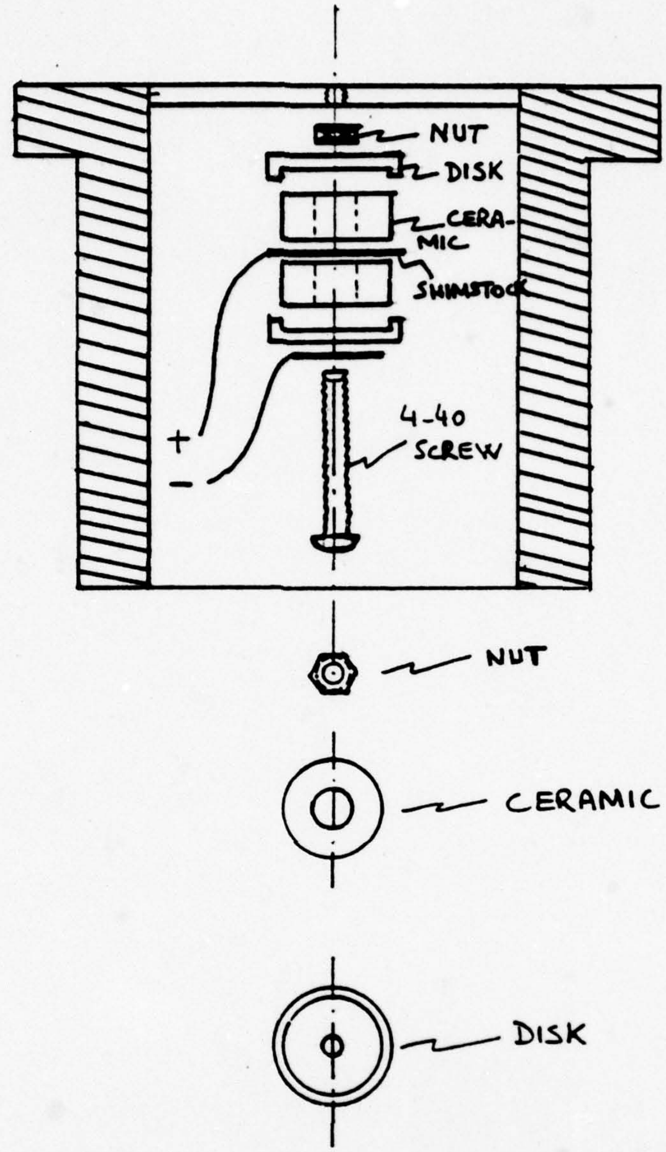

Figure 9. Driver Elements and Position on the Transducer

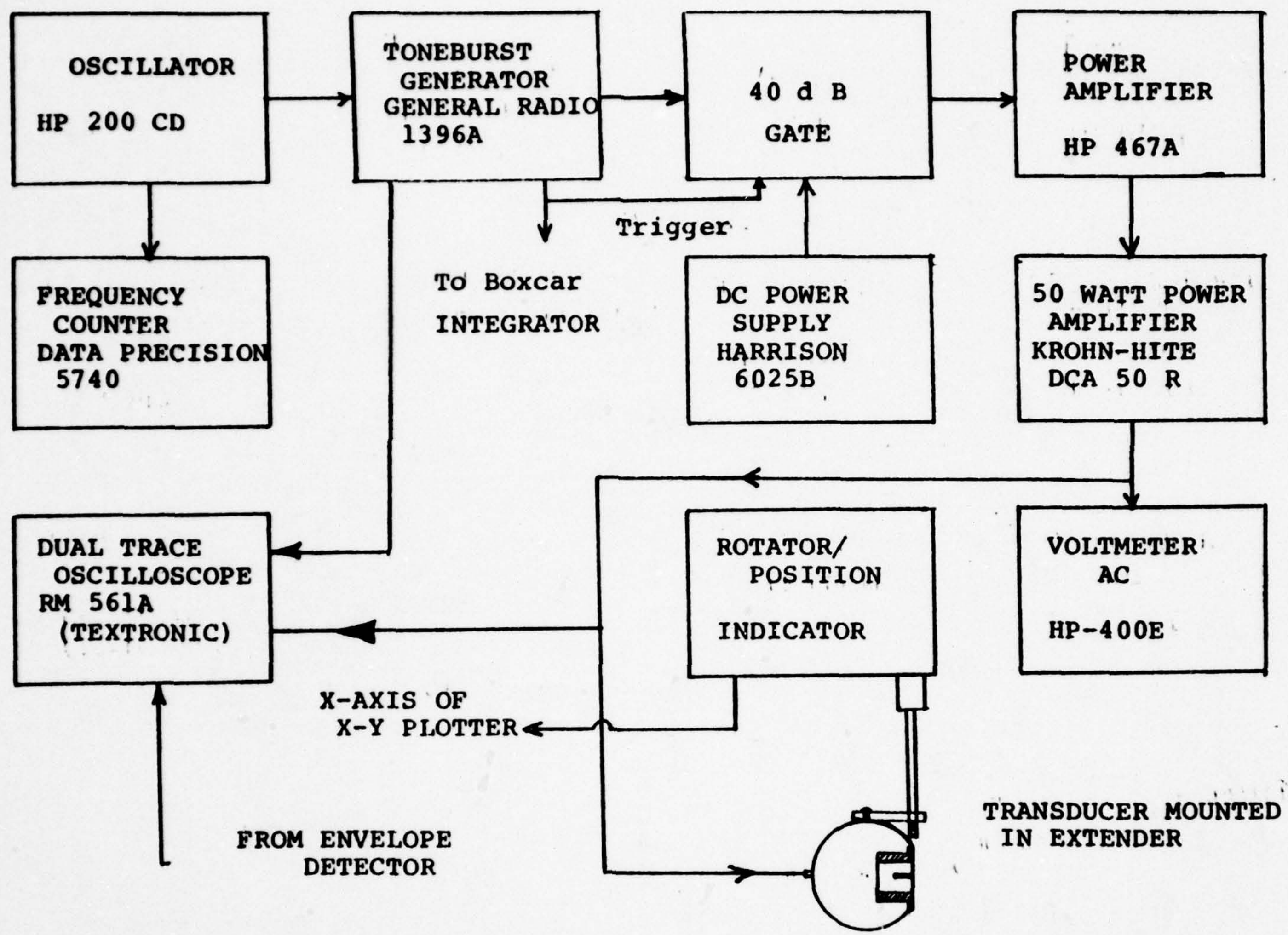

Figure 10. Radiation Pattern Measurement Apparatus (Transmitting)

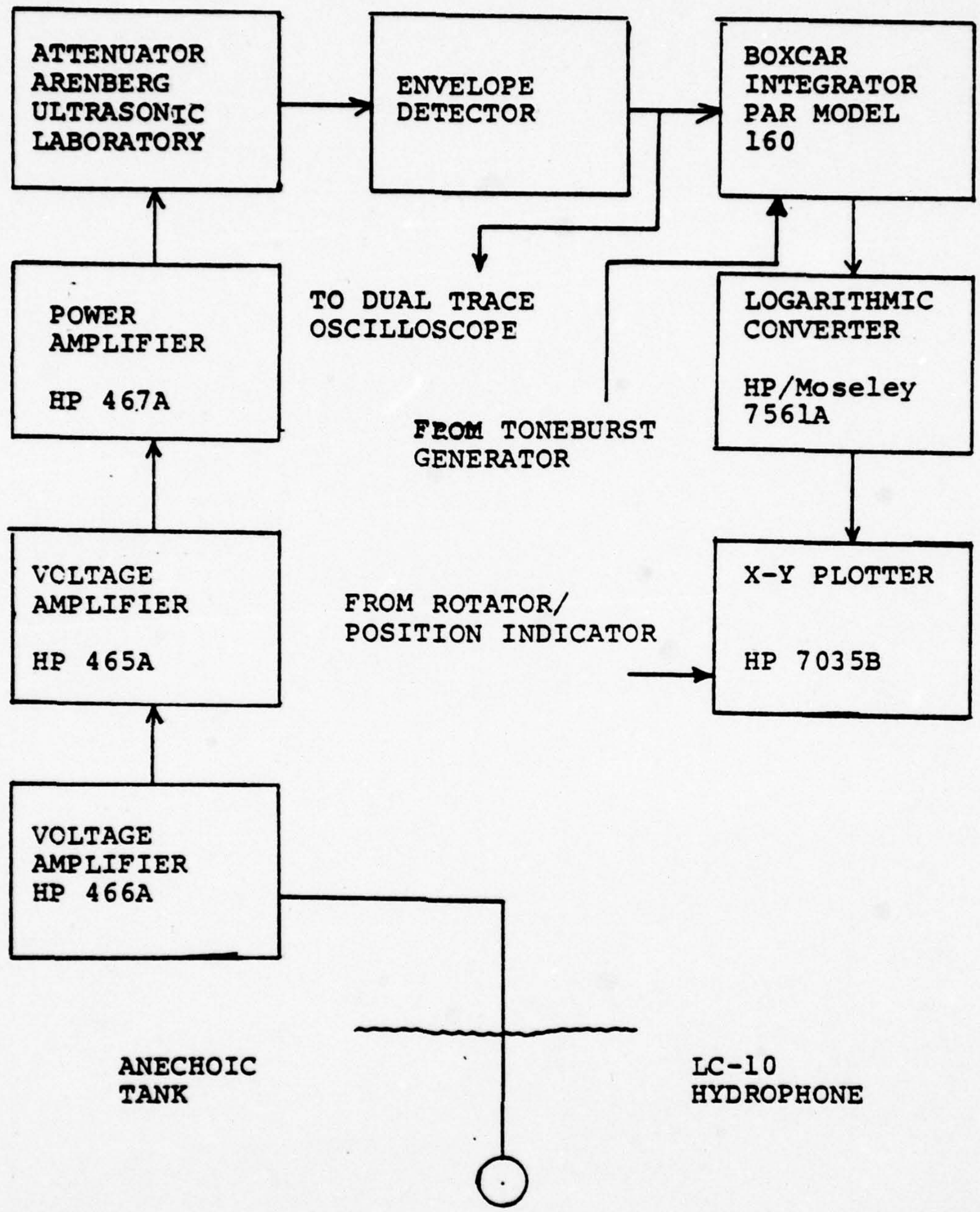

Figure 11. Radiation Pattern Measurement Apparatus (Receiving)

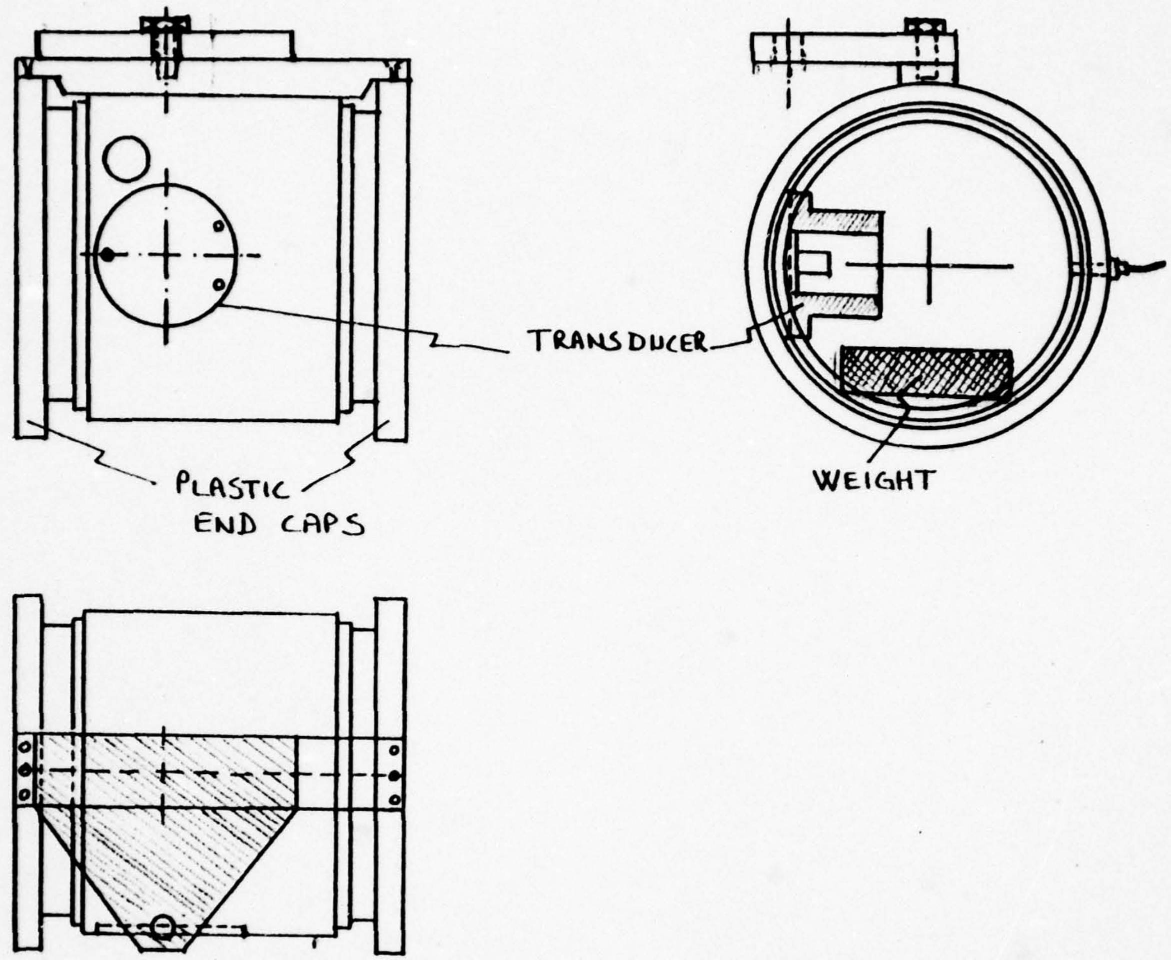

Figure 12. Cylindrical Baffle

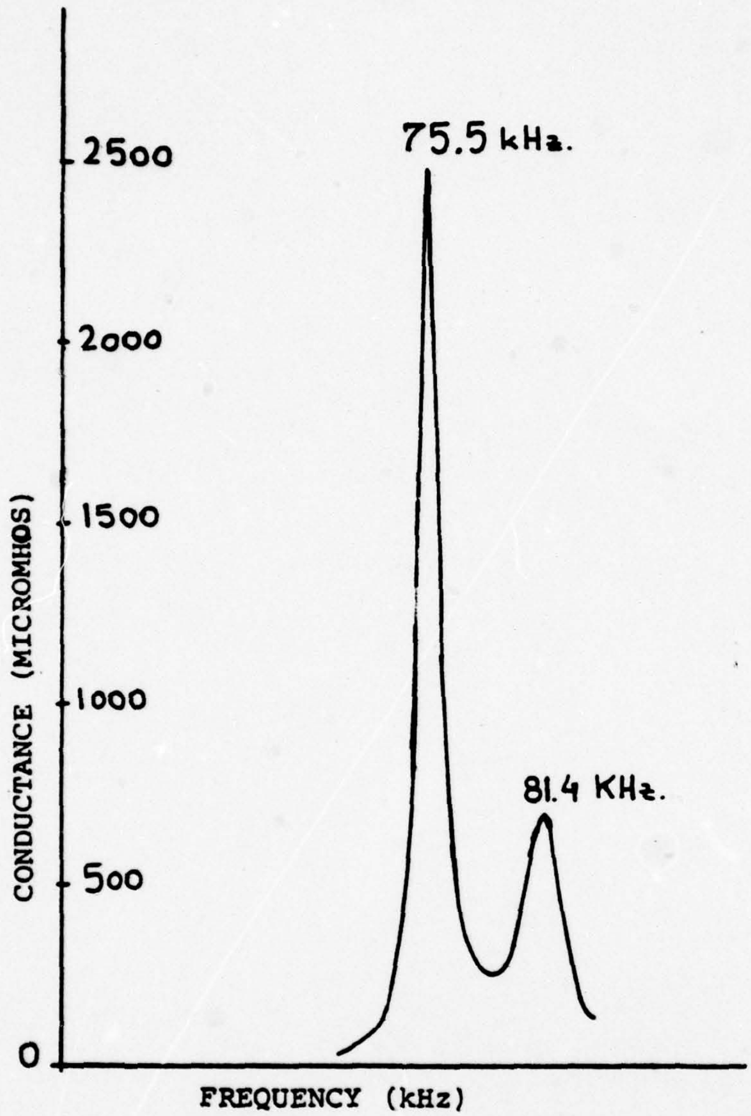

Figure 13. Conductance/Frequency Plot
Driver Alone (with nut)
in Air

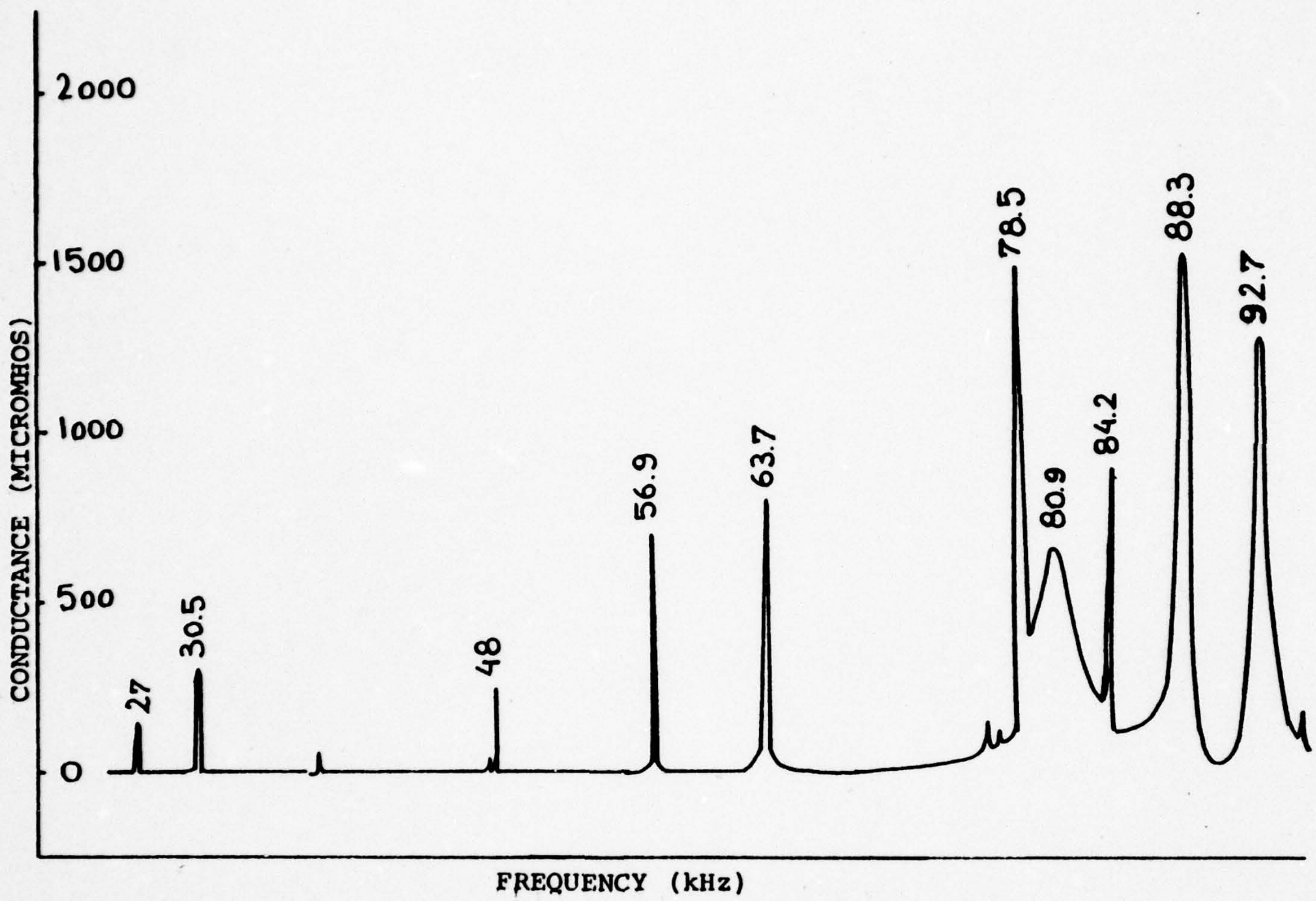

Figure 14. Conductance/Frequency Plot. Transducer in Air.

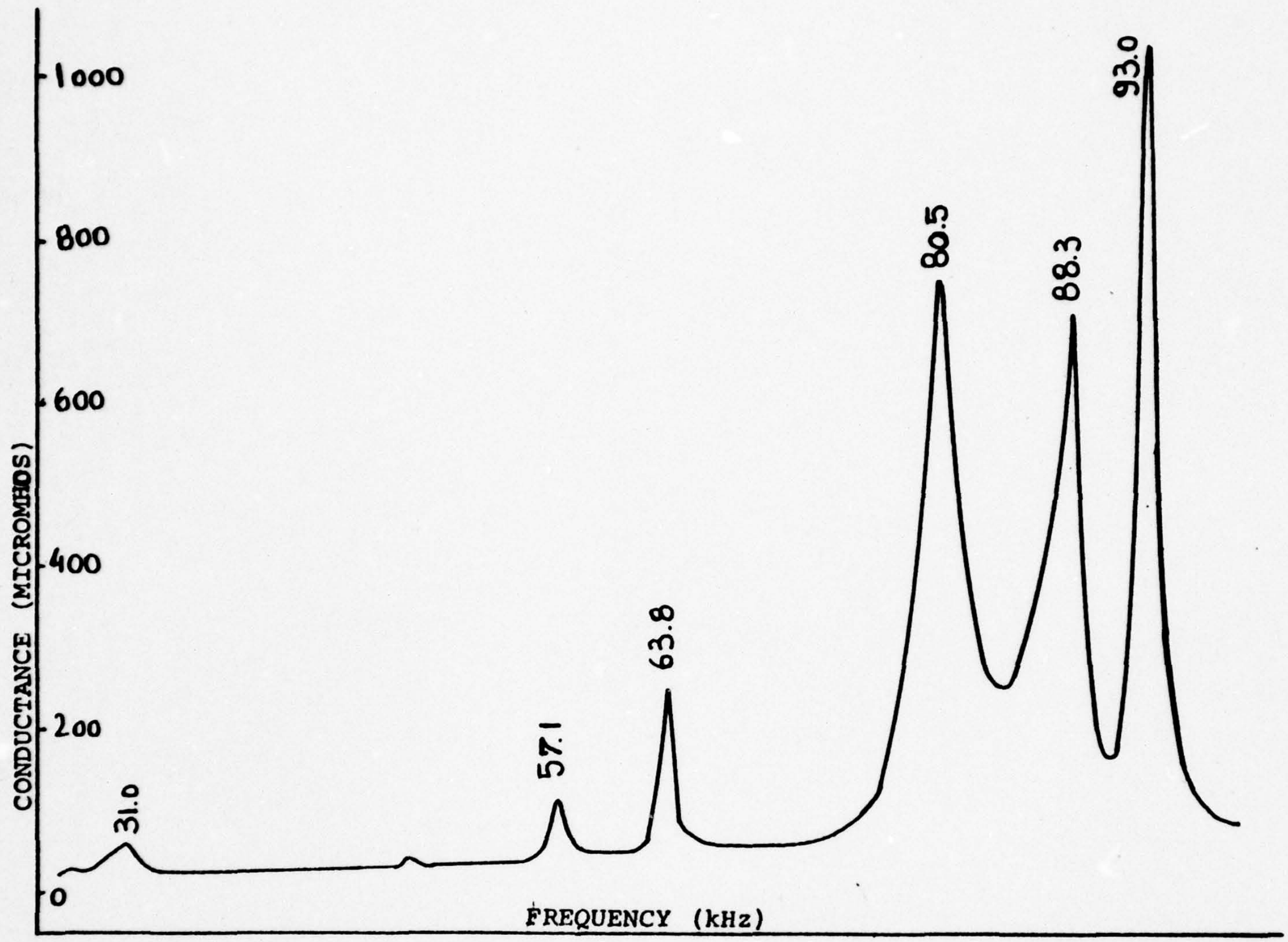

Figure 15. Conductance/Frequency Plot. Transducer mounted in Baffle in Air.

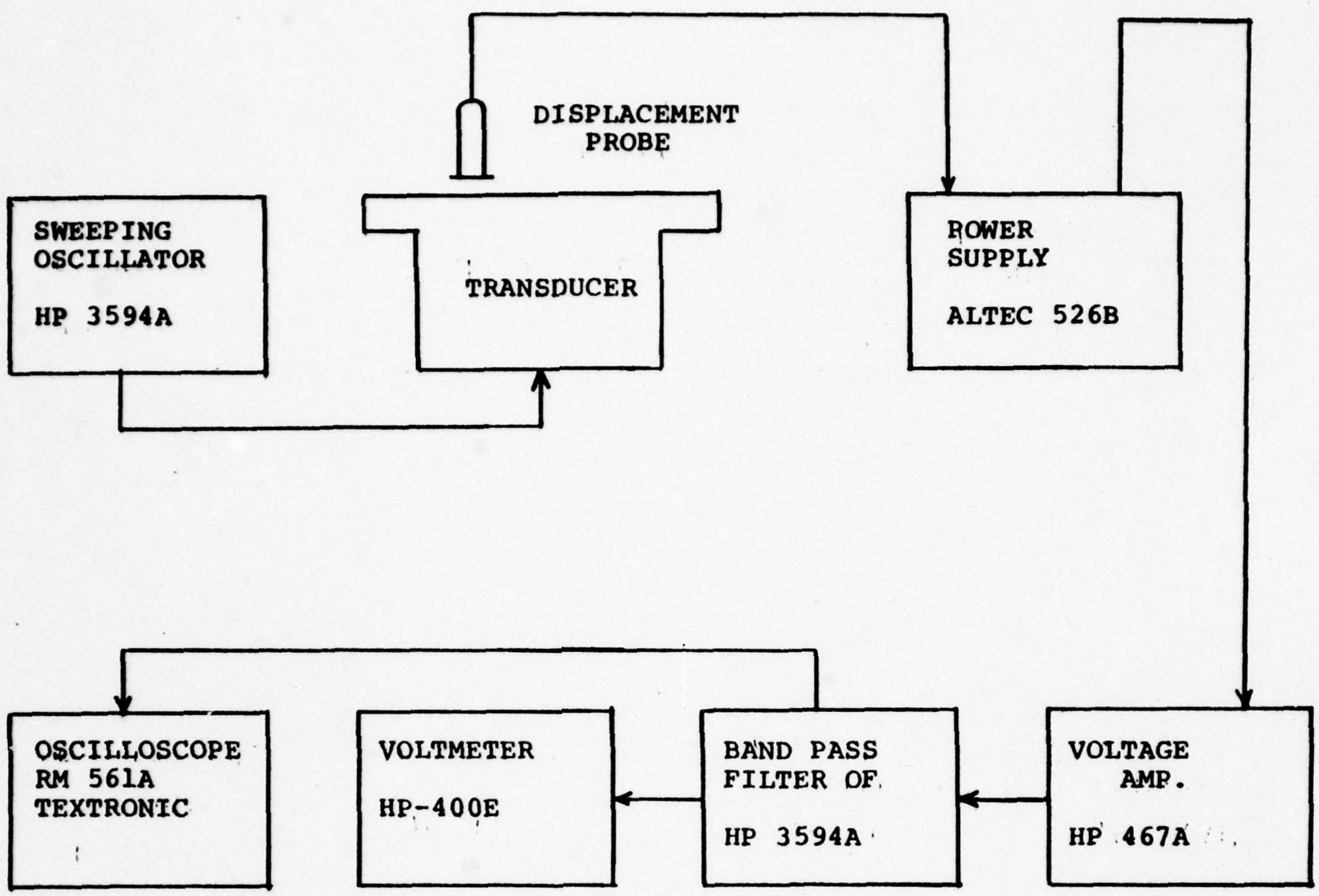

Figure 16. Relative Plate Displacement Measurement Apparatus.

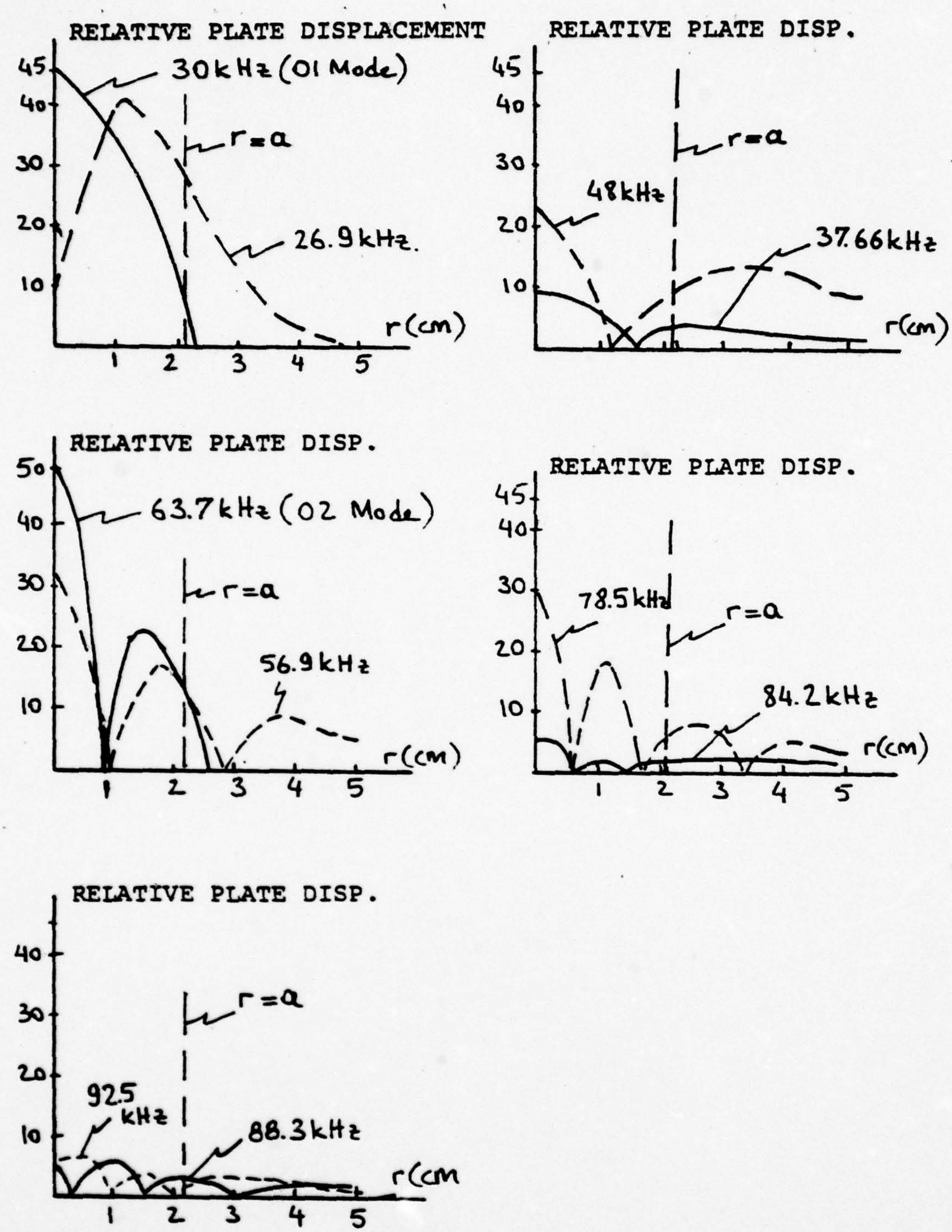

Figure 17. Relative Plate Displacement of Transducer. (Unmounted, in Air)

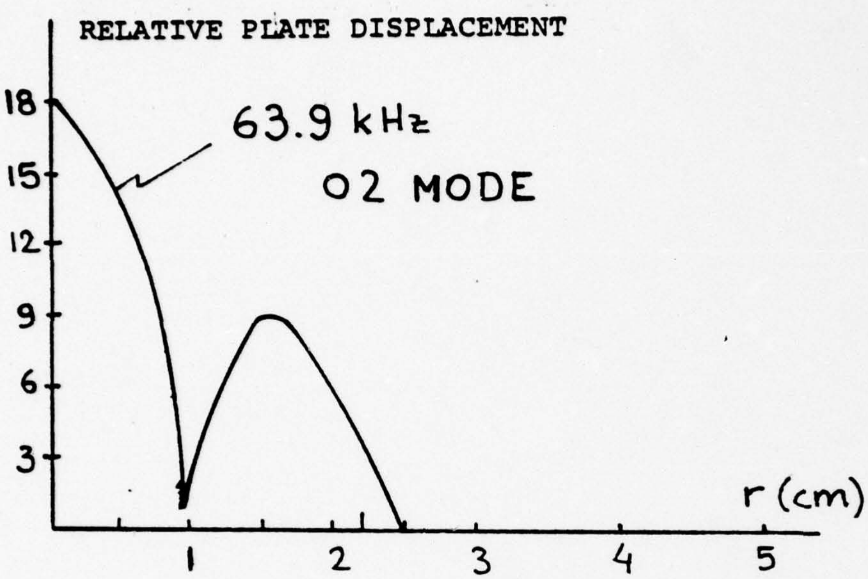

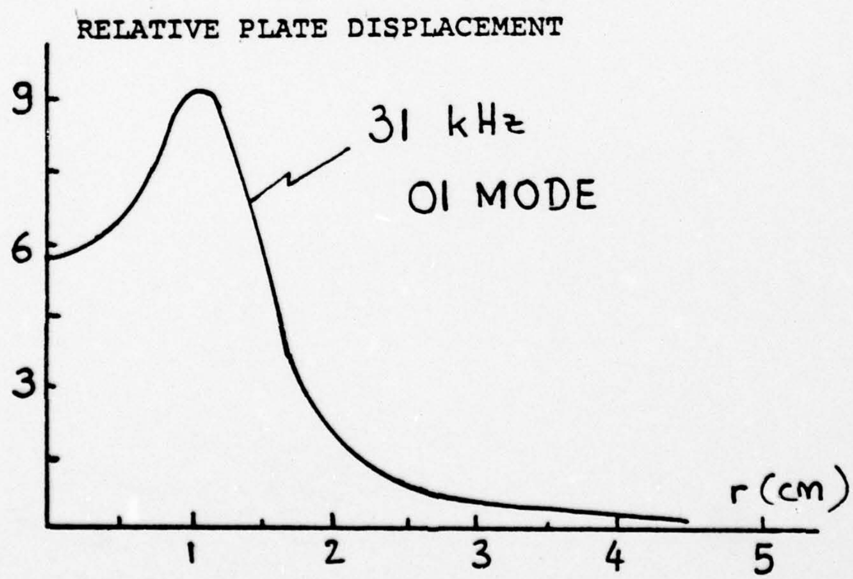

Figure 18. Relative Plate Displacement for 01 and 02 mode (transducer mounted in baffle in air)

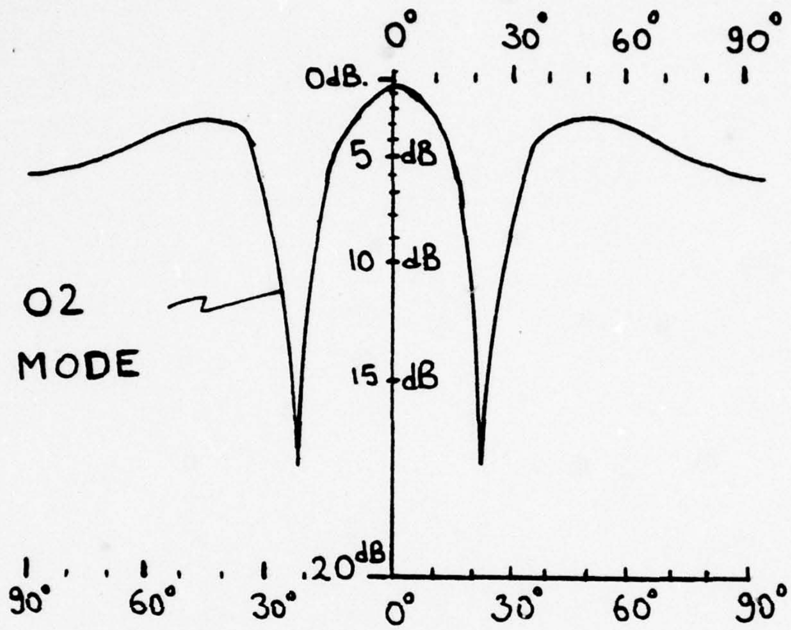

DEGREES OFF MAIN AXIS

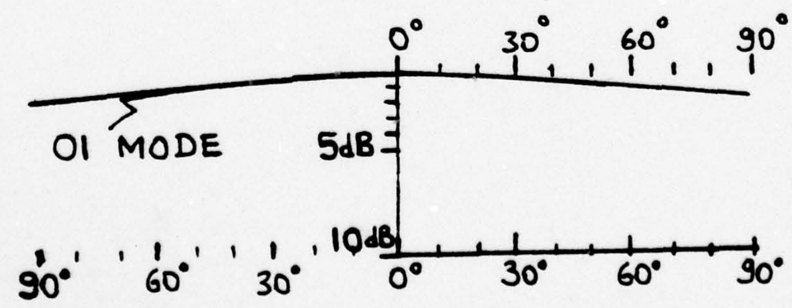

DEGREES OFF MAIN AXIS

Figure 19. Theoretical Radiation Patterns of 01 and 02 Mode.

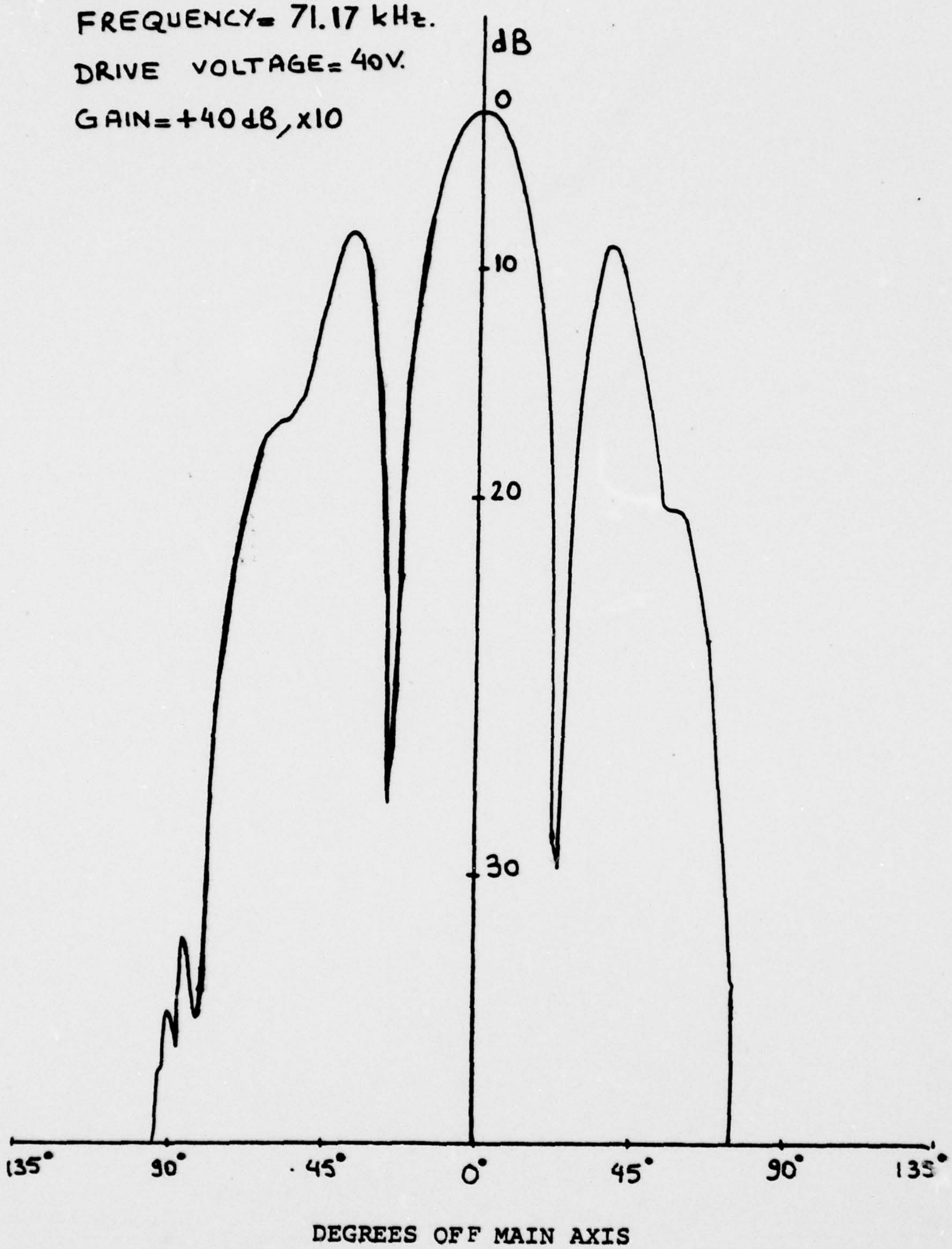

Figure 20. Radiation Pattern (small area, perpendicular axis)

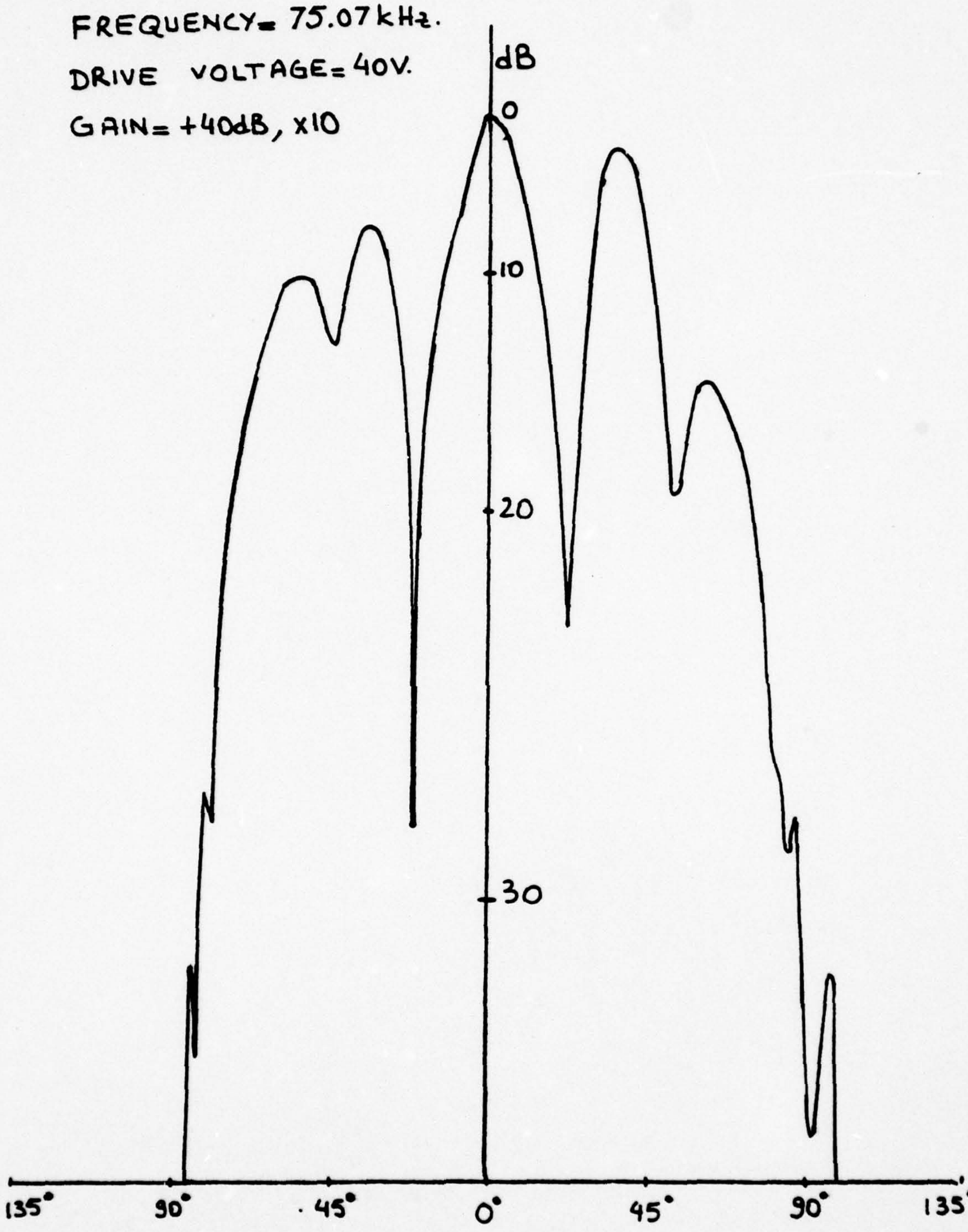

Figure 21. Radiation Pattern (small area, perpendicular axis)

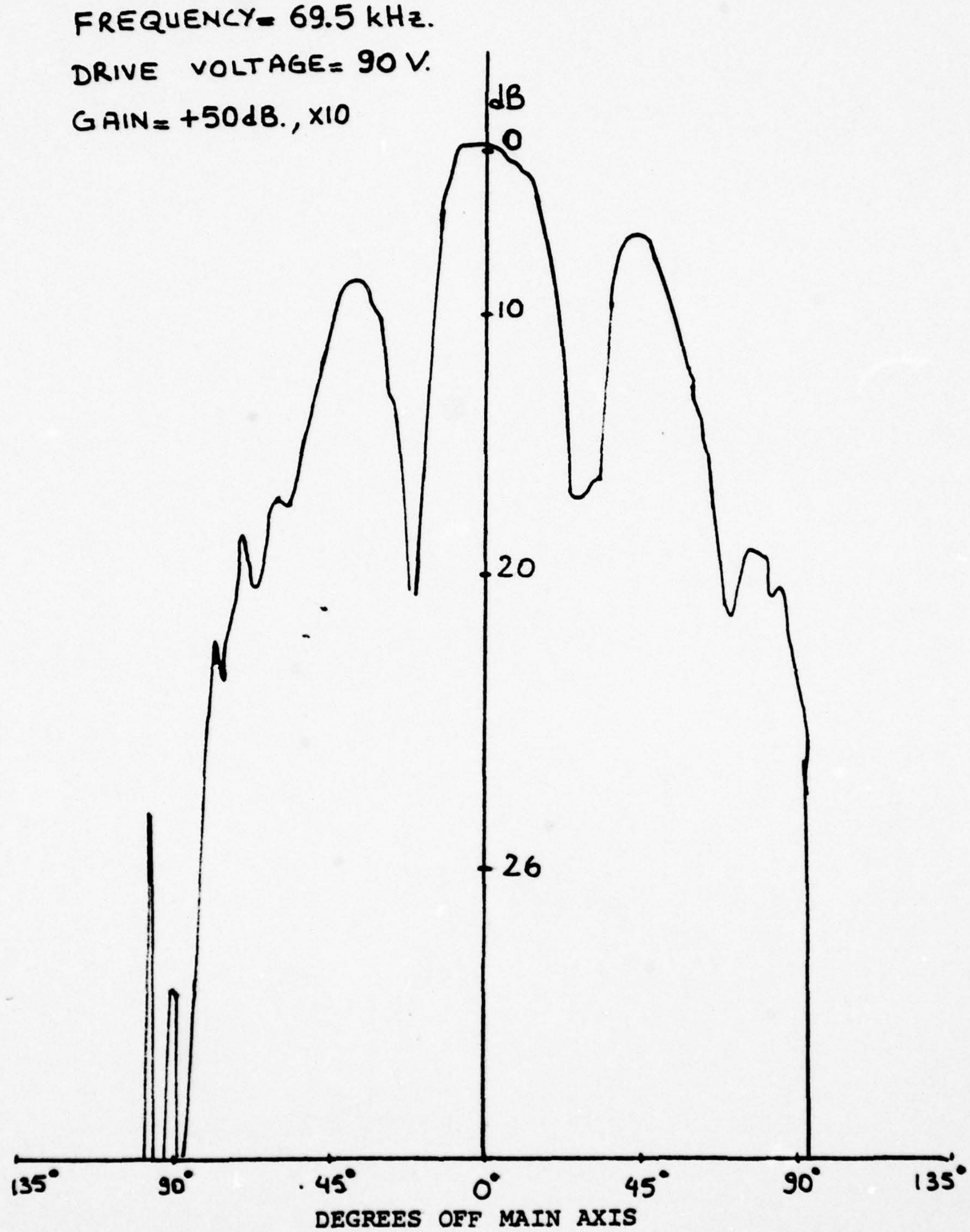

Figure 22. Radiation Pattern (small area, perpendicular axis)

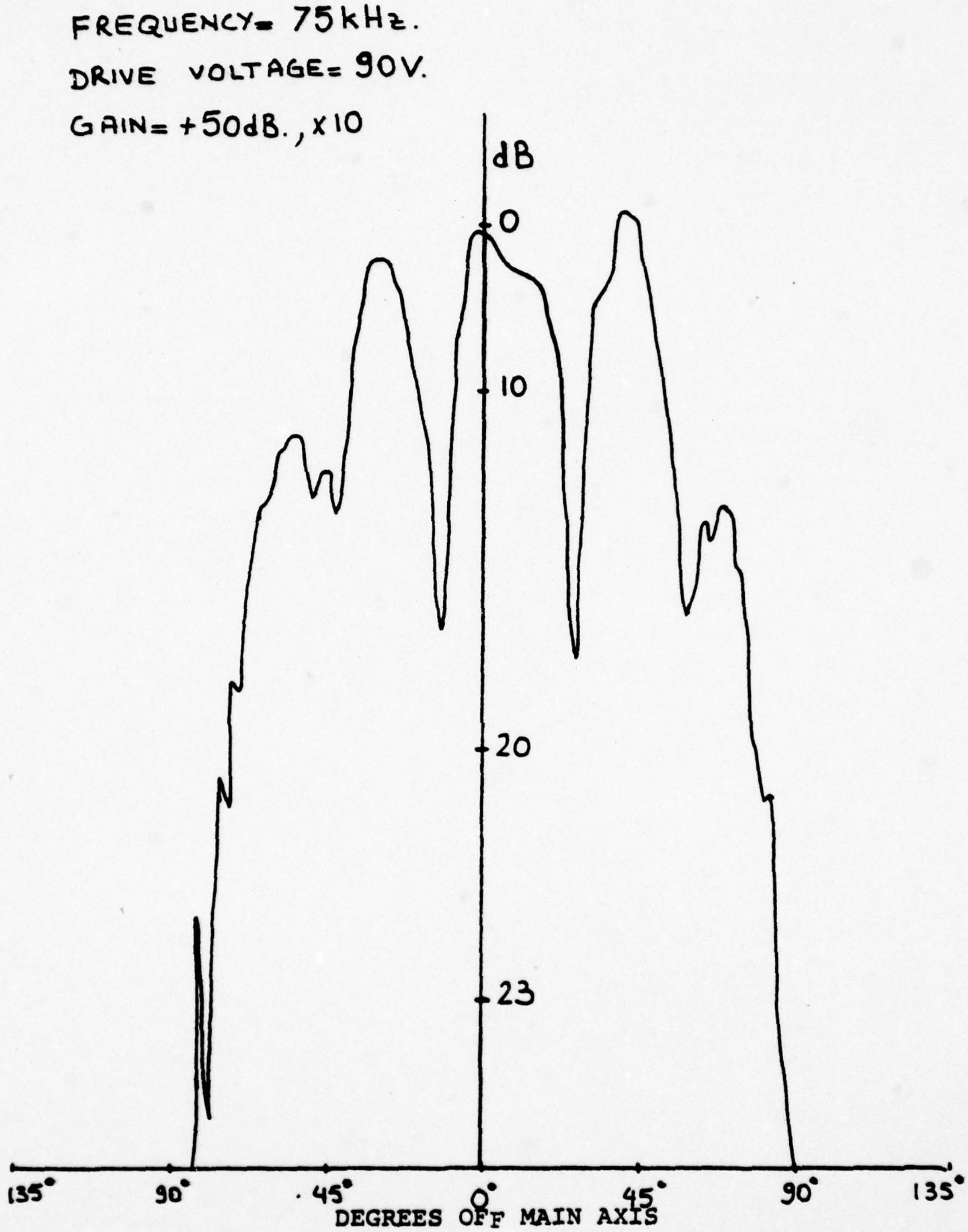

Figure 23. Radiation pattern (small area, cylindrical axis)

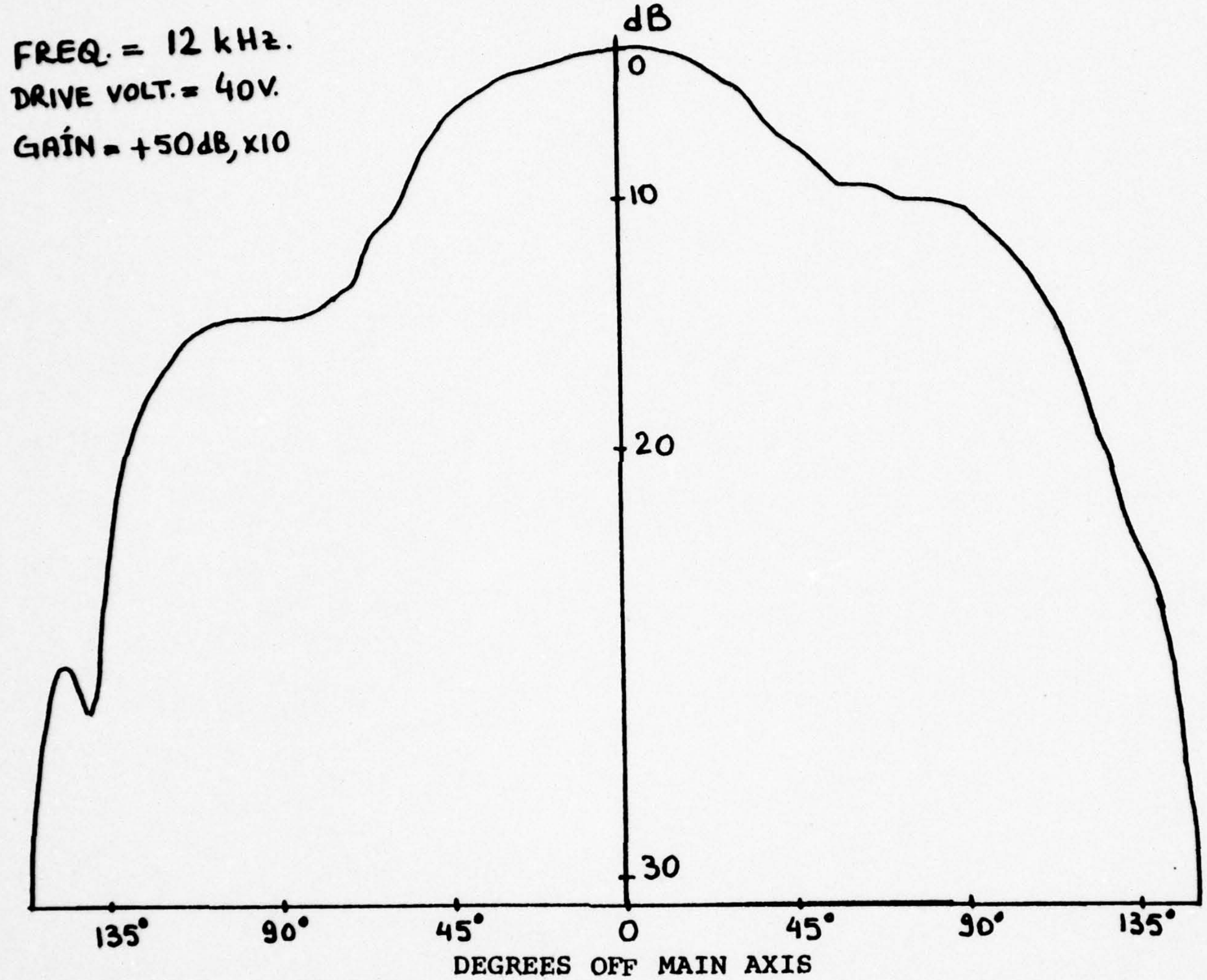

Figure 24. Radiation Pattern (large area, perpendicular axis)

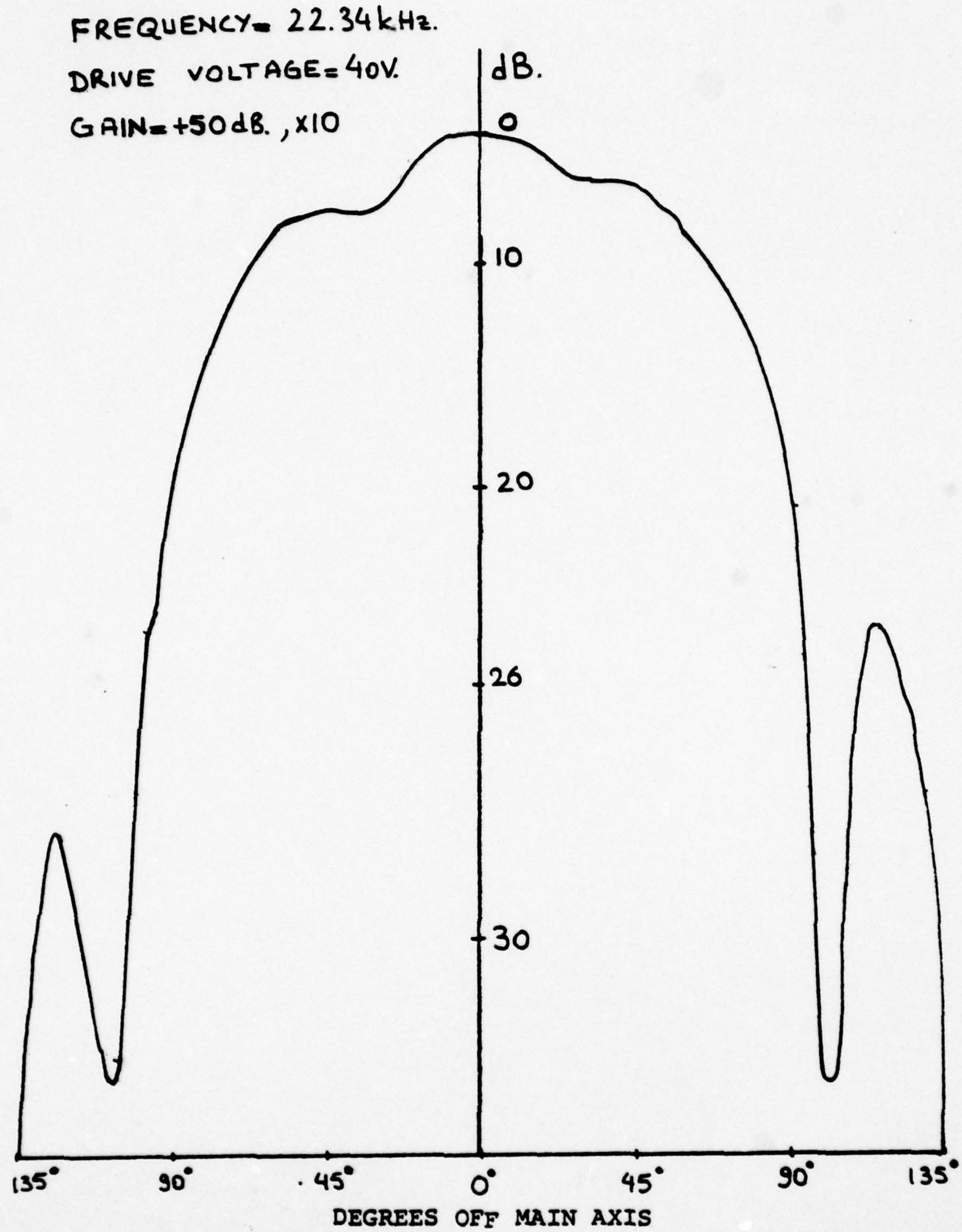

Figure 25. Radiation Pattern (large area, perpendicular axis)

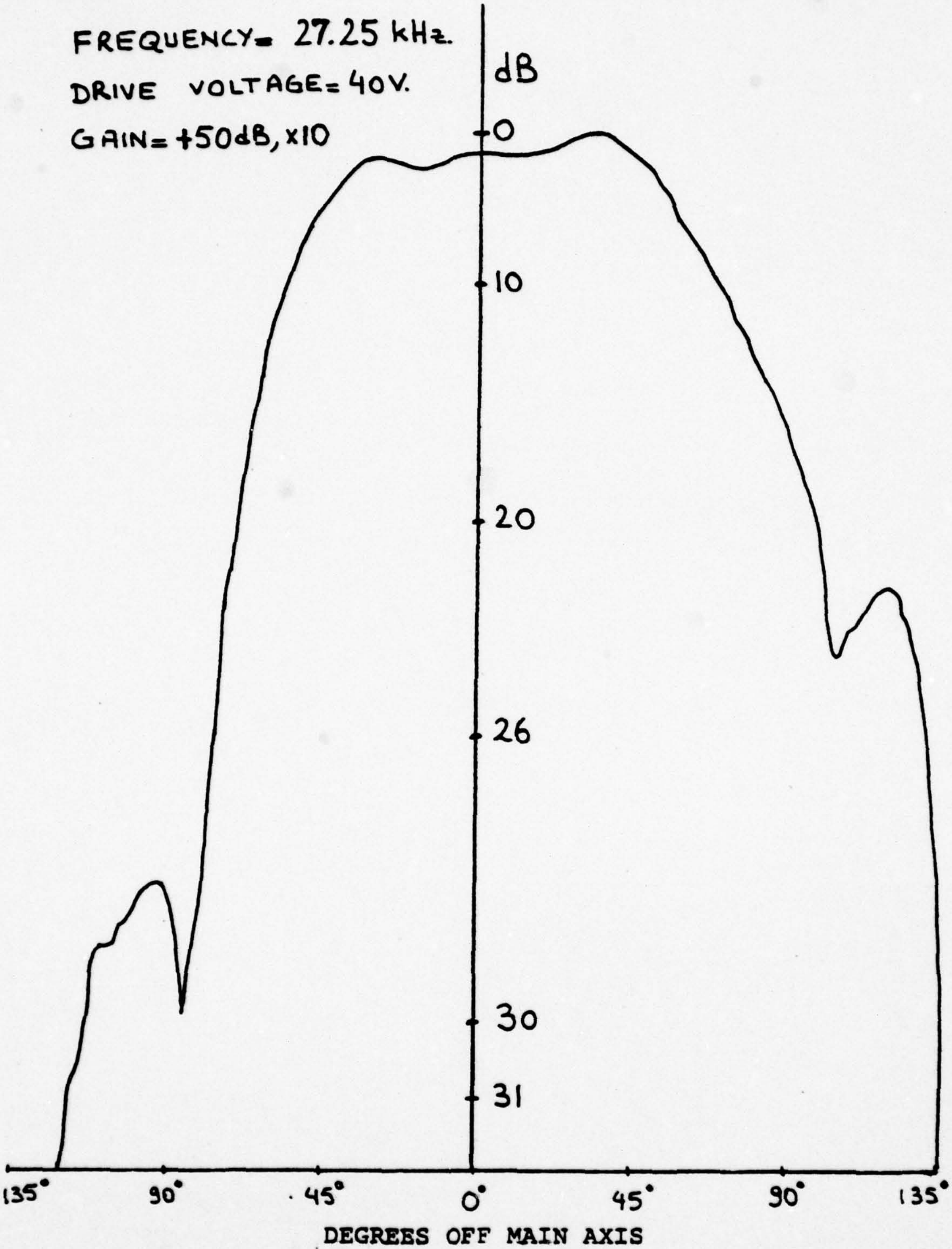

Figure 26. Radiation Pattern (large area, perpendicular axis)

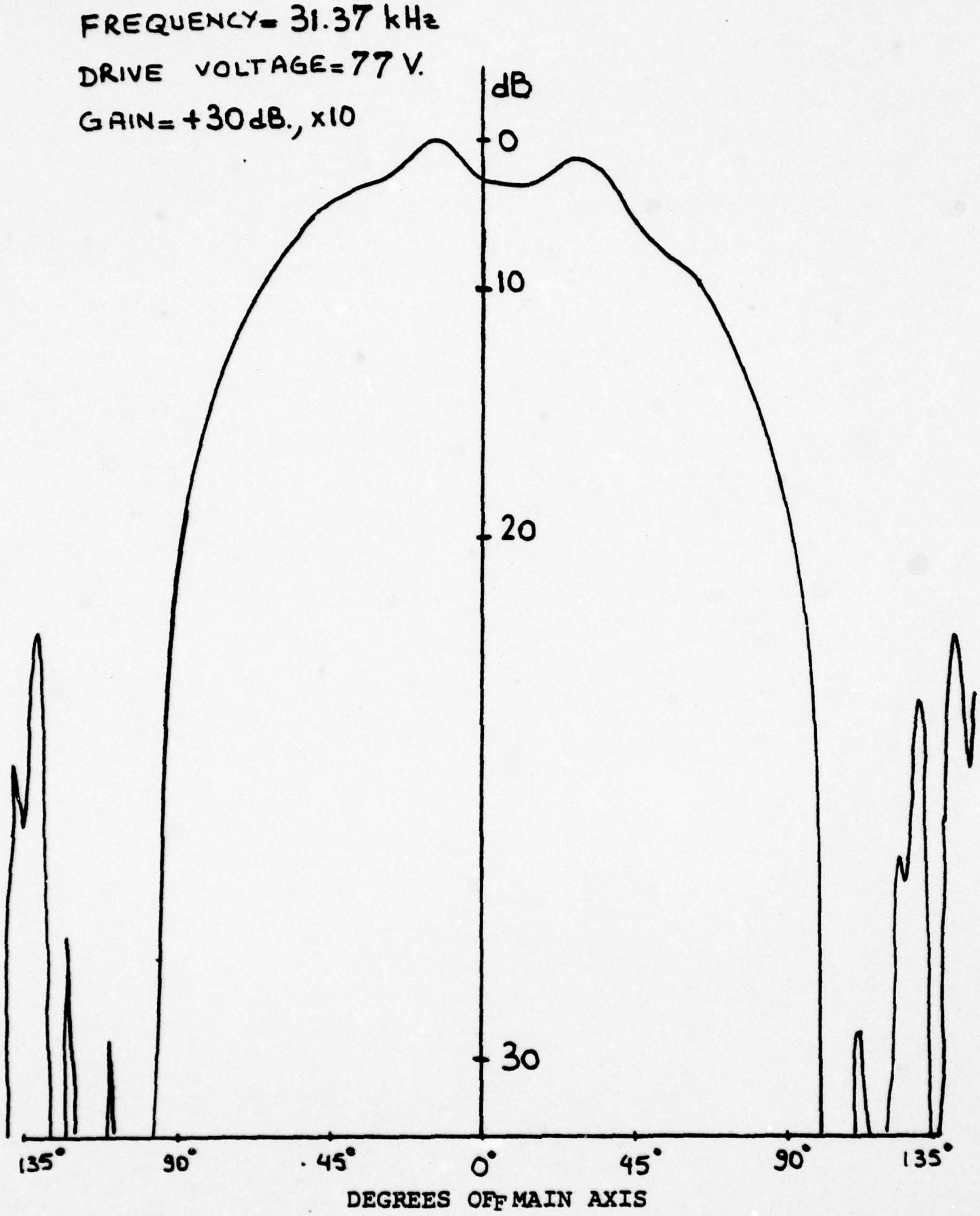

Figure 27. Radiation Pattern (small area, perpendicular axis)

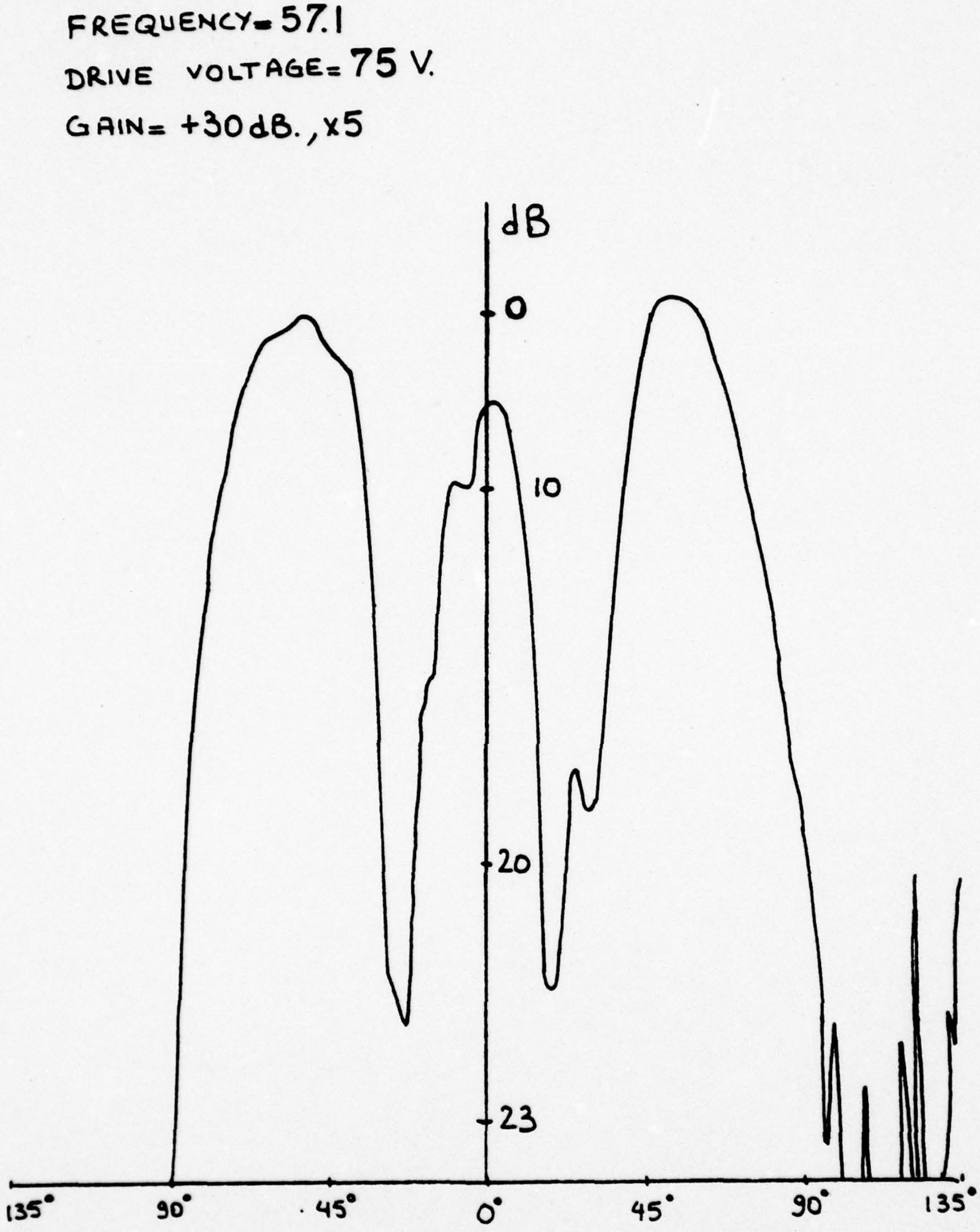

Figure 28. Radiation Pattern (small area, perpendicular axis)

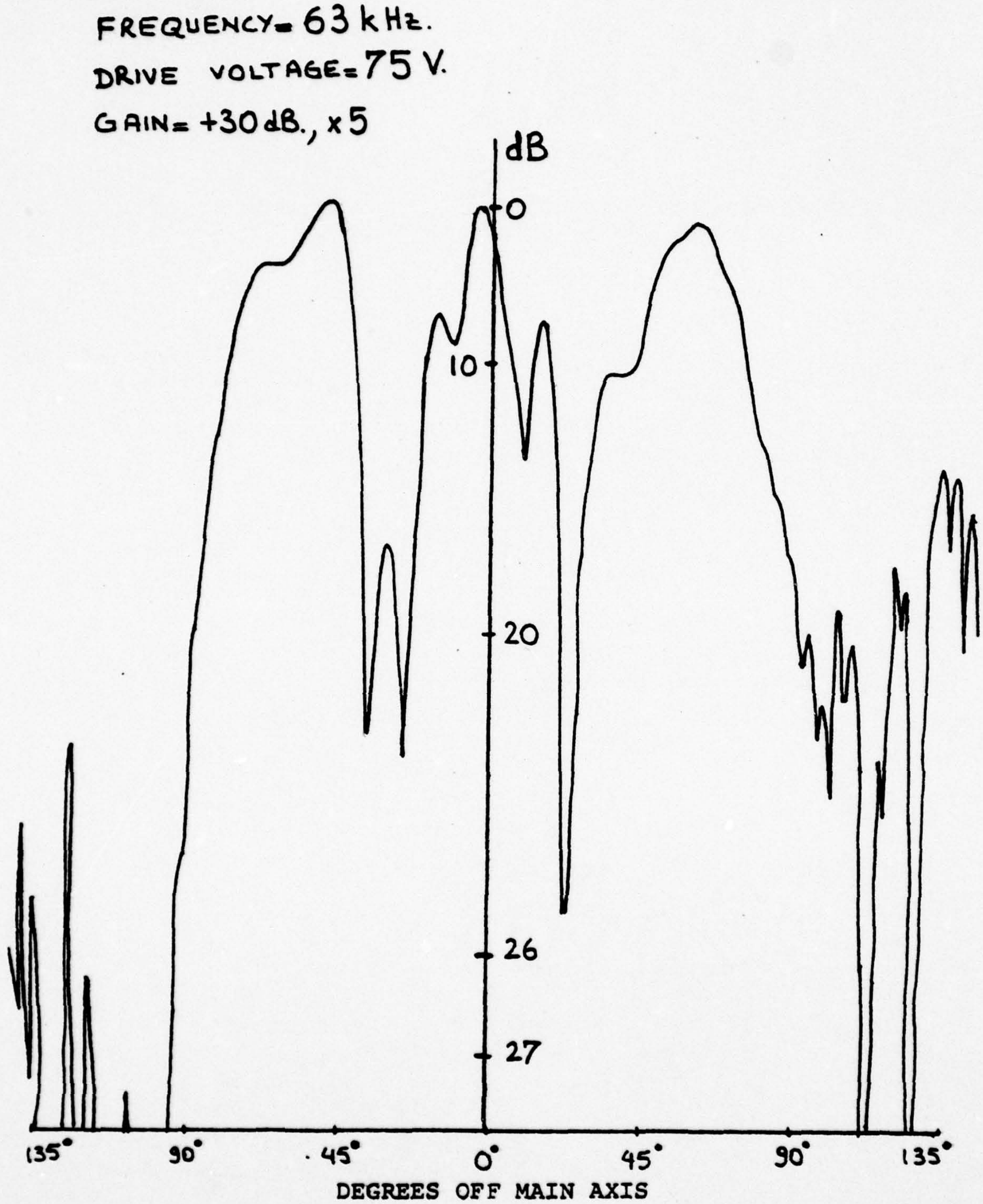

Figure 29. Radiation Pattern (small area, perpendicular axis)

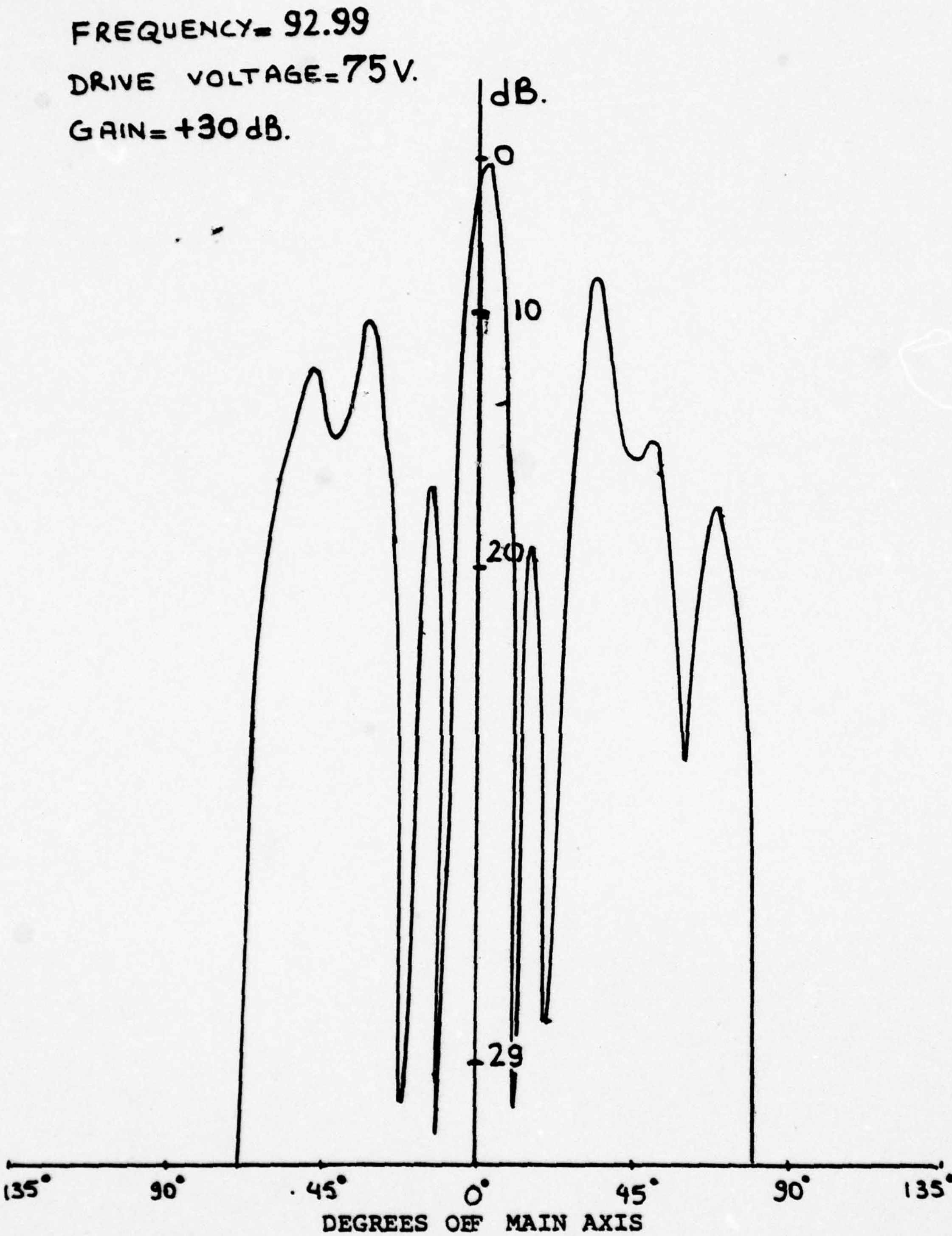

Figure 30. Radiation Pattern (small area, perpendicular axis)

APPENDIX A

COMPUTER PROGRAMS FOR FAR FIELD PRESSURE
AND ASSOCIATED PARAMETERS

Alper's original programs were not changed very much. For the main program, the outputs of the Program, Roots, and the Program, Caller, (for getting sum)are needed. After getting the output of Program, Roots, Program, Caller output is obtained by using these results. Finally, the main program will be run by using the obtained parameters and sums. For this reason some Formats were changed to fit inputs and outputs each other. The only problem which still was not solved is that of Subroutine Bessel.

```
CCC JOB CARD
FTN (OPT=2,R=3)
LGO.
"
      PROGRAM ROOTS(INPUT,OUTPUT,PUNCH,TAPE5=INPUT,TAPE6=OUTPUT,
     *   TAPE7)
C
C     DEFINITION OF VARIABLES.
C
C        ANS          TABLE OF ANSERS FROM ROOT FINDING ROUTINE
C        A1           SQUARE ROOT OF A1SQRD.
C        A1SQRD        DIMENSIONLESS TERM IN DELTA FUNCTION.
C        A2           SQUARE ROOT A2SQRD.
C        A2SQRD DIMENSIONLESS TERM IN DELTA FUNCTION
C        A3SQRD        DIMENSIONLESS TERM IN DELTA FUNCTION.
C        BES          SUBROUTINE FOR DETERMINE BESSEL FUNCTION
C        BOA1         VALUE OF BESSEL FUNCTION-
C        BOA2       ORDER    GIVEN BY SECOND CHARACTER (0,1,OR2)
C        B1A1         ARGUMENT IS GIVEN BY LAST TWO CHARACTERS
C        B1A2         -A1 OR A2..
C        B2A1
C        B2A2
C        CAPK         ONE-HALF OF (1.0 MINUS POISSONS RATIO).
C        DEL          RATIO OF BESSEL FUNCTION VALUES OF A1 TO A2
C        DELTA        ROUTINE FOR EVALUETING DELTA FUNC TION OF OMEGA.
C        EN         , NORMALIZATION TERM USED IN LATER PROCESSING.
C        FCNZERO        ROOT FINDING ROUTINE.
C        GSQRD        ONE-TWELTH OF THE SQUARE OF THE RATIO OF
C                     PLATE THICKNESS TO PLATE RADIUS
C        G            SQUARE ROOT  OF GSQRD.
C        I,J          LOCAL INCICIES   USE DETERMINES MEANING.
C        NROOTS       NUMBER OF ROOTS FOUND BY ROOT FINDING ROTINE.
C        OBEGIN        INITIAL VALUE OF OMEGA INTERVAL OF INTEREST
C        OEND         TERMINAL VALUE OF OMEGA INTERVAL OF INTEREST
C        OMEGA        PRIMARY INDEPENDENT VARIABLE.
C        OTOL         TOLERANCE FOR OMEGA AND DELTA.
C        RBEGIN       INITIAL VALUE OF PLATE RATIO (RPLATE).
C        REND         TERMINAL VALUE OF PLATE RATIO.
C        RPLATE       RATIO OF PLATE THICKNESS TO PLATE RADIUS.
C        RPOISN       POISSONS RATIO.
C        RSPEED       RATIO OF SPEED OF SOUND IN FLUID TO
C                     SHEAR WAVESPEED IN PLATE.
C        RSTEP        INCREMENT DESIRED IN STEPPING PLATE RATIO
C                     FROM RBEGIN TO REND.
C        SIGMA1       DIMENSIONLESS TERM IN DELTA FUNCTION.
C        SIGMA2       DIMENSIONLESS TERM IN DELTA FUNCTION.
C        SHEAR        TIMESHENKOS SHEAR COEFFICIENT.
C        TEMP         TEMPORARY WORKING STORAGE FOR USE BY BES.
```

```
C        U,V,W,X,Y,Z LOCAL VARIABLES USAGE DETERMINES MEANING
C
      COMMON/TABLE1/A1,A2,A1SQRD,A2SQRD,A3SQRD,CAPK,G,GSQRD,
     * RPLATE,RPOISN,RSPEED,SIGMA1,SIGMA2,SHEAR
      COMMON/TABLE2/B0A1,B0A2,B1A1,B1A2,B2A1,B2A2,DEL,EN
      DIMENSION ANS(2050)
C
      EXTERNAL DELTA
C
   10 FORMAT(9(F7.3,1X))
   20 FORMAT(///1H1,10H** NOTE **,2X,I5,17H ROOTS FOUND FOR ,F15.8)
   30 FORMAT(1X,I4,F11.6,4F16.10)
   40 FORMAT(1H1,3X,9HJ    OMEGA,6X,6HA1SQRD,10X,6HA2SQRD,9X,
     *8HDELTA(J),10X,4HN(J)//)
C     READ IN CONSTANTS ,BEGINING AND ENDING VALUES FOR THE PLATE
C     RATIO AND OMEGA WITH THEIR INCREMENT OR TOLERANCE,AND THEN
C     CALCULATE THE REMANING CONSTANTS. SET PLATE RATIO TO INITIAL
C     VALUE.
      READ(5,10) RPOISN,RSPEED,SHEAR,RBEGIN,REND,RSTEP,
     * OBEGIN,OEND,OTOL
C
      CAPK=0.5*(1.0-RPOISN)
      RPLATE=RBEGIN
  100  GSQRD=(RPLATE*RPLATE)/12.0
      G=SQRT(GSQRD)
C     CALL ROOT FINDING SUBROUTINE.
      CALL FCNZERO(DELTA,OBEGIN,OEND,OTOL,0,NROOTS,ANS)
C     WRITE PUNCH OUT RESULTS.
      IF(NROOTS.GT.0) GO TO 150
      WRITE(6,20) NROOTS,RPLATE
      GO TO 200
  150 WRITE(6,40)
      DO 180 J=1,NROOTS
      I=2*(J-1)+1
      OMEGA=ANS(I)
      CALL PARAM(OMEGA)
      WRITE(6,30) J,OMEGA,A1SQRD,A2SQRD,DEL,EN
      WRITE(7,30) J,OMEGA,A1SQRD,A2SQRD,DEL,EN
  180 CONTINUE
C     STEP PLATE RATIO AND CONTINUE ITERATION IF MAXIMUM HAS NOT BEEN
C     EXCEEDED.
  200 RPLATE=RPLATE+RSTEP
      IF(RPLATE.LE.REND) GO TO 100
      CALL EXIT
      END

      SUBROUTINE PARAM(OMEGA)
C
```

```
      CCMMON/TABLE1/A1,A2,A1SQRD,A2SQRD,A3SQRD,CAPK,G,GSQRD,
     * RPLATE,RPOISN,RSPEED,SIGMA1,SIGMA2,SHEAR
      CCMMON/TABLE2/BOA1,BOA2,B1A1,B1A2,B2A1,B2A2,DEL,EN
C     CALL DELTA FUNCTION TO SET VALUES FOR GIVEN OMEGA.
      X=DELTA(OMEGA)
C     SET THE VALUE OF PI AND CALCULATE DEL.
      PI=3.141592653589
      DEL=BOA1/BOA2
C     SET THE SIGN FACTOR TO AGREE WITH THE SIGN OF A2SQRD.
      SIGN=1.0
      IF(A2SQRD.LT.0.0) SIGN=-1.0
C     CALCULATE EN.
      EN=PI*(0.5*(BOA1*BOA1+B1A1*B1A1)+(DEL*DEL*0.5)*(BOA2*BOA2+
     *B1A2*B1A2(-)2.0*A1*BOA1*B1A1(/)A1SQRD-A3SQRD*CAPK)
     * +GSQRD*(SIGMA1-1.0)*(SIGMA1-1.0)*A1SQRD*0.5
     *  *(B1A1*B1A1-BOA1*B2A1)
     * +GSQRD*(SIGMA2-1.0)*(SIGMA2-1.0)*A2*A2
     * *DEL*DEL*0.5*(B1A2*B1A2-BOA2*B2A2)
     * -GSQRD*2.0*A1*(SIGMA1-1.0)*BOA1*B1A1)
C     PROCESSING IS COMPLETE -RETURN TO CALLING PROGRAM.
      RETURN
      END

      FUNCTION DELTA(OMEGA)
C
      CCMMON/TABLE1/A1,A2,A1SQRD,A2SQRD,A3SQRD,CAPK,G,GSQRD,
     * RPLATE,RPOISN,RSPEED,SIGMA1,SIGMA2,SHEAR
      CCMMON/TABLE2/BOA1,BOA2,B1A1,B1A2,B2A1,B2A2,DEL,EN
      DIMENSION TEMP(200)
C     CALCULATE FORMULA PARTS X,Y,AND Z.
      U=(1.0/SHEAR)-CAPK
      V=G*RSPEED*OMEGA
      W=U*U+(4.0*CAPK)/(V*V)
      X=SQRT(W)
      Y=RSPEED*RSPEED*OMEGA*OMEGA
      Z=(1.0/SHEAR)+CAPK
C     CALCULATE THE SQUARES OF A1,A2, AND A3
      A1SQRD=0.5*Y*(Z+X)
      A2SQRD=0.5*Y*(Z-X)
      A3SQRD=Y-(SHEAR/GSQRD)
C     CALCULATE A1 AND THE TWO SIGMAS.
      A1=SQRT(A1SQRD)
      SIGMA1=A2SQRD/(A3SQRD*CAPK)
      SIGMA2=A1SQRD/(A3SQRD*CAPK)
C     IF A2 IS IMAGINARY, I.E.ITS SQUARE IS NEGATIVE,TRANSFER DOWN
C     TO USE THE ALTERNATE FORMULA FOR DELTA.
      IF(A2SQRD.LT.0) GO TO 100
C     CALCULATE A2,CALL THE APPROPRIATE BESSEL  FUNCTION AND RETURN
```

```
C       THE VALUE OF THE DELTA FUNCTION TO THE CALLING ROUTINE.
        A2=SQRT(A2SQRD)
        CALL BES(0,A1,0,BOA1,TEMP)
        CALL BES(0,A2,0,BOA2,TEMP)
        CALL BES(1,A1,0,B1A1,TEMP)
        CALL BES(1,A2,0,B1A2,TEMP)
        CALL BES(2,A1,0,B2A1,TEMP)
        CALL BES(2,A2,0,B2A2,TEMP)
        DELTA=A1*(SIGMA1-1.0)*B1A1*BOA2-A2*(SIGMA2-1.0)*B1A2*
       *    BOA1
        RETURN
C       CALCULATE A2,CALL THE APPROPRIATE BESSEL FUNCTION,AND
C       RETURN THE VALUE OF THE DELTA FUNCTION TO THE CALLING ROUTINE.
  100   X=-A2SQRD
        A2=SQRT(X)
        CALL BES(0,A1,0,BOA1,TEMP)
        CALL BES(0,A2,1,BOA2,TEMP)
        CALL BES(1,A1,0,B1A1,TEMP)
        CALL BES(1,A2,1,B1A2,TEMP)
        CALL BES(2,A1,0,B2A1,TEMP)
        CALL BES(2,A2,1,B2A2,TEMP)
        DELTA=A1*(SIGMA1-1.0)*B1A1*BOA2&A2*(SIGMA2-1.0)
       *    *B1A2*BOA1
        RETURN
        END

        SUBROUTINE BES(NO,X,KODE,RESULT,T)
C       C3 UCOS BES
        DIMENSION T(200)
  107   FORMAT(55H1NEGATIVE ORDER NOT ACCEPTED IN BESSEL FUNCTION ROUTINE)
        DO 100 I=1,200
  100   T(I)=0.0
        KLAM=1
        KO=NO+1
        IF(X) 6,1,6
    1   IF(NO) 4,2,3
    2   T(KO)=1.0
        RESULT=1.0
        RETURN
    4   IF(KO) 5,10,3
    3   RESULT=0
        RETURN
   10   RESULT=9.999999999E200
        RETURN
    5   PRINT 107
        STOP1
    6   IF(NO) 5,7,7
    7   IF(KODE) 8,9,8
```

```
8     KLAM=KLAM+1
9     JC=2.*FIX(F(X))
      MO=NO
      IF(MO-JO) 11,12,12
11    MO=JO
12    MO=MO+11
      T(MO)=0.
      LUB=MO-1
      T(LUB)=1.0E-290
      GO TO (23,511),KLAM
23    F=2*LUB
      MO=MO-3
      I2=MO
24    F=F-2.
      T(I2+1)=F/X*T(I2+2)-T(I2+3)
      IF(I2) 25,26,25
25    I2=I2-1
      GO TO 24
26    SUM=T(1)
      DO 40 J=3,MO,2
40    SUM=SUM+2.*T(J)
      F=1./SUM
      DO 50 J=1,KO
50    T(J)=T(J)*F
      RESULT=T(KO)
      RETURN
51    F=2*LUB-2
      MO=MO-3
      I2=MO
511   T(I2+1)=F/X*T(I2+2)+T(I2+3)
      IF(I2) 52,53,52
52    I2=I2-1
      F=F-2.
      GO TO 511
53    SUM=T(1)
      DO 70 J=2,MO
70    SUM=SUM+2.*T(J)
      F=1./SUM*EXP(F(X))
      DO 80 J=1,KO
80    T(J)=T(J)*F
      RESULT=T(KO)
      RETURN
      END
      SUBROUTINE FCNZERO(LC,LB,UB,TL,NR,SC,LST)
C
C     TITLE- REAL ZEROS OF ASINGLE-VALUED FUNCTION
C     PURPOSE -TO FIND THE REAL ZEROS OF ASINGLE-VALUED FUNCTION OF
C     ONE REAL VARIABLE BY A MODIFIED METHOD OF FALSE POSITION
```

```
      DIMENSION BND(4),LST(2050)
      TYPE REAL LBOUT,INPUT,LB,LST,K4,LC
      TYPE INTEGER TW,FSC,R,S,T,V,SC
      COMMON/A/INPUT,OUTPUT,LIM,VAL,Z0,Z1,FZ0,FZ1
      LIM=1000
      DELTAX=0.0
      VAL=0.02
      K4=0.367879441
      TW=FSC=SC=R=V=0
      DX=DELTAX
      IF(DX.EQ.0)1,2
    1 DX=UB-LB
    2 IF(NR.EQ.0)3,4
    3 NR=512
    4 DUMMY=INPUT=LB
      LBOUT=LC(DUMMY)
    5 SC=R=0
      BND(1)=LB
      BND(2)=LBOUT
    6 IF(BND(1).EQ.UB)7,8
    7 IF(ABS(BND(2)).LT.TL)9,20
    9 LST(R+1)=BND(1)
      LST(R+2)=BND(2)
      SC=SC+1
   10 GO TO 20
    8 INPUT=BND(1)+DX
      IF(INPUT.GT.UB)11,12
   11 INPUT=UB
   12 BND(3)=DUMMY=INPUT
      BND(4)=LC(DUMMY)
      IF(BND(2).EQ.0)17,13
   13 IF(BND(2).LT.0)14,15
   14 IF(BND(4).GT.0)17,19
   15 IF(BND(4).LT.0)17,19
   17 DO 18 I=1,4
      LST(R+I)=BND(I)
   18 CONTINUE
      R=R+4
      SC=SC+1
      IF(SC.GE.512)25,19
   19 BND(1)=BND(3)
      BND(2)=BND(4)
      GO TO 6
   20 IF(SC.EQ.FSC)21,22
   21 TW=TW+1
      GO TO 23
   22 TW=1
   23 IF(SC.LT.NR.AND.TW.LT.4)24,25
```

```
24 DX=K4*DX
   FSC=SC
   GO TO 5
25 T=(SC-1)*4+1
   DO 32 S=1,T,4
   IF(LST(S+1).EQ.0)26,27
26 LST(V+1)=LST(S)
   LST(V+2)=LST(S+1)
   GO TO 31
27 IF(LST(S+1).LT.0)28,29
28 ZO=LST(S)$      FZO=LST(S+1)
   Z1=LST(S+2)$   FZ1=LST(S+3)
   GO TO 30
29 Z1=LST(S)$     FZ1=LST(S+1)
   ZO=LST(S+2)$    FZO=LST(S+3)
30 CALL CONVERG (LC,TL)
   LST(V+1)=INPUT
   LST(V+2)=OUTPUT
31 V=V+2
32 CONTINUE
33 RETURN
   END

   SUBROUTINE CONVERG (LCN,TLN)
C
   TYPE REAL K3,INPUT ,LCN
   COMMON/A/INPUT,OUTPUT,LIM,VAL,ZO,Z1,FZO,FZ1
   FACTOR=1.0
   K2=0
   FOROUT=K3=1.0E100
34 DUMMY=INPUT=(FZ1*ZO-FZO*Z1)/(FZ1-FZO)
   OUTPUT=LCN(DUMMY)
   K2=K2+1
   IF(ABS(OUTPUT).LT.TLN.AND.ABS(Z1-ZO).LT.TLN)50,35
35 IF(K2.EQ.1) GO TO42
   RATIO=ABS((FORIN-INPUT)/(Z1-ZO))
   IF(RATIO.LT.VAL.AND.FOROUT*OUTPUT.GT.0)36,42
36 FACTOR=FACTOR*10.0
37 IF(RATIO*(FACTOR+1.0).GE.1.0)38,39
38 FACTOR=FACTOR/2.
   GO TO 37
39 SPEC=INPUT
   ALSO=OUTPUT
   DUMMY=INPUT=INPUT-FACTOR*(FORIN-INPUT)
   OUTPUT=LCN(DUMMY)
   K2=K2+1
   IF(ALSO.LT.0)40,41
40 FORIN=ZO=SPEC
```

```
      FOROUT=FZ0=ALSO
      GO TO 42
   41 FORIN=Z1=SPEC
      FOROUT=FZ1=ALSO
   42 IF(OUTPUT.EQ.0)50,43
   43 IF(OUTPUT.LT.0)44,45
   44 FORIN=Z0=INPUT
      FOROUT=FZ0=OUTPUT
      GO TO 46
   45 FORIN=Z1=INPUT
      FOROUT=FZ1=OUTPUT
   46 IF(ABS(OUTPUT).LT.TLN.AND.ABS(Z1-Z0).LT.TLN)50,47
   47 IF(Z0.EQ.0.0.AND.K2.LE.LIM) GO TO 34
      IF(K2.GT.LIM.OR.ABS((Z0-Z1)/Z0).LT.0.0000000001)48,34
   48 PRINT 49,K2,Z0,FZ0,Z1,FZ1
   49 FORMAT(1X,I4,4(3X,E17.10))
   50 RETURN
      END
 789
   0.3     0.42     0.86     0.04     0.2      0.04     2.       10.      0.0001
 6789
```

```
REQUUEST(TAPE10,*Q)
FTN (OPT=2,R=3)
LGO.
CATALOG(TAPE10,ID=   ,RP=30)
"
      PROGRAM CALLER(INPUT,OUTPUT)
C
      DIMENSION A1SQRD(25),A2SQRD(25),PSI(180),SUM1(60,25),SUM2(60,25),
     *   TAU(180,60)
      DOUBLE PHI1,PHI2,PSI,SUM1,SUM2,TAU,TAW
C
   10 FORMAT(16X,2F16.10,32X)
   20 FORMAT(1H0,23HA1  CONVERGENCE FAILURE. ,2X,2HK=,I3,2X,2HJ=,I3,2X,
     *   5HPHI1=,D32.25,2X,5HSUM1=,D32.25)
   30 FORMAT(1H0,23HA2  CONVERGENCE FAILURE. ,2X,2HK=,I3,2X,2HJ=,I3,2X,
     *   5HPHI2=,D32.25,2X,5HSUM2=,D32.25)
 2468 FORMAT(1X,2HJ=,I2,3X,2HK=,I2,3X,6HTMAX1=,E14.6,3X,10HSUM1(K,J)=,
     *   D14.6,3X,6HTMAX2=,E14.6,3X,10HSUM2(K,J)=,D14.6)
C     READ IN VALUES FOR A1SQRD AND A2SQRD.
      DO 100 J=1,25
      READ 10,A1SQRD(J),A2SQRD(J)
  100 CONTINUE
C     COMPUTE VALUES OF PSI
      DO 110 I=1,180
      QUE=I
      PSI(I)=-0.25/(QUE*QUE)
  110 CONTINUE
C     COMPUTE VALUES OF TAU.
      DO 130 K=1,60
      XK=K-1
      DO 120 I=1,180
      QUE=I
      TAU(I,K)=PSI(I)*(XK+QUE)/(XK+QUE+1.0)
  120 CONTINUE
  130 CONTINUE
C       COMPUTE VALUES OF SUMS
      DO 160 J=1,25
      DO 150 K=1,60
      TMAX1=0.0
      TMAX2=0.0
      XK=K-1
      PHI1=1.0/(XK+1.0)
      PHI2=PHI1
      SUM1(K,J)=PHI1
      SUM2(K,J)=PHI2
      QUEMAX=1.6*SQRT(A1SQRD(J))+40.0
      JAY=INT(QUEMAX)
      DO 140 I=1,JAY
```

```
      TAW=TAU(I,K)
      PHI1=TAW*A1SQRD(J)*PHI1
      T1=DABS(PHI1)
      TMAX1=AMAX(TMAX1,T1)
      SUM1(K,J)=SUM1(K,J)+PHI1
  140 CONTINUE
      IF(DABS(PHI1/(SUM1(K,J)-PHI1)).LT.10.E-24) GO TO 142
      PRINT 20,K,J,PHI1,SUM1(K,J)
      RETURN
  142 VAL=ABS(A2SQRD(J))
      QUEMAX=1.6*SQRT(VAL)+40.0
      JAY=INT(QUEMAX)
      DO 145 I=1,JAY
      TAW=TAU(I,K)
      PHI2=TAW*A2SQRD(J)*PHI2
      SUM2(K,J)=SUM2(K,J)+PHI2
      T2=DABS(PHI2)
      TMAX2=AMAX1(TMAX2,T2)
  145 CONTINUE
      PRINT 2468,J,K,TMAX1,SUM1(K,J),TMAX2,SUM2(K,J)
      IF(DABS(PHI2/(SUM2(K,J)-PHI2)).LT.10.E-24)
      PRINT 30,K,J,PHI2,SUM2(K,J)
      RETURN
  150 CONTINUE
  160 CONTINUE
      WRITE(10) SUM1,SUM2
CTERMINATE PROGRAM.
      RETURN
      END
789
DATA -OUTPUT OF PROGRAM ROOTS
6789
```

```
CCC JOB CARD
ATTACH (TAPE10,ID=  )
REWIND (TAPE10)
FTN (OPT=2,R=3)
LGO.
      PROGRAM CALLER(INPUT,OUTPUT,TAPE10,TAPE11,TAPE12,PUNCH)
C
      COMMON/TABLE1/A(25),A1SQRD(25),A2SQRD(25),C(25,60),DEL(25),
     *  EN(25),FORCE,FREQ,GEE(25,25),H,MAXJ,OMEGA(25),PI,R4(25),
     *R4D(25),SUM1(60,25),SUM2(60,25),T(25),Z
      TYPE COMPLEX A,R4,R4D
      TYPE DOUBLE C,FREQ,GEE,PI,SUM1,SUM2,T
      COMMON/TABLE2/ETA,S1(25),WORK1(50,50),WORK2(70,60),XI
      TYPE DOUBLE ETA,S1,WORK2,XI
      TYPE COMPLEX ABYS1,COEF,D,HOLD,PRESS1,PRESS2
      DIMENSION COEF(25,26),D(25),HOLD(25,26)
C
   10 FORMAT(5X,F11.10,4F16.10)
   11 FORMAT(1X,I4,F11.6,F16.10)
   15 FORMAT(1X,2HN=,I3,1X,5HA(N)=,E20.10,1X,E20.10,2X,6HOMEGA=,F6.2,
     *  2X,5HNMAX=,I3)
   20 FORMAT(1H1,29X,4HZ=,E20.10,24X,8HFORCE=,E20.10/)
   25 FORMAT(1H0,4X,1HJ,12X,5HOMEGA,19X,6HA1SQRD,19X,6HA2SQRD,21X,
     *  3HDEL,23X,2HEN/)
   30 FORMAT(1H,I5,5(5X,E20.10))
   35 FORMAT(1H1,60X,9HGEE ARRAY/)
   40 FORMAT(1H,4(1X,D32.25))
   45 FORMAT(1H1,56X,17HCOEFFICIENT ARRAY//1H ,52X,4HH = ,E20.10/)
   50 FORMAT(1H,E20.10,1X,E20.10,4X,E20.10,1X,E20.10,4X,E20.10,1X,
     *  E20.10)
   55 FORMAT(1H1,4X,1HN,23X,2HR4,43X,3HR4D,39X,1HT/)
   60 FORMAT(1H,I5,3X,E20.10,2X,E20.10,4X,E20.10,2X,E20.10,4X,D32.25)
   65 FORMAT(1H1,23X,9HH/A=0.04,27X,7HOMEGA =,F6.2,26X,10HNUMBER OF ,
     *  13HEIGENVALUES =,I3//1H0,10X,1HN,32X,1HD,59X,1HA/1H ,28X,
     *   9HREAL PART,11X,14HIMAGINARY PART,26X,9HREAL PART,11X,
     *  14HIMAGINARY PART/)
   70 FORMAT(1H,6X,I5,12X,E20.10,2X,E20.10,18X,E20.10,2X,E20.10)
   75 FORMAT(1H1)
   80 FORMAT(1H0,7HROOTS =,I3,3X,7HOMEGA =D21.10,2X,5HETA =,D11.3,3X,
     *  4HXI =,D11.3,3X,10HPRESSURE =,E21.10,2X,E20.10)
   85 FORMAT(1H1,12X,9HH/A =0.04,18X,23HNUMBER OF EIGENVALUES=,I3,
     *  18X,4HXI=,F6.1,18X,9HETA= 1.0//1H,5X,5HOMEGA,30X,8HPRESSURE,
     *  37X,8HPRESSURE,24X,8HPRESSURE/1H,26X,9HREAL PART,15X,
     *  14HIMAGINARY PART,20X,9HMAGNITUDE,22X,11HPHASE ANGLE/)
   90 FORMAT(1H,4X,F6.2,11X,E20.10,6X,E20.10,12X,E20.10,12X,E20.10)
   95 FORMAT(1H1,12X,9HH/A=0.04,18X,23HNUMBER OF EIGENVALUES =,I3,
     *  18X,4HXI=,F6.1,16X,7HOMEGA =,F16.10//1H,6X,3HETA,31X,
     *  8HPRESSURE,37X,8HPRESSURE,24X,8HPRESSURE/1H ,26X,9HREAL PART,
```

```
     *    15X,14HIMAGINARY PART,20X,9HMAGNITUDE,22X,11HPHASE ANGLE/)
C        READ IN TABLE VALUES ASSOCIATED WITH ROOTS.
         DO 100 J=1,25
         READ 10,OMEGA(J),A1SQRD(J),A2SQRD(J),DEL(J),EN(J)
   100   CONTINUE
C        READ IN SUMS.
         READ(10) SUM1,SUM2
C        FOR MAXJ TESTING ONLY
C        PRINT HEADERS AND SET LINE COUNT TO INITIAL VALUE.
         MAXJ=16
         SXI0=0.0
         SXI100=100.0
   105   WRITE(11,95) MAXJ,SXI0
         WRITE(12,85) MAXJ,SXI100
         LINES=0
C        SET CONSTANT VALUES.
         PI=3.14159265358979323846264340
         FORCE=1.0
         ETA=1.0D
         FREQ=0.21D
         XI=0.0D
         Z=0.04*0.42*0.42/PI
         SETA=ETA
   110   H=0.132*0.42*0.42*FREQ*FREQ
         SFREQ=FREQ
C         FOR FREQUENCY PLOT AT THIS POINT
C        CALL SUBROUTINE TO GENERATE OBLATE PARAMETERS.
         CALL OBLATE
C         SET NUMBERS OF TERMS TO BE CONSIDERED AND THE FACTORS WHICH
C        DEPEND ON THIS NUMBER.
   150   NROWS=MAXJ
         NCOLS=NROWS+1
C        CALL THE ROUTINE WHICH SOLVES FOR D.
   160   CALL DSOLVE(COEF,D,HOLD,NROWS,NCOLS)
C        CALL THE ROUTINE WHICH SOLVES FOR A.
   170    CALL ACALC(D,NROWS)
C        CALCULATE PRESSURE.
   180   PRESS1=(0.0,0.0)
         PRESS2=(0.0,0.0)
         DO 190 J=1,MAXJ
         ABYS1=A(J)*S1(J)
         PRESS1=PRESS1+ABYS1*R4(J)
         JAY=2*(J/2)
         IF(J.EQ.JAY)ABYS1=-ABYS1
         PRESS2=PRESS2+ABYS1
   190   CONTINUE
         PRESS1=PRESS1*(0.0,1.0)*FREQ*FREQ
         PRESS2=PRESS2*(-FREQ/100.0D)*CEXP((0.0,-1.0)*FREQ*100.0D)
```

```
      SIZE1=CABS(PRESS1)
      SIZE2=CABS(PRESS2)
C
      X=REAL(PRESS1)
      Y=AIMAG(PRESS1)
      ANGLE1=180.0/PI*ATAN2(Y,X)
      X=REAL(PRESS2)
      Y=AIMAG(PRESS2)
      ANGLE2=180.0/PI*ATAN2(Y,X)
C     PRINT OUT RESULTS
      GO TO 300
  194 DO 198 I=1,25
      DO 196 J=1,60,4
      PRINT 40,C(I,J),C(I,J+1),C(I,J+2),C(I,J+3)
  196 CONTINUE
  198 CONTINUE
  199 PRINT 40,(S1(I),I=1,25)
  200 PRINT 20,Z,FORCE
  210 PRINT 25
  220 DO 230 J=1,25
      PRINT 30,J,OMEGA(J),A1SQRD(J),A2SQRD(J),DEL(J),EN(J)
  230 CONTINUE
      GO TO 250
  240 PRINT 35
      PRINT 40,GEE
  250 PRINT 45,H
      GO TO 280
  257 KAY=1+(NROWS*NCOLS-1)/20
      DO 270 J=1,KAY
      DO 260 I=1,20,3
      PRINT 50,COEF(I,J),COEF(I+1,J),COEF(I+2,J)
  260 CONTINUE
  270 CONTINUE
  280 PRINT 55
      DO 290 J=1,25
      N=2*(J-1)
      PRINT 60,N,R4(J),R4D(J),T(J)
  290 CONTINUE
  300 PRINT 65,SFREQ,MAXJ
      DO 310 N=1,MAXJ
      PUNCH 15,N,A(N),SFREQ,MAXJ
      PRINT 70,N,D(N),A(N)
  310 CONTINUE
  320 IF(LINES.LT.50) GO TO 330
      LINES=0
      WRITE(11,85) MAXJ,SXI0
      WRITE(12,85) MAXJ,SXI100
C
```

```
  330 LINES=LINES+1
      WRITE(11,90)  SFREQ,PRESS1,SIZE1,  ANGLE1
      WRITE(12,90)  SFREQ,PRESS2,SIZE2,  ANGLE2
C
CRESET DRIVING FREQUENCY AND BEGIN ANOTHER
C       ITERATION OR TERMINATE PROGRAM
        FREQ=FREQ+0.1D
        IF(FREQ.LT.10.1D) GO TO 110
C       TERMINATE THE PROGRAM.
  500 RETURN
      END

      SUBROUTINE OBLATE
C
      COMMON/TABLE2/ETA,S1(25),A(50,50),CTERM(70,60),X
C
      COMMON/TABLE1/DUMMY1(100),C(25,60)DUMMY2(51),H,DUMMY3(1277),
     *   PI,R4(25),R4D(25),DUMMY4(6000),T(25),DUMMY5
      TYPE DOUBLE C,CTERM,ETA,PI,S1,T
      TYPE COMPLEX R4,R4D
C
      TYPE DOUBLE AA,AAA,AH,AR,ARATIO,ARG,ARRAY,ATERM,BLIST,BOOK,CL,
     1COEFF1,COEFF2,COEFF3,CORA,CORB,CWRON,DE,DH,DL,DLIST,DN,DX,E1,E2,
     2E3,EJN,EM,ENR,ENRC,ESTORE,ESUM,EYE,FACT,FN1,FN2,FNM,GLIST,H,
     3OUTPUT,PAPER,PCL,PEN,PL8,PL9,PLA,PLB,PLC,PLD,R1,R2,R3,RAD1,RAD1D,
     4RAD2,RAD2D,RATIO,RSTORE,RSUM,S,SSUM1,SUBSUM,TEMP,TERM,TERM1,TERM2,
     5TERM3,TWRON,W,X,X1,XL,XX,EIG,Q,CRAD2,CRAD2D,DW,COEF,ANORM, P,
     6      FBCT,                                 S1TERM,SUM,CCOEF,
     7          DRATIO,DNEG,ANGLE,            FSTRAT
      DIMENSION          BLIST(250),ENR(250),GLIST(250),AIG(50),P(150),
     1DLIST(200),DN(200),EIG(50),          CCOEF(100)
      COMMON  FACT(300),FBCT(300)
   86 FORMAT(1X,I3,2X,5(D24.17,1X),1X,I3)
   87 FORMAT(1H1,56X,*OBLATE RADIAL FUNCTIONS*,///,47X,*H= *,D10.3,8X,
     1*X= *,D9.2,9X,* M= *,I3,///,3X,*L*,13X,*R1*,23X,*R1D*,22X,*R2*,
     223X,*R2D*,18X,*EIGENVALUE*,9X,*ACC*/)
C
      M=0
      L1=0
      ICL=2
                NL=16
      IF(ETA.EQ.1.0D) ANGLE=0.0D
      IF(ETA.EQ.1.0D) GO TO 69
      IF(ETA.EQ.0.0D) ANGLE=PI/(2.0D)
      IF(ETA.EQ.1.0D) GO TO 69
      ANGLE=DATAN(DSQRT(1.0D/(ETA*ETA)-1.0D))
   69 FBCT(1)=1.D-280
      DO 52 J=1,255
```

```
   52 FBCT(J+1)=J*FBCT(J)
      FACT(1)=1.0D
      DO 51 J=1,170
   51 FACT(J+1)=J*FACT(J)
      FACT(171)=FACT(171)*(1.D-290)
      DO 53 J=171,296
   53 FACT(J+1)=J*FACT(J)
      CCOEF(2)=-.25D
      DO 90 K=1,59
      CCOEF(K+2)=-CCOEF(K+1)/((K+1)*(K+1)*4.D)
      CTERM(1,K+1)=FBCT(K+K+K+K+1)/FBCT(K+K+1)*(FACT(K+1)*FACT(K+1)
     1/FACT(K+K+1))
 1865  FORMAT(1X,5HCCOEF,2X,5HCTERM,2X,D32.25,5X,D32.25)
      LIMC=70-K
      DO 90 J=1,LIMC
      CTERM(J+1,K+1)=CTERM(J,K+1)*(K+K+K+K+J+J-1)*(K+K+K+K+J+J)*(K+J)*
     1(K+J)/((K+K+J+J-1)*(K+K+J+J)*(K+K+J)*J)
 1875 FORMAT(1X,5HCTERM,2X,D32.25)
   90 CONTINUE
      EM=M
      LF=L1+(NL-1)*IDL
      AA=-H*H
      AAA=AA*AA
      N=50
      N1=LF-M+1
      DO 41 J=1,N
      DO 41 I=1,N
   41 A(I,J) =0.
      DO 42 I=1,N
      XL= M+I-1
   42 A(I,I)=XL*(XL+1.)+AA*(2.*XL*(XL+1.)-2.*EM*EM-1.)/((2.*XL-1.)*
     1(2.*XL+3.))
      NM2=N-2
      DO 43 I=1,NM2
      XL=M+I-1
      A(I,I+2)=(AA/(2.*XL+3.))*SQRT(((XL+2.+EM)*(XL+1.+EM)*
     1(XL+2.-EM)*(XL+1.-EM))/((2.*XL+5.)*(2.*XL+1.)))
   43 A(I+2,I)=A(I,I+2)
      ANORM1=AA
      ANORM2=LF*(LF+1.)
      CALL EIGEN(A,AIG,N,N1,ANORM1,ANORM2)
      DO 7 I=1,N1
    7 EIG(I)=AIG(I)
   38 XX=X*X+1.D
      ARG=H*X
    6 PRINT 87,H,X,M
      DO 400IL=1,NL
      L=L1+(IL-1)*IDL
```

AD-A066 388 NAVAL POSTGRADUATE SCHOOL MONTEREY CALIF F/G 20/1
COMPARISON OF THEORETICAL AND EXPERIMENTAL SOUND RADIATION PATT--ETC(U)
DEC 78 T O KIYAR

UNCLASSIFIED NL

2 OF 2
ADA
066388

END
DATE
FILMED
5-79
DDC

```
      ODDEVE=2+2*(L/2)-L
      OEV=2*(L-2*(L/2))
      PLB=2.D*EM+1.D
      IFC=0
      IUCT=(L-M)/2
      IRIO=IUCT+1
      IR=IRIO+1
      CL=EIG(L-M+1)
      IF(2*IUCT.NE.(L-M)) GO TO 10
   11 ID=2
       IB=75
      IC=2*M
      GLIST(1)= EM(%EM+1.D)+AA*(PLB-2.D)/((PLB-2.D)*(PLB+2.D))
      GO TO 12
   10 ID=3
       IB=74
      IC=2*M+1
      GLIST(1)=(EM+1.D)*(EM+2.D)+(6.D*EM+3.D)/(PLB*(PLB+4.D))*AA
   12 LIM=150
      IIB=IB-1
      DO 13 I=ID,LIM,2
      EYE=I
      INDEX=(I-ID+2)/2
      BLIST(INDEX)=EYE*(EYE-1.D)*(PLB+EYE-1.D)*(PLB+EYE-2.D)*AAA/
     1((PLB+2.D*EYE-4.D)*(PLB+2.D*EYE)*(PLB+2.D*EYE-2.D)*(PLB+2.D*EYE-
     22.D))
      INDEX=(I-ID+4)/2
   13 GLIST(INDEX)=(EM+EYE)*(EM+EYE+1.D)+.5D*AA*((1.D)-(PLB*PLB-2.D
     1*PLB)/((PLB+2.D*EYE-2.D)*(PLB+2.D*EYE+2.D)))
   17 ENR(1)=CL-GLIST(1)
      IF(IUCT.EQ.0) GO TO 1800
      DO 18 I=1,IUCT
   18 ENR(I+1)=-BLIST(I)/ENR(I)-GLIST(I+1)+CL
 1800 ENR(IB)=-BLIST(IB)/GLIST(IB+1)-CL)
      IP=IIB+IR
      DO 19 I=IR,IIB
      IPI=IP-I
   19 ENR(IPI)=-BLIST(IPI)/(GLIST(IPI+1)-CL+ENR(IPI+1))
      ENRC=-BLIST(IRIO)/(GLIST(IR )-CL+ENR(IR))
      DE=ENRC*ENRC/BLIST(IRIO)
       CORB=DE
      DO 20 I=IR,IB
      DE=ENR(I)*ENR(I)/BLIST(I)*DE
      CORB=CORB+DE
   20 IF(DABS(DE/CORB).LT.1.D-27) GO TO 23
   23 CORA=1.D
      DE=1.D
      IF(IUCT.EQ.0) GO TO 27
```

```
      DO 26  I=1,IUCT
      DE=BLIST(IRIO-I)/(ENR(IRIO-I)*ENR(IRIO-I)) *DE
      CORA=CORA+DE
   26 IF(DABS(DE/CORA).LT.1.D-27) GO TO 27
   27 DL=(ENRC-ENR(IRIO))/(CORA+CORB)
      CL=CL+DL
      IF(DABS(DL/CL).LT.1D-24) GO TO 22
      IFC=IFC+1
      IF(IFC.LT.50) GO TO 17
   22 CONTINUE
      EIG(L-M+1)=CL
   31 AR=ID
      DN(1)#((2.D*EM+2.D*AR-1.D)*(2.D*EM+2.D*AR+1.D)*ENR(1))/
     1((2.D*EM+AR)*(2.D*EM+AR-1.D)*AA)
      D(%J)=DN(J-1)*((2.D*EM+2.D*AR-1.D)*(2.D*EM+2.D*AR+1.D)
     1*ENR(J))/((2.D*EM+AR)*(2.D*EM+AR-1.D)*AA)
      DW=DN(J)*(FACT(2*(M+J)+ID-1)/FACT(ID+2*J-1))
      IF((2*(M+J)+ID-1).GT.170)DW=DW*1.D+290
   30 W=W+DW
      DLIST(1)=FACT(L+M+1)/((ACT%L-M+1)*(W+FACT(IC+1)))
      ANORM=DLIST(1)**2*2.D/(-2.D*ODDEVE+5.D)
      DO 32 J=1,70
      DLIST(J+1)=DN(J)*DLIST(1)
   32 ANORM=ANORM+DLIST(J+1)**2*2.D/(4.D*J-2.D*ODDEVE+5.D)
      DLIST(72)=0.D
      DNEG=DLIST(1)
      TERM=FACT(M+M+ID+ID-3)/(2.D**(ID-2)*FACT(M+ID-1))
      FSTRAT=TERM*DLIST(1)
      TERM2=DABS(FSTRAT)
      DO 34 I=2,71
      TERM=-TERM*(M+M+I+I+ID+ID-6) *(M+M+I+I+ID+IC-7)/(4.D*(I-1)*(M+I+ID
     1-3))
      TERM1=TERM*DLIST(I)
      TERM2=DMAX1(TERM2,DABS(TERM1))
   34 FSTRAT=FSTRAT+TERM1
      IAC=26-DLOG10(TERM2/DABS(FSTRAT))
      IF(IAC.GT.25)  IAC=25
      LLL=L/2+1
      C(LLL,1)=1.D
      DO 82 K=2,60
      KE=DEV*(K-1)
      SUM=CTERM(1,K)*DLIST(K)
C
      INDEX=71
      IF(H.LT.1.D) INDEX=51
      LIMC=INDEX-K
      IF(LIMC.LT.1) GO TO 81
      DO 80 J=1,LIMC
```

```
      JE=J+J+1
      TERM=CTERM(J+1,K)*DLIST(K+J)*(JE+KE)/JE
      SUM=SUM+TERM
 1900 FORMAT(1X,4HTERM,2X,3HSUM,2X,D32.25,5X,D32.25)
   80 IF(DABS(TERM/SUM).LT.1.E-26) GO TO 81
   81 C(LLL,K)=CCCEF(K)*SUM
 1910 FORMAT(1X,6HCCONST,2X,D32.25)
   82 CONTINUE
      IF(L.EQ.L1) CALL POLY(M,142,ANGLE,P)
      S1(LLL)=0.D
      DO 500 J=1,71
      INDEX=2*J-ODDEVE+1
      S1TERM=DLIST(J)*P(INDEX)
      S1(LLL)=S1(LLL)+S1TERM
  500 IF(DABS(S1TERM/S1(LLL)).LT.1.E-26) GO TO 501
  501 CONTINUE
  237 PLC=FACT(L-M+1)*FACT(2*M+1)*DLIST(1)*H**M/(FACT(L+M+1)*PLB)
      INDEX=(L-M)-((L-M)/4)*4+1
      GO TO (240,242,244,246),INDEX
  240 RAD1=PLC
      RAD1D=0.D
      RAD2=(M+M-1)*PI*FACT(M+1)*FACT(L-M+1)*(H/2.D)**M*FSTRAT*FSTRAT
     1/(FACT(M+M+1)*FACT(L+M+1)*2.D*H*DNEG)
      RAD2D= 1.D/(H*RAD1)
      GO TO 326
  242 RAD1=0.D
      RAD1D=PLC*(2.D*EM+1.D)*H/(2.D*EM+3.D)
      RAD2=-1.D/(H*RAD1D)
      RAD2D=(M+M-3)*(M+M-1)*FACT(M+1)*FACT(L-M+1)*PI*(H/2.D)**M*
     1FSTRAT*FSTRAT/(FACT(M+M+1)*FACT(L+M+1)*2.D*H*H*DNEG)
      GO TO 326
  244 RAD1=-PLC
      RAD1D=0.D
      RAD2=(M+M-1)*PI*FACT(M+1)*FACT(L-M+1)*(H/2.D)**M*FSTRAT*FSTRAT
     1/(-FACT(M+M+1)*FACT(L+M+1)*2.D*H*DNEG)
      RAD2D=+1.D/(H*RAD1)
      GO TO 326
  246 RAD1=0.D
      RAD1D=-PLC*(2.D*EM+1.D)*H/(2.D*EM+3.D)
      RAD2=-1.D/(H*RAD1D)
      RAD2D= -(M+M-3)*(M+M-1)*FACT(M+1)*FACT(L-M+1)*PI*(H/2.D)**M*
     1FSTRAT*FSTRAT/(FACT(M+M+1)*FACT(L+M+1)*2.D*H*H*DNEG)
  326 IF(IAC.LT.0) IAC=0
      PRINT 96,L,RAD1,RAD1D,RAD2,RAD2C,EIG(L-M+1),IAC
      LLL=L/2+1
      Z1=RAD1
      Z2=RAD2
      R4(LLL)=CMPLX(Z1,-Z2)
```

```
      Z1=RAD1D
      Z2=RAD2D
      RAD(LLL)=CMPLX(Z1,-Z2)
      T(LLL)=ANORM/2.D
  400 CONTINUE
      RETURN
      END

      SUBROUTINE EIGEN(A,VALU,N,N1,ANORM1,ANORM2)
C
      DIMENSION A(50,50),VALU(50),DIAG(50),Q(50),VALL(55)
      NN=N-2
      DO 160 I=1,NN
      II=I+2
      DO 160 J=II,N
      T1=A(I,I+1)
      T2=A(I,J)
      IF(T2.EQ.0.D) GO TO 160
      T=1./SQRT(T1*T1+T2*T2)
      SIN=T2*T
      COS=T1*T
      DO 105 K=1,N
      T2=COS*A(K,I+1)+SIN*A(K,J)
      A(K,J)=COS*A(K,J)-SIN*A(K,I+1)
  105 A(K,I+1)=T2
      DO 125 K=I,N
      T2=COS*A(I+1,K)+SIN*A(J,K)
      A(J,K)=COS*A(J,K)-SIN*A(I+1,K)
  125 A(I+1,K)=T2
  160 CONTINUE
      DO 15 I=1,N
      DIAG(I)=A(I,I)
      Q(I)=A(I,I-1)*A(I,I-1)
      VALL(I)=ANORM1
   15 VALU(I)=ANORM2
      I=1
      MATCH=N
   18 TAU=(VALL(I)+VALU(I))/2.
      IF(MATCH.NE.I-1) LATCH=MATCH
      MATCH=0
      T0=0.
      T1=1.E-100
      DO 20 J=1,N
      T2=(DIAG(J)-TAU)*T1-Q(J)*T0
      IF((T1.NE.0.).AND.((T2*T1).LE.0.)) MATCH=MATCH+1
      T0=T1
   20 T1=T2
       IF(MATCH.LT.I) GO TO 26
```

```
      DO 25 K=I,MATCH
   25 VALU(K)=TAU
   26 NATCH=MATCH+1
       IF(LATCH.LT.NATCH) GO TO 40
      DO 30 K=NATCH,LATCH
   30 IF(TAU.GT.VALL(K))    VALL(K)=TAU
   40 IF((VALU(I)-VALL(I)).GT.(1.E-4)) GO TO 18
      I=I+1
      MATCH=N
      IF(I.LE.N1) GO TO 40
      RETURN
      END

      SUBROUTINE POLY(M,LN,ANGLE,P)
C
      TYPE DOUBLE FACT,FBCT,P,ANGLE,S,SN
      TYPE FACT,FBCT,P,ANGLE,S,SN
      DIMENSION P(150)
      COMMON FACT(300),FBCT(300)
      LNN=LN+1
      DO 2 N=1,LNN
    2 P(N)=0.0D
      MP=M+1
      SN=DSIN(ANGLE)
      IF((ANGLE.NE.0.).AND.((ANGLE.LT.3.1415926).OR.(ANGLE.GT.3.1415926
     19))) GO TO 6
      IF(M.NE.0)RETURN
      DO 5 N=1,LNN
    5 P(N)=1.D
       IF(ANGLE.EQ.0<
      DO 4 N=2,LNN,2
    4 P(N)=-P(N)
      GO TO 14
    6 IF((ANGLE.LT.1.570796320).OR.(ANGLE.GT.1.570796329)) GO TO 10
      IF(M.EQ.0) 3,9
    3 P(1)=1.D
      MA=2
      GO TO 1
    9 MA=M
    1 DC 7N=MA,LN
      P(N+1)=FACT(N+M)/(FACT((N+M)/2)*FACT((N-M)/2+1)*2.D**(N-1))
       IF(2*((M+N)/2).NE.(M+N))   P(N+1)=C.D
    7 IF(2*((N-M)/4<.NE.(N-M)/2)   P(N+1)=-P(N+1)
      GO TO 14
   10 P(MM)=SN**M*FACT(2*M+1)/(FACT(MM)*2.D**M)
   11 DO 13 N=MM,LN
      S=0.D
      IN=(N-M-1)/2
```

```
      II=0
      DO 12  I=II, IN
   12 S=S+FACT(2*M+I*2+1)*FBCT(2*N-2*I+1 )*DCOS((N-M-2*I)*ANGLE)/(  2.D**
     1(M+N)*FBCT(N-I+1)*FACT(MM+I)*FACT(I+1)*FACT(N-M-I+1))
      P(N+1)=SN**M*FACT(MM)/(FACT(2*M+1)*2.D**(N-2*M-1))*S
   13 IF(2*((M+N)/2).EQ.M+N)  P(N+1)=P(N+1)+SN**M*FACT(MM)*(FACT(N+MM)/
     1(FACT((N+M)/2+1)*FACT((N-M)/2+1)))**2/(FACT(2*M+1)*2.D**(2*N-M))
   14 CONTINUE
      RETURN
      END

      SUBROUTINE  SIMCX(ORIG,MCT,MAT,ANS)
C
      NCT=MCT+1
      CALL ACTCX(ORIG,MCT,NCT,MAT,ANS)
      RETURN
      END

      SUBROUTINE  ACTCX(ORIG,MCT,NCT,MAT,ANS)
C
      TYPE INTEGER V
      TYPE COMPLEX MAT,ORIG,ANS,B0,B2,B4,B6,B8,B10,B11,B13,B15
      DIMENSION MAT(MCT,NCT),ORIG(MCT,NCT),ANS(MCT)
   10 FORMAT(1X,E17.10,E17.10)
   15 FORMAT(25H  THIS MATRIX IS SINGULAR/)
   18 FORMAT(1HO*  VALUE OF DETERMINANT IS*, E17.10,E17.10 /)
   23 FORMAT(8X,*ORIGINAL CONSTANTS*,21X,*DERIVED CONSTANTS*/)
   21 FORMAT(1X,E17.10,E17.10,5X,E17.10,E17.10)
   28 FORMAT(1H1)
      JSING=JFIN=MCT
      JTOT=MCT*NCT
      IX=0$  B4=(0.0,0.0)$   B11=(1.0,0.0)
      DO 2  I=1,JTOT
      MAT(I)=ORIG(I)
    2 CONTINUE
      JCT=MCT-1
      DO 3  J=1,JCT
      KK=J+1
      GO  TO  25
   24 DO  4  K=KK,MCT
      B8=MAT(K,J)/MAT(J,J)
      DO  5  L=J,NCT
      B10=B8*MAT(J,L)
    5 MAT(K,L)=MAT(K,L)-B10
    4 CONTINUE
    3 B11=B11*MAT(J,J)
      LOW=-MCT$  MO=-1
      DO 6  INM=LOW,MO
```

```
      M=IABS(INM)
      B0=-MAT(M,NCT)
      B2=MAT(M,M)
      B4=(0.0,0.0)
      IF(IX) 7,22,7
22    IX=IX+1
      GO TO 8
7     MO2=-JFIN
      DO 9 IVN=LOW,MO2
      N=IABS(INN)
9     B4=B4+MAT(M,N)*ANS(N)
      B0=B0-B4$   JFIN=JFIN-1
8     IF(B2) 29,13,29
29    ANS(M)=B0/B2
6     CONTINUE
      PRINT 28
      PRINT 10,(ANS(II),II=1,MCT)
      PRINT 18,B11
      GO TO 26
25    V=J
      IF(MAT(J,J))12,11,12
11    IF(V.EQ.JSING)13,14
13    PRINT 28$ PRINT15
      RETURN
14    V=V+1
      IF(MAT(V,J))16,11,16
16    DO 17 JJ=J,NCT
      B6=MAT(J,JJ)
      MAT(J,JJ)=MAT(V,JJ)
17    MAT(V,JJ)=B6
      B11=-B11
12    JSING=JSING-1
      GC TO 24
26    PRINT 23
      DO 20 LL=1,MCT
      B13=(0.0,0.0)
      DO 19 MM=1,MCT
19    B13=ORIG(LL,MM)*ANS(MM)+B13
      B15=-ORIG(LL,NCT)
      PRINT21,B15,B13
20    CONTINUE
27    RETURN
      END
      SUBROUTINE ACALC(D,NROWS)
C
      COMMON/TABLE1/A(25),A1SQRD(25),A2SQRD(25),C(25,60),DEL(25),
     *   EN(25),FORCE,FREQ,GEE(25,25),H,MAXJ,OMEGA(25),PI,R4(25),
     *   R4D(25),SUM1(60,25),SUM2(60,25),T(25),Z
```

```
      TYPE COMPLEX A,R4,R4D
      TYPE DOUBLE C,FREQ,GEE,PI,SUM1,SUM2,T
      TYPE COMPLEX D
      DIMENSION  D(NROWS)
C     CLEAR THE A ARRAY.
      DO 100 N=1,MAXJ
      A(N)=(0.0,0.0)
  100 CONTINUE
C       CALCULATE A TERMS.
      DO 120 N=1,MAXJ
      DO 110 J=1,MAXJ
      A(N)=A(N)+D(J)*GEE(J,N)
  110 CONTINUE
      A(N)=A(N)*((0.0,-1.0)/(T(N)*R4D(N)))
  120 CONTINUE
C     RETURN CALLING PROGRAM.
      RETURN
      END

      SUBROUTINE DSOLVE(COEF,D,HOLD,NROWS,NCOLS)
C
      COMMON/TABLE1/A(25),A1SQRD(25),A2SQRD(25),C(25,60),DEL(25),
     *   EN(25),FORCE,FREQ,GEE(25,25),H,MAXJ,OMEGA(25),PI,R4(25),
     *   R4D(25),SUM1(60,25),SUM2(60,25),T(25),Z
      TYPE COMPLEX A,R4,R4D
      TYPE DOUBLE C,FREQ,GEE,PI,SUM1,SUM2,T
      DIMENSION COEF(NROWS,NCOLS),D(NROWS),HOLD(NROWS,NCOLS)
      TYPE COMPLEX COEF,D,HOLD,RATIO
C     CLEAR STORAGE AREAS.
      DO100 I=1,NROWS
      D(I)=(0.0,0.0)
      DO 90 J=1,NCOLS
      COEF(I,J)=(0.0,0.0)
      HOLD(I,J)=(0.0,0.0)
   90 CONTINUE
  100 CONTINUE
C     CALCULATE Q TERMS COEFFICIENTS.
      CALL GEECALC
      DO 130 N=1,NROWS
      RATIO=R4(N)/(T(N)*R4D(N))
      DO 120 J=1,NROWS
      DO 110 I=1,NROWS
      COEF(I,J)=COEF(I,J)+RATIO*GEE(I,N)*GEE(J,N)
  110 CONTINUE
  120 CONTINUE
  130 CONTINUE
C     MULTIPLY THE Q TERMS BY THE H CONSTANT.
      DO 150 J=1,NROWS
```

```
      DO 140 I=1,NROWS
      COEF(I,J)=COEF(I,J)*H
  140 CONTINUE
  150 CONTINUE
C     SUSRACT THE APPROPRIATE TERMS FROM DIAGONAL Q ELEMENTS.
      DO 160 J=1,NROWS
      I=J
      COEF(I,J)=COEF(I,J)-Z*EN(J)*(FREQ*FREQ-OMEGA(J)*OMEGA(J))
  160 CONTINUE
C     CALCULATE THE VALUES OF THE CONSTANT VECTOR.
      RATIO=FORCE/(2.0*PI)
      DO 170 I=1,NROWS
      COEF(I,NROWS)=-RATIO*(1.0-DEL(I))
  170 CONTINUE
C     CALL THE SUBROUTINE WHICH SOLVES FOR D.
      CALL SIMCX(COEF,NROWS,HOLD,D)
C     RETURN TO THE CALLING PROGRAM
      RETURN
      END

      SUBROUTINE GEECALC
C
      COMMON/TABLE1/A(25),A1SQRD(25),A2SQRD(25),C(25,60),DEL(25),
     *   EN(25),FORCE,FREQ,GEE(25,25),H,MAXJ,OMEGA(25),PI,R4(25),
     *   R4D(25),SUM1(60,25),SUM2(60,25),T(25),Z
      TYPE COMPLEX A,R4,R4D
      TYPE DOUBLE C,FREQ,GEE,PI,SUM1,SUM2,T
   10 FORMAT(1H0,20HCONVERGENCE FAILURE.,2X,2=J#,I3,2X,2HN=,I3,2X,
     *   6HTERM1=,D32.25,2X,6HPART1=,D32.25)
   20 FORMAT(1H0,20HCONVERGENCE FAILURE.,2X,2HJ=,I3,2X,2HN=,I3,2X,
     *   6HTERM2=,D32.25,2X,6HPART2=,D32.25)
C     CALCULATE THE GEE ASSOCIATED WITH EACH J AND N BY CALCULATING ITS
C     TWO PARTS,CHECKING FOR CONVERGENCE, AND THEN COMBINING THEM.
 8642 FORMAT(1H1,5HFREQ=,F17.10)
      DO 140 N=1,MAXJ
      DC 130 J=1,MAXJ
      TMAX1=0.0
      TMAX2=0.0
C     CALCULATE TWO PARTS.
      PART1=0.0D
      PART2=0.0D
      DC 100 K=1,60
      TERM1=C(N,K)*SUM1(K,J)
      PART1=PART1+TERM1
      TERM2=C(N,K)*SUM2(K,J)
      PART2=PART2+TERM2
      IF(MAXJ.NE.20) GO TO 100
      T1=DABS(TERM1)
```

```
      TMAX1=AMAX1(TMAX1,T1)
      T2=DABS(TERM2)
      TMAX2=AMAX1(TMAX2,T2)
  100 CONTINUE
C     CHECK FOR CONVERGENCE.
      IF(DABS(TERM1/(PART1-TERM1)).LT.10.E-12) GO TO 110
      PRINT 10,J,N,TERM1,PART1
      CALL EXIT
  110 IF(DABS(TERM2/(PART2-TERM2)).LT.10.E-12) GO TO 120
      PRINT 20,J,N,TERM2,PART2
      CALL EXIT
C     COMBINE PARTS AND STEP LOOPS.
  120 GEE(J,N)=0.5D*PART1-0.5D*PART2*DEL(J)
      IF(MAXJ.NE.20) GO TO 130
 2468 FORMAT(1X,2HN=,I2,3X,2HJ=,I2,3X,6HTMAX1=,E14.6,3X,6HPART1=,D14.6,
     *3X,6HTMAX2=,E14.6,3X,6HPART2=,D14.6/1X,7HDEL(J)=,E14.6,3X,
     *9HGEE(J,N)=,D14.6)
      PRINT 2468,N,J,TMAX1,PART1,TMAX2,PART2,DEL(J),GEE(J,N)
  130 CONTINUE
  140 CONTINUE
C     RETURN TO CALLING PROGRAM.
  150 RETURN
      END
789
DATA -OUTPUT OF PROGRAM ROOTS
6789
```

LIST OF REFERENCES

1. Sevdik, Omer, Development of a Flexural Disk Transducer for Acoustic Tracking of Underwater Vehicles, M. S. Thesis, Naval Postgraduate School, Monterey, CA, 1976.

2. Morse, Philip M. and Ingard, Uno K., Theoretical Acoustics, pp. 213-219, McGraw-Hill, 1968.

3. Malecki, I., Physical Foundations of Technical Acoustics, pp. 505-509, Pergamon Press, 1969.

4. Mindlin, R. D., "Influence of Rotatory Inertia and Shear on Flexural Motions of Isotropic, Elastic Plates," Journal of Applied Mechanics, Vol. 18, pp. 31-38, March 1951.

5. Feit, David, "Pressure Radiated by a Point-Excited Elastic Plate," The Journal of Acoustical Society of America, Vol. 40, Number 6, pp. 1489 - 1494, 1966.

6. Alper, Stanley and Magrab, Edward B., "Radiation from the Forced Harmonic Vibrations of a Clamped Circular Plate in an Acoustic Fluid," The Journal of the Acoustical Society of America, Vol. 48, Number 3 (Part 2), pp. 681-691, 1970.

7. Jarvis, James L., Experimental Investigation of the Effects of Fluid Loading on Flexural Waves in Plates, M. S. Thesis, Naval Postgraduate School, Monterey, 1977.

8. Rayleigh, J. W. S., The Theory of Sound, Vol. II, Dover Publications, 1945.

9. Deresciewicz, H., and Mindlin, R. D., "Axially Symmetric Flexural Vibrations of a Circular Disk," Journal of Applied Mechanics, pp. 86-88, March 1951.

10. Mindlin, R. D. and Deresciewicz, H., "Thickness-Shear and Flexural Vibrations of a Circular Disk," Journal of Applied Physics, Vol. 25, Number 10, pp. 1329-1332, October 1954.

11. Reismann, H., and Greene, T. E. "Forced Axisymmetric Motions of Circular Plates," Developments in Mechanics, Proceedings of the Tenth Midwestern Mechanics Conference, Colorado State University, pp. 329-947, August 21-23, 1967.

12. Tranter, C. J., Integral Transforms in Mathematical Physics, 3rd Ed., p. 16, John Wiley & Sons, Inc., 1966.

13. Sommerfeld, A., Partial Differential Equations, Academic Press, Inc., New York 1949, p. 251.

14. Brekhovskikh, L. M., Waves in Layered Media, Academic Press, Inc., New York, 1960, pp. 242-258.

15. Junger, M. C. and Feit, D., Sound Structures and Their Interaction, MIT Press, 1972, p. 168.

16. Alper, Stanley, Radiation from the Forced Harmonic Vibrations of a Clamped Circular Plate in an Acoustic Fluid. Ph.D. Thesis. The Catholic University of America, Washington, D.C., 1970.

17. Van Buren, A. L., King, B. J., Baier, R. V., Hanish, S., Tables of Angular Spheroidal Wave Functions. Naval Research Laboratory, Washington, D.C., June 30, 1975.

18. Flammer, Carson, Spheroidal Wave Functions. Stanford University Press, 1957.

INITIAL DISTRIBUTION LIST

		No. Copies
1.	Defense Documentation Center Cameron Station Alexandria, Virginia 22314	2
2.	Library, Code 0142 Naval Postgraduate School Monterey, California 93940	2
3.	Department Chairman, Code 61 Department of Physics and Chemistry Naval Postgraduate School Monterey, California 93940	1
4.	Professor O. B. Wilson, Code 61 Wl Department of Physics and Chemistry Naval Postgraduate School Monterey, California 93940	5
5.	Department Library, Code 61 Department of Physics and Chemistry Naval Postgraduate School Monterey, California 93940	1
6.	Mr. R. L. Marimon, Code 70 Naval Undersea Warfare Engineering Station Keyport, Washington 98345	2
7.	Mr. Charles Brown, Code 7033 Naval Undersea Warfare Engineering Station Keyport, Washington 98345	1
8.	Mr. Michael L. Barlow, Code 7042 Naval Undersea Warfare Engineering Station Keyport, Washington 98345	1
9.	Dr. Stanley Alper, OMT/C64 National Oceanic and Atmospheric Administration 6001 Executive Blvd. Rockville, Maryland 20852	1
10.	Professor W. B. Zeleny, Code 61 Zl Department of Physics and Chemistry Naval Postgraduate School Monterey, CA 93940	1
11.	Deniz K. Komutanligi Bakanliklar - Ankara, TURKEY	5

12. Middle East Technical University
Library
Ankara, TURKEY 1

13. Istanbul Teknik Universitesi
Kutuphanesi
Taskisla - ISTANBUL, TURKEY 1

14. Bogazigi Universitesi
Kutuphanesi
Bebek - ISTANBUL, TURKEY 1

15. Deniz Harb Okulu Komutanligi
Kutuphanesi
Heybeliada - ISTANBUL, TURKEY 1

16. Dz. Yzb. Tekin Kiyar
Tatlipinar cad. Ozlem Sok. No=3/3
B-Blok Mutluol Apt.
Sehremini - ISTANBUL, TURKEY 3